NASA Contractor Report 179458

(NASA-CR-179458) PROPFAN TEST ASSESSMENT TESTBED AIRCRAFT FLUTTER MODEL TEST REPORT (Lockheed-Georgia Co.) 102 p Avail: NTIS HC A06/MF A01 CSCL 01A

N87-29413

Unclas
G3/02 0099102

Propfan Test Assessment Testbed Aircraft Flutter Model Test Report

C.M.J. Jenness
Lockheed-Georgia Company
Marietta, Georgia

Prepared for
Lewis Research Center
under Contract NAS3-24339

National Aeronautics
and Space Administration

Lewis Research Center
Cleveland, Ohio 44135

FOREWORD

The flutter model test program described herein was conducted by the Lockheed Georgia Company as a part of the Propfan Test Assessment under contract NAS3-24339 with the NASA-Lewis Research Center. Mr. C.M. Jenness was the Lockheed project engineer and Mr. J.F. Lubomski was the NASA technical monitor for the flutter model program.

The wind tunnel tests were performed in the Transonic Dynamics Tunnel at the NASA Langley Research Center. Mr. C. H. Ruhlin was the NASA Langley project engineer and Mr. O. J. Crooks was the Lockheed test engineer.

The flutter model detail design and fabrication were performed by Calcusearch, Incorporated (Atlanta, Georgia) under the direction of Mr. D. C. Cone.

PRECEDING PAGE BLANK NOT FILMED

LIST OF FIGURES

PRECEDING PAGE BLANK NOT FILMED

PAGE VI INTENTIONALLY BLANK

LIST OF FIGURES (CONT'D)

LIST OF SYMBOLS

Symbol	Definition
b	Reference length
BL	Buttock line - Lateral distance from fuselage plane of symmetry (Fig. 1)
C	Flexibility influence coefficient (defined in Tables 21 and 22)
D	Propfan diameter
EI	Beam bending stiffness
FS	Fuselage station - Distance along fuselage reference line from a point .20m (8 in.) forward of nose radome (Fig. 1)
GJ	Beam torsional stiffness
$I_{xx_o}, I_{yy_o}, I_{zz_o}$	Centroidal mass moments of inertia about x, y, and z axes, respectively
in.	Inches
kg	Kilograms
lb	Pounds
M	Mach number
M_D	Design dive Mach number
m	Meters
N	Newtons
n	Propfan rotation speed
q	Dynamic pressure
s	Seconds
V	Velocity
V_D	Design dive velocity
V/nD	Propfan advance ratio
WL	Water line - Vertical distance from static ground line at nose gear (Fig. 1)

PRECEDING PAGE BLANK NOT FILMED

PAGE X INTENTIONALLY BLANK

LIST OF SYMBOLS (CONT'D)

Symbol	Definition
WS	Wing station - Spanwise distance in wing reference plane
x,y,z	Distances along longitudinal, lateral, and vertical axes, respectively
$\bar{x},\bar{y},\bar{z}$	Center of gravity locations along x, y, and z axes, respectively
ρ	Atmospheric density
ω	Frequency of oscillation

SUMMARY

The Propfan Test Assessment (PTA) program includes flight tests of a propfan powerplant mounted on the left wing of a modified Gulfstream II testbed aircraft. A static balance boom is mounted on the right wing tip for lateral balance. Flutter analyses indicate that these installations reduce the wing flutter speed and that torsional stiffening and the installation of a flutter stabilizing tip boom are required on the left wing for adequate flutter safety margins.

Wind tunnel tests of a 1/9th scale high speed flutter model of the testbed aircraft were conducted in the NASA Langley Transonic Dynamics Tunnel during August 1985. One objective of the tests was to substantiate the analytically predicted wing flutter safety of the single propfan testbed preliminary design and a similar design with propfan powerplants on both wings. A second objective was to obtain data with which to validate the flutter analysis methods being used in the aircraft final design. The test program included the design, fabrication, and testing of the flutter model and the correlation of the flutter test data with analysis results.

The model was designed to simulate the operation of the testbed aircraft throughout its flight test envelope and to demonstrate a 20 percent flutter speed margin above limit dive speed. It was dynamically scaled for testing at full scale Mach numbers in Freon 12, which limited the maximum test dynamic pressure to about 9000 N/m^2 (188 lb/ft^2).

The model wings and fuselage utilized single spar, segmented shell construction. Two complete wings were fabricated, one of which represented the unmodified Gulfstream II with static balance booms on each tip and the other of which represented the torsionally stiffened testbed design with a propfan powerplant and flutter stabilizing boom on each side. The unsymmetrical single propfan configuration was represented by installing one-half of each wing design. The unpowered propfan powerplants included dynamically scaled power sections, gearboxes, and propfans. The 0.30m (12 in) diameter propfans had graphite reinforced epoxy blades which could be set at different pitch angles to vary the windmilling speed. Equivalent weight nonrotating spinners could be substituted for the propfans.

The model was tested on a very compliant two-cable mount system which produced minimal effects on the wing flutter stability. It was instrumented with a combination of strain gage bridges and miniature accelerometers to measure its loads and dynamic response.

The test procedure consisted of speed buildups at several tunnel total pressures until flutter occurred or the test envelope limits ($1.2V_D$, M = 0.90) were reached. The propfan blade pitch was set at 52.5° in order to achieve the nominal rotation speed at approximately M = 0.9.

Fifteen configurations were tested. Ten of these represented the nominal aircraft preliminary designs and were intended to verify their predicted flutter safety margins. Included were tests of the single and twin propfan configurations without flutter booms, and a test of the single propfan configuration with a simulated failure of the gearbox-to-power section connections. No flutter or near-flutter conditions occurred in any of these tests.

The other five tests were made with destabilizing wing booms to obtain flutter data for analysis validation. Flutter or near-flutter points were obtained in three of these tests. The twin propfan configuration fluttered in a 16 Hz symmetric mode at M = .77 and 8857 N/m^2 (185 lb/ft^2) dynamic pressure. The single propfan configuration fluttered in a 15 Hz unsymmetric mode at M = .79 and 9193 N/m^2 (188 lb/ft^2) with a spinner, and was near flutter at M = .77 and 9000 N/m^2 (188 lb/ft^2) with a windmilling propfan.

Excellent correlations with the test data were achieved in post-test flutter analysis using actual model properties. It was concluded that the flutter analysis method used was capable of accurate flutter predictions for both the (symmetric) twin propfan configuration and the (unsymmetric) single propfan configuration. The same method will be used for the final flutter analysis of the aircraft.

The flutter analysis also revealed that the differences between the tested model configurations and the current aircraft design caused the (scaled) model flutter speed to be significantly higher than that of the aircraft, at least for the single propfan configuration without a flutter boom. Thus, it cannot be concluded from the model tests alone that the current (or final) aircraft designs necessarily have adequate flutter safety margins. Verification of the aircraft final design should, therefore, be based on flutter predictions made with the test validated analysis method.

INTRODUCTION

The Propfan Test Assessment (PTA) is a NASA-sponsored program to evaluate by flight tests the structural integrity and noise characteristics of an efficient, high-speed propeller known as a propfan. The PTA Program is being carried out by the Lockheed-Georgia Company under Contract NAS3-24339 with the NASA-Lewis Research Center. It was initiated in August 1984, following the evaluation of the results of system studies performed by the Lockheed-Georgia and Douglas Aircraft Companies (Ref. 1 and 2).

The PTA Program will utilize a 2.74 meter (9-foot) diameter, 8-blade propfan developed by the Hamilton Standard Division of United Technologies in the Large-Scale Advanced Prop-Fan (LAP) Program. The propfan drive system consists of a modified Allison Model 570 industrial engine and modified Allison T56 reduction gearbox. The propfan powerplant will be mounted on the left wing of a modified Gulfstream American GII testbed aircraft (Figure 1). A static balance boom will be installed on the right wing tip to counterbalance the weight of the propfan powerplant. The program also includes the preliminary design of a twin propfan GII testbed configuration.

Preliminary flutter analyses indicated that the propfan installation adversely affects the GII wing flutter stability and that modifications are required to provide adequate flutter safety margins during the propfan flight testing. The flutter modifications include the addition of external doublers on the left wing upper and lower surfaces to provide increased torsional stiffness inboard of the propfan nacelle and a flutter stabilizing "dynamic balance" boom on the left wing tip. The same modifications are made to both wings of the twin propfan testbed configuration. The testbed fuselage and empennage are structurally unmodified from the GII design.

The flutter prevention program consists of flutter analyses, a flutter model test, a ground vibration (resonance) test, and a flight flutter test. The flutter model test was included in the program primarily because of the uncertain effects of the propfan at high subsonic Mach numbers and of the considerable unsymmetry of the single propfan configuration.

The objectives of the model test are to substantiate the analytically predicted flutter safety margins of the single and twin propfan testbed preliminary designs and to validate the methods used in the aircraft final flutter analyses. To meet these objectives, a 1/9-scale high-speed flutter model capable of representing the single and twin propfan testbed configurations was designed and fabricated. The model includes dynamically scaled propfan powerplants with windmilling propfans to represent the essential aerodynamic and gyroscopic effects of the props. The model was tested at full-scale Mach numbers in the NASA Transonic Dynamics Tunnel (TDT) at the Langley Research Center from 12 to 30 August 1985. The tests are believed to be unique in that propeller effects were investigated at Mach numbers up to 0.90.

This report describes the design, construction, and testing of the flutter model. The results of post-test analysis correlations with the test data are also included.

MODEL DESCRIPTION

SCALING

The flutter models were designed to simulate the operation of the testbed aircraft throughout its flight test envelope and to demonstrate a 20 percent flutter speed safety margin above limit dive speed (Figure 2). The models were designed for testing in Freon 12 in the NASA Langley Transonic Dynamics Tunnel (TDT). The Freon 12 test medium was necessary because its low sonic velocity reduces the dynamic pressure to about one-fourth of that in air at the same Mach number. This reduces the required strength of the models to achievable levels.

The models were dynamically scaled, with the exception of the propfan blades and empennage, which have higher-than-scaled stiffnesses and (approximately) scaled mass properties. This approach reduced the risk of encountering flutter of these components, which might have prevented the successful testing of the wing.

The model design scales are shown in Table 1. A geometric scale of 1/9 was selected because it permitted the use of the same propfan blades used on the PTA stability and control model, and it was compatible with the TDT test section dimensions (4.88m x 4.88m or 16 ft x 16 ft).

The Mach, density, velocity and dynamic pressure scales were established by ratioing the "design point" conditions for the aircraft and model. The most accurate dynamic simulation of the aircraft occurs in the vicinity of the design point. The design point was $1.2V_D$ at M=1.0 (Figure 2). The corresponding model design point was located within the TDT operating envelope at M=1.0 and a dynamic pressure of 8426 N/m^2 (173 psf). The Freon density and sonic velocity at this point were determined from the TDT operating data in Reference 3 and were used to establish the density and velocity scales. The remaining scales (frequency, weight, mass moment of inertia, and stiffness) were derived from the others by means of standard dynamic similarity laws.

WING CONFIGURATIONS

Three wing configurations were tested. They were the bare wing, single propfan, and twin propfan configurations. Photographs of the three are shown in Figures 3-5. The bare wing configuration (Figure 3) represented an unmodified Gulfstream II (GII) wing with a 1134kg (2500 lb) static balance boom on each tip. Its purpose was to substantiate the predicted flutter stability of the right wing of the single propfan testbed aircraft, without the complicating effects of an unsymmetrical left wing. The twin propfan configuration (Figure 4) represented the stiffened GII wing design with propfan powerplants and 136kg (300 lb) flutter stabilizing booms on both sides. Its purpose was to substantiate the predicted flutter stability of the twin propfan testbed aircraft preliminary design. It was also used to obtain symmetrical flutter data for analysis validation and for comparison with the unsymmetrical flutter data obtained with the single propfan configuration.

The single propfan configuration (Figure 5) represented the unsymmetrical flight test aircraft (preliminary) design, with its propfan powerplant and flutter boom on the left side and static balance boom on the right. Its left wing semispan was the same as that of the twin propfan configuration and its right semispan the same as that of the bare wing configuration. The same fuselage and empennage were used with all three wing configurations. The single propfan configuration was used to substantiate the predicted flutter safety of the highly unsymmetrical testbed aircraft design. It was also used to obtain unsymmetrical flutter data for analysis validation and comparison with the symmetrical twin propfan flutter data. For these tests, destabilizing, aft slung wing tip booms were substituted for the flutter stabilizing booms in order to induce well defined flutter instabilities within the model test envelope. Tests of the single and twin propfan configurations were made with windmilling propfans (Figure 5a) and with equivalent weight non-rotating spinners (Figure 5b).

CONSTRUCTION

The single propfan model general arrangement is shown in Figure 6. The model wings and fuselage are constructed with hollow aluminum spars and segmented, fiberglass-reinforced, wooden aerodynamic fairings which are attached to the spars with aluminum "bridges". The spars provide the scaled stiffness and part of the mass and inertia properties of the corresponding aircraft components. The fairings provide the external shape and remaining mass and inertia properties. Fuel mass properties are represented by removable metal weights which attach directly to the wing spars. Two complete wings are provided, one representing the twin propfan configuration and the other representing the bare wing configuration. The single propfan configuration is represented by installing the twin propfan left wing semispan and the bare wing right semispan. The wings are built without twist to alleviate the excessive outer wing down loading which would otherwise occur at high dynamic pressures. A 25% chord roll trim tab is located on each right wing semispan. It is operated through a worm gear and torque tube by an electric motor located in the fuselage.

The propfan powerplants (Figure 7) consist of masses representing the power section, gearbox, and propfan, which are supported by springs representing the engine mounts and a built-up aluminum truss representing the nacelle structure. Each propfan consists of 8 graphite-epoxy blades mounted in an aluminum hub. The hub is bolted to a steel shaft which turns on two ball bearings in the simulated gearbox. The blade pitch is adjustable so that the windmilling speed can be varied. The blades are identical to those on the stability and control model and are designed for rotation speeds up to 18,000 rpm. The maximum rotation speed during flutter model testing was approximately 7500 rpm.

The fuselage spar has a wing attachment fitting which simulates the roll and yaw flexibilities of aircraft wing attachment. Pulley brackets for the cable mount system are bolted to the fuselage spar forward and aft of the wing fitting. A Y-shaped aluminum box structure attaches the simulated jet engines to the aft fuselage spar. Flexures at its ends simulate the vertical and pitch flexibilities of the aircraft engine pylons.

Because they are not stiffness scaled, the fin and stabilizer are unsegmented monocoque surfaces. They consist of aluminum root and tip ribs and spars with bonded fiberglass-cloth-reinforced epoxy skins. Plastic foam cores stabilize the skins. The fin skins extend over and are bolted to the aft fuselage spar. A rudder of similar construction provides yaw trim. It is operated through a worm gear drive and torque tube by an electric motor located in the fuselage. The stabilizer is attached to the fin through a pivot fitting and jackscrew, which provides +/- 5 degrees pitch trim. The jackscrew is operated through a jointed torque tube by an electric motor located in the fuselage.

PRODUCT ASSURANCE

The model design and fabrication were carried out in compliance with the quality assurance criteria specified in the NASA-Langley Wind-Tunnel Model Systems Criteria handbook (Ref. 4), as summarized below. Calibration of the test instrumentation is described in the Instrumentation section of this report.

The model detail design and fabrication were vendor supplied. Quality assurance controls were initially established and incorporated into the "Propfan Test Airplane Flutter Model Specification" (Ref. 5), which was a part of the vendor purchase agreement. Requirements for design reviews, inspection, acceptance, and delivery were specified. A design review of each major model component was accomplished prior to its fabrication. Periodic visits to the vendor's facility were made to ensure specification compliance, resolve problems, and approve necessary design changes.

The critical wing and fuselage spars were 100-percent X-ray inspected at Lockheed after welding and heat treatment. Certifications of the materials and heat treatment processes used were provided by the vendor. These documents, along with the interpreted X-ray films were submitted to the NASA-Langley TDT Facility Safety Officer with the "Propfan Test Assessment Testbed Aircraft Flutter Model System Safety" report (Ref. 6) for approval prior to the wind tunnel test.

The inspection and acceptance of the model were accomplished at the vendor's facility. A combination of static loads, stiffness, mass property, and resonance tests was performed to verify vendor-supplied data and compliance with specifications. Shipment to the Lockheed facility was accomplished by Lockheed personnel.

CABLE MOUNT SYSTEM

The model was restrained in the TDT test section by the cable mount system shown schematically in Figure 8. The flying cable mount system consisted of a forward cable oriented in a vertical plane and a rear cable oriented in a horizontal plane. The ends of the forward cable attached to the test section floor and ceiling at tunnel station 13.54 (533) and passed over pulleys located in the model forward fuselage at FS 0.804 (31.64). The rear cable loop passed over pulleys located in the model aft fuselage at FS 1.686 (66.36) to pulleys mounted on the test section walls at tunnel station 29.01 (1142) to a remotely controlled tensioning device located outside the test section. The rear cable tension was normally maintained at 667N (150 lb) by a soft spring in this device.

The flying cable system was very compliant in the vertical, lateral, and angular degrees of freedom and therefore did not significantly affect the wing flutter stability. For example, the maximum rigid body mode frequency (pitching) at zero airspeed was approximately one-tenth of the wing flutter frequency.

Emergency restraint was supplied by the four-cable snubber system shown in Figure 8. The cables attached to the model fuselage, at FS 1.273 (50.1), passed over pulleys located in the test section wall slots and then to a tensioning and damping device located outside the test section. The normally slack snubber cables could be quickly tensioned to 356N (80 lb) by a pneumatic cylinder in this device. A spring-damper cartridge maintained tension and provided damping for each cable.

A dynamic stability analysis of the model and cable mount system was performed to ensure adequate stability of the model with and without the snubber cables tensioned.

INSTRUMENTATION

MODEL SENSORS

The model was instrumented with a combination of strain gage bridges and miniature accelerometers to measure the loads and dynamic response. Hall-effect pulse transducers and frequency counters were used to monitor the propfan rotation speeds. Sixteen of these channels were displayed and recorded on two 8-channel pen recorders. Thirteen channels were also recorded on an FM tape recorder, along with a time code and voice recorded information. The recorded channels varied with the wing configuration being tested, as shown in Tables 2-4.

Six to eight of the strain gage channels were calibrated and monitored to ensure that the model maximum design loads were not exceeded. Included were the wing vertical bending, fuselage vertical and lateral bending, left jet engine pylon bending and left propfan nacelle vertical and lateral bending strain gage channels. These outputs were low-pass filtered to yield "static" loads. Generally, the wing bending and torsion and aft fuselage vertical bending and torsion strain gages and the fuselage nose and propfan gearbox accelerometers (when applicable) were monitored (and recorded) for indications of approaching flutter.

The wind tunnel parameters were obtained via the TDT facility data acquisition system. Static and stagnation pressure, stagnation temperature, Mach number and dynamic pressure were continuously displayed and were printed out for each tab point. High speed (128 ft/sec) movie cameras located on either side and downstream of the model were used to record significant model responses.

CALIBRATION AND ACCURACY

Calibrations of the strain gage channels used to monitor the model static loads were made in the wind tunnel by applying approximate design loads to the model and adjusting the sensitivity so that full scale deflection of the pen recorder would occur at the design load level. The resulting accuracy of the static loads measurements was estimated to be ±5 percent. Precise measurements were not required because of the large (100%) safety margins built into the model.

The model dynamic response channels were not calibrated because only frequency and relative amplitude data were required. The estimated accuracy of the flutter frequency measurements is ±2%. The propfan rotation speed measurements are estimated to be within ±1%.

The principal quantitative data required from the test were the wind tunnel parameters at the flutter points and at the maximum conditions reached. The measurement accuracy of these data is discussed in Reference 1, and are generally as follows:

Dynamic pressure	±1%
Mach number	±.002

TEST PROCEDURE

MODEL TEST ENVELOPE

The model test envelope (Figure 9) was established by applying the design scales to the testbed aircraft dynamic pressures at 1.2 V_D. The maximum model test Mach number was limited to 0.9 by the TDT facility safety requirements. This limitation was considered unimportant in that the minimum flutter dynamic pressure was predicted to occur at M = .865.

For each configuration tested, buildups in dynamic pressure and Mach number were made along several lines of approximately constant total pressure until flutter occurred or the test envelope conditions were reached. Generally, the tunnel was pumped down to the minimum test pressure (usually 7180-9575 N/m^2 (150-200 lb/ft^2) before beginning a test. A speed buildup was made at this pressure, after which the airspeed was reduced to zero, and Freon was bled into the tunnel to increase the pressure for the next pass.

PROPFAN WINDMILLING SPEED

At a given blade pitch angle, the propfans windmilled at an approximately constant advance ratio (V/nD). Since the speed of sound remained almost constant during the test, the propfan rotation speed varied almost linearly with Mach number, as shown in Figure 10. Thus, the scaled rotation speed of 7560 RPM could be achieved at only one Mach number. The blade pitch was set at 52.5° so that this rotation speed was reached at appoximately M = .90. Flutter analyses performed prior to the test indicated that the wing flutter speed was insensitive to propfan advance ratio. This being the case, it was not worthwhile to test each configuration at several different blade pitch angles in order to achieve the design rotation speed at several different Mach numbers.

SUMMARY OF PROBLEMS AND CORRECTIVE ACTION

CABLE MOUNT STABILITY

A model pitch-plunge instability was encountered when the snubber system was engaged during the initial testing of the bare wing configuration. The 2.6 to 2.8 Hz instability occurred at dynamic pressures of 2400 to 3100 N/m^2 (50-65 lb/ft^2), with rear flying cable tensions ranging from 445 to 890N (100 to 200 lb). The instability was eliminated by moving the model center-of-gravity froward 0.076m (3 in.) by adding 2.96 kg to the nose ballast. The same nose ballast increment was used for the single and twin propfan configuration tests. Also, the snubber cable pulleys were moved forward by 0.23m (9 in.).

ROLL TRIM

Difficulties were experienced in maintaining roll trim each time the wing configuration was changed. The roll trim flap located on the right side of the wing was less effective than expected and was inadequate to compensate for the rolling moments caused by the lift unsymmetry.

The problem was alleviated by: (1) shimming the outer wing sections to reduce the lift unsymmetry, and (2) adding a chord extension to the trim tab to increase its effectiveness.

MODEL LOADS

The loads experienced by the wing and horizontal stabilizer were higher than predicted. Because the facility safety requirements prohibit testing with loads in excess of the maximum design values, this situation threatened to restrict the model test envelope. The problem was alleviated in two ways. The wing root bending moments were reduced by shimming the wing sections to introduce a small amount of washout to the untwisted wing. The horizontal stabilizer design down load was increased by 35 percent, and a static test was performed to demonstrate a 50-percent margin of safety.

TEST RESULTS

SUMMARY

A summary of the test configurations and results is given in Table 5. For each test (configuration) the run and tab point numbers, wing configuration, fuel condition, prop rotation direction and wing boom configuration are given along with comments indicating the maximum dynamic pressure reached and whether or not flutter occurred. Plots of dynamic pressure versus Mach number for each test are shown in Figures 11 through 25. For most configurations, tests were made at several total pressures. The variation of dynamic pressure with Mach number for each of these passes is shown in the figures by dashed lines which lead to tab points indicating the maximum conditions reached. Where no flutter occurred, an open symbol and a tab point number are shown. Where flutter occurred, a solid symbol is used, and the flutter frequency is also indicated. Table 6 lists the Mach number, dynamic pressure, velocity, density, Reynolds number, prop RPM and model response description for each tab point shown in the figures.

DESIGN VERIFICATION TESTS

Tests 1 through 9 and 13 were made to substantiate the predicted flutter safety of the single and twin propfan testbed aircraft preliminary designs. Nominal 1134 kg (2500 lb) balance booms and/or 136 kg (300 lb) flutter stabilizing booms were simulated for all except tests 9 and 13, in which the flutter booms were removed. The minimum (12½%) fuel condition was simulated for all except tests 4 through 6, in which the most flutter critical (by analysis) intermediate fuel condition of 1250 kg (10,000 lb) was simulated. No flutter or near flutter conditions occurred for these tests, including those made without flutter booms.

Test 6 simulated a severe failure condition in which the torquemeter and struts connecting the propfan gearbox to the engine power section were assumed to have failed. Because it represented a failure condition, this test was intended to reach only the V_D boundary. The test was terminated at .97 V_D when a spring representing the lower gearbox (engine) mount buckled and allowed the gearbox and prop to pitch down several degrees. Because the strength of the full scale mount was not simulated on the model, this failure did not imply that a similar failure would be likely on the aircraft. No wing or whirl flutter conditions were observed on this test prior to the mount failure.

ANALYSIS VALIDATION TESTS

Tests 10 through 12, 14, and 15 were made with destabilizing wing tip booms to obtain data for validation of the method being used for the aircraft flutter analysis. Three destabilizing boom configurations were tested on the twin propfan configuration in an attempt to induce a flutter instability within the model test envelope. They were: (1) the nominal 136 kg (300 lb) flutter booms installed in reverse (aft slung); (2) the same booms modified by increasing their mass to simulate 235 kg

PRECEDING PAGE BLANK NOT FILMED

(519 lb), and (3) large destabilizing booms simulating 264 kg (582 lb) each and having approximately three times the centroidal pitching moment of inertia of the flutter booms. Mass data for the boom configurations are given in Table 17.

Although high levels of dynamic response were observed with all three destabilizing boom configurations, sustained flutter occurred only with the large destabilizing booms. Flutter occurred in a 16 Hz symmetric wing bending, torsion mode at M = .77 and 8857 N/m^2 (185 lb/ft^2) dynamic pressure (Figure 22). When the same boom was tested on the single propfan configuration (test 14), flutter occurred in a 15 Hz unsymmetric mode at M = .79 and 9193 N/m^2 (192 lb/ft^2) (Figure 24). The same configuration with a windmilling propfan instead of a nonrotating spinner was very close to sustained flutter at M = .77 and 9000 N/m^2 (188 lb/ft^2) when the test was terminated to avoid unnecessary risk of model damage (Figure 25).

DISCUSSION OF RESULTS

MODEL FLUTTER ANALYSIS

Post-test flutter analyses of the flutter model were performed for correlation with the data from tests 12, 14, and 15. The analysis method was the same as that being used for the full-scale testbed aircraft. The lumped mass, beam-type structural representation utilized actual model mass and stiffness data and was adjusted to achieve good normal mode correlation with resonance test data.

A comparison of the caculated and measured normal mode frequencies is given in Table 7 for the twin propfan configuration and in Table 8 for the single propfan configuration with nominal booms. The agreement was within 3 percent for all except two single propfan configuration modes which differed by 5 and 6 percent. The measured modes are further described in Figures 42, 43, and 44 of the Appendix.

The unsteady aerodyamic derivatives used in the analyses were predicted with a subsonic doublet lattice method. The wing derivatives were adjusted to obtain agreement with the steady lift-curve-slope variation with Mach number which was measured on the Gulfstream II aerodynamic model. Doublet lattice aerodynamic derivatives were also used on the vertical and horizontal stabilizer surfaces. Quasi-steady propfan aerodynamic derivatives calculated by Hamilton Standard were used for correlations with test 15.

The unsymmetry of the single propfan configuration required the representation of the complete model (both sides) in the analysis. Although the twin propfan configuration was symmetrical and could have been represented by a half-model, a complete model was also used for it for expediency. The resulting math models contained 49 (single) and 52 (twin) component modes which were used to compute 35 normal modes for the flutter analyses. Two percent structural damping (g = .02) was used for all modes.

ANALYSIS - TEST DATA CORRELATION

The flutter boundaries predicted for the twin and single propfan model configurations with large destabilizing booms are shown in Figures 27, 28, and 29. Also shown in the figures are the data from tests 12, 13, and 15. Excellent correlation with the test data was achieved for all three cases. The flutter frequency was somewhat overpredicted for the twin propfan configuration, but was very close for the single propfan configuration. Because only one flutter (or near-flutter) test point was obtained for each case, the predicted flutter boundaries could not be fully validated. However, the lack of flutter at tab point 376 (test 12) suggests that the shape of the predicted boundary for the twin propfan configuration is reasonable.

Although the predicted single propfan flutter boundary is higher than that of the twin propfan at Mach numbers below 0.8, it has a more pronounced "dip" and is about 7 percent lower in dynamic pressure (3.5%

lower in speed) at M = 0.865. This was unexpected, because the flutter speed for an unsymmetrical configuration is generally higher than that of a summetrical configuration representing its more critical wing. The more pronounced dip seen here was caused by the greater sensitivity of the single propfan flutter instability to the density variation with Mach number in the TDT.

The predicted flutter boundary for the single propfan configuration with a windmilling propfan was negligibly higher than that without propfan effects. This insensitivity to prop aerodynamic and gyroscopic effects is consistent with the test data and observations of sub-critical response made during the tests.

AIRCRAFT DESIGN VERIFICATION

No flutter or near-flutter conditions occurred in the tests representing the aircraft (preliminary) design configurations, including those representing a propfan powerplant failure and the loss of the flutter boom. These results are consistent with the aircraft preliminary flutter analyses, which predict flutter boundaries above 1.2 V_D, except for the cases without flutter booms. In these cases, flutter is predicted to occur within the aircraft flight test envelope. However, the stability (net damping) of the predicted flutter mode varies very gradually with airspeed, and small changes in damping result in large flutter speed changes. Also, the stability of this mode has been shown by analysis to be sensitive to other parameters, including outer wing mass and propfan nacelle flexibility.

The model differs from the current (scaled) aircraft design in several respects. The most critical wing fuel conditions are empty and 4535 kg (10,000 lb). No fuel is located in the outer wing for either of these conditions. The model wing could not be made light enough to represent the empty fuel condition, in spite of its efficient thin wall aluminum spar. The excess mass is distributed across the span and is equivalent to 12½ percent of the Gulfstream II capacity fuel mass, or about 1135 kg (2500 lb). The aircraft flutter analyses indicate that increased outer wing mass increases the stability of the sensitive boom-off flutter mode.

The model propfan nacelle flexibilities also differ from the (scaled) aircraft design. The frequencies of the model engine-nacelle normal modes are generally lower than the scaled (predicted) aircraft modes, which indicates that the model engine mount and/or nacelle structural flexibilities are greater than desired. Aircraft flutter analyses indicate that increased nacelle flexibility increases the stability of the sensitive boom-off wing flutter mode.

A third difference between the model and the (scaled) aircraft is the nose ballast added to the model for cable mount dynamic stability. The ballast represents 3227 kg (7100 lb) on the aircraft. Its effect on the critical flutter mode was not separately determined.

An analysis was performed to determine the net effect of these differences on the stability of the single propfan model without a flutter boom. The predicted flutter speed was well above 1.2 V_D, which is consistent with the test results, but indicates that the model is more stable than the aircraft for this configuration. Therefore, the absence of flutter in the test of this configuration does not indicate that the flutter stabilizing boom is unnecessary for the testbed aircraft.

The effects of these differences on the flutter stability of the other test configurations are probably less significant, but were not determined by comparative flutter analyses. Therefore, the test results alone cannot be used to verify that the final aircraft design will have adequate flutter safety margins. They do indicate, however, that no serious flutter instabilities of the aircraft have been overlooked in the analysis.

CONCLUSIONS AND RECOMMENDATIONS

The results of the design verification tests generally confirm the predicted wing and whirl flutter stability of the preliminary design configurations tested. However, the model tests did not accurately simulate the most critical current configurations, and the differences were shown by analysis to increase the stability and flutter speed of the model relative to the current aircraft design, at least for the single propfan configuration without a flutter boom.

This leads to the following conclusions:

- No unexpected flutter instabilities are caused by the rotating propfan or the unsymmetry of the single propfan testbed configuration.
- The wing flutter stability is essentially the same with rotating propfans as with equivalent weight non-rotating spinners.
- The flutter stability of the symmetrical twin propfan configuration is approximately the same as that of the unsymmetrical single propfan configuration.

It is also reasonable to conclude from the model analysis/test data correlation that the flutter analysis methods being used in the aircraft design are capable of accurately predicting its wing flutter characteristics, including the effects of mass and stiffness unsymmetry and propfan aerodynamic and gyroscopic coupling. The verification of the aircraft flutter safety margins would, therefore, be based on test validated analytical predictions rather than the model test results. The structural representation used in the aircraft flutter analysis should be validated by normal mode correlations with ground vibration test data.

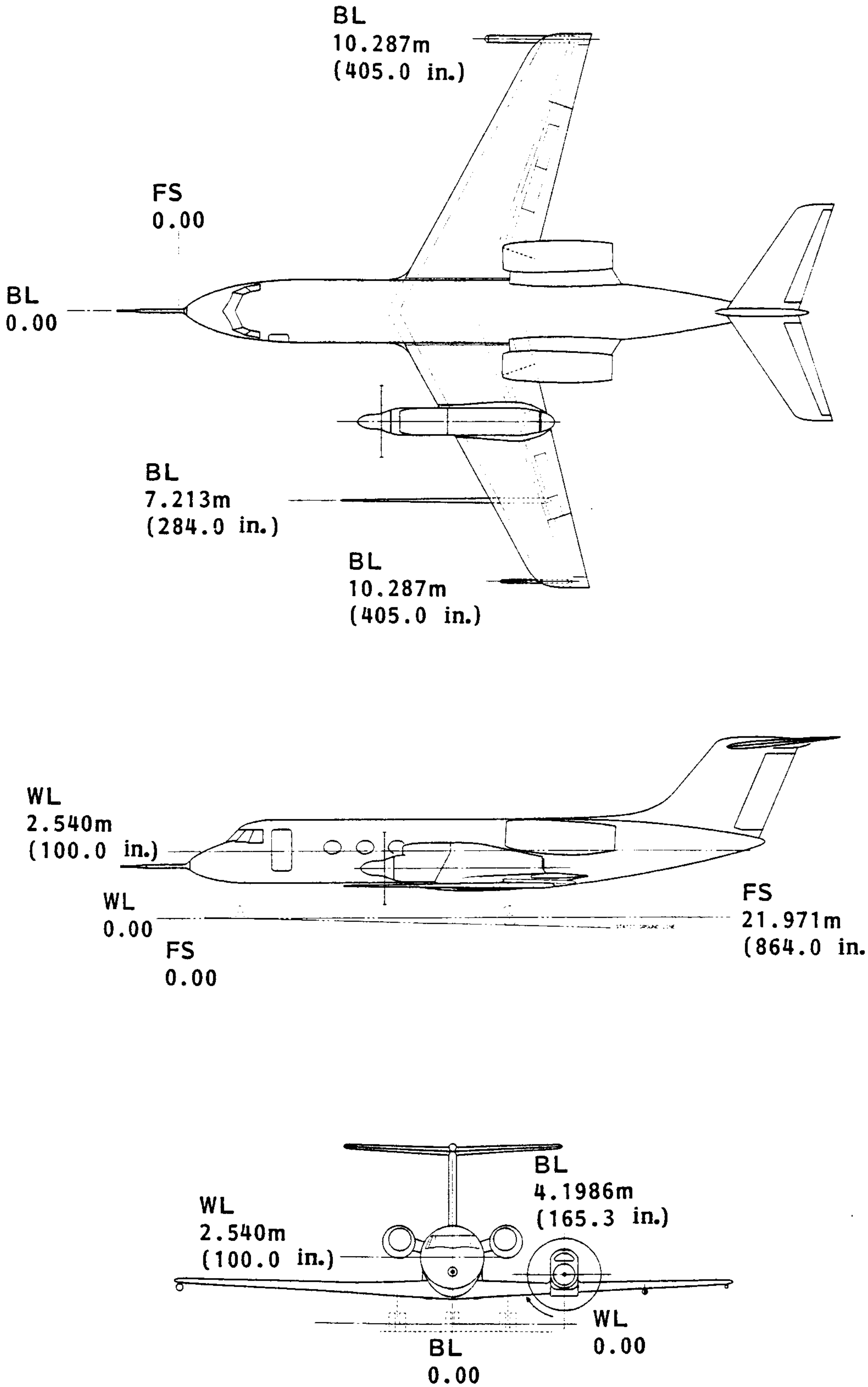

Figure 1. Modified Gulfstream II Propfan Testbed Aircraft

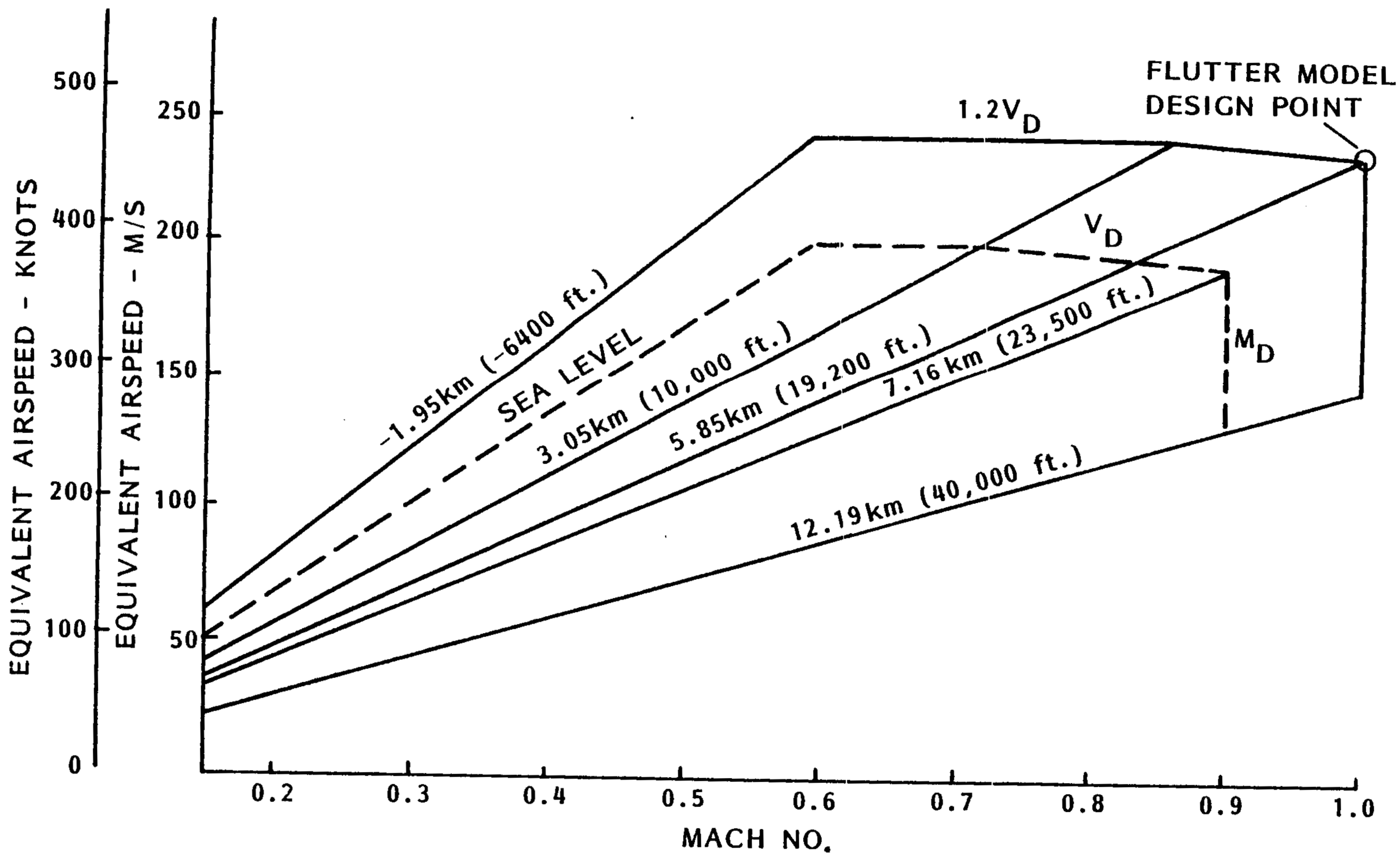

Figure 2. Propfan Testbed Aircraft Design Flight Test Envelope and Flutter Safety Margin

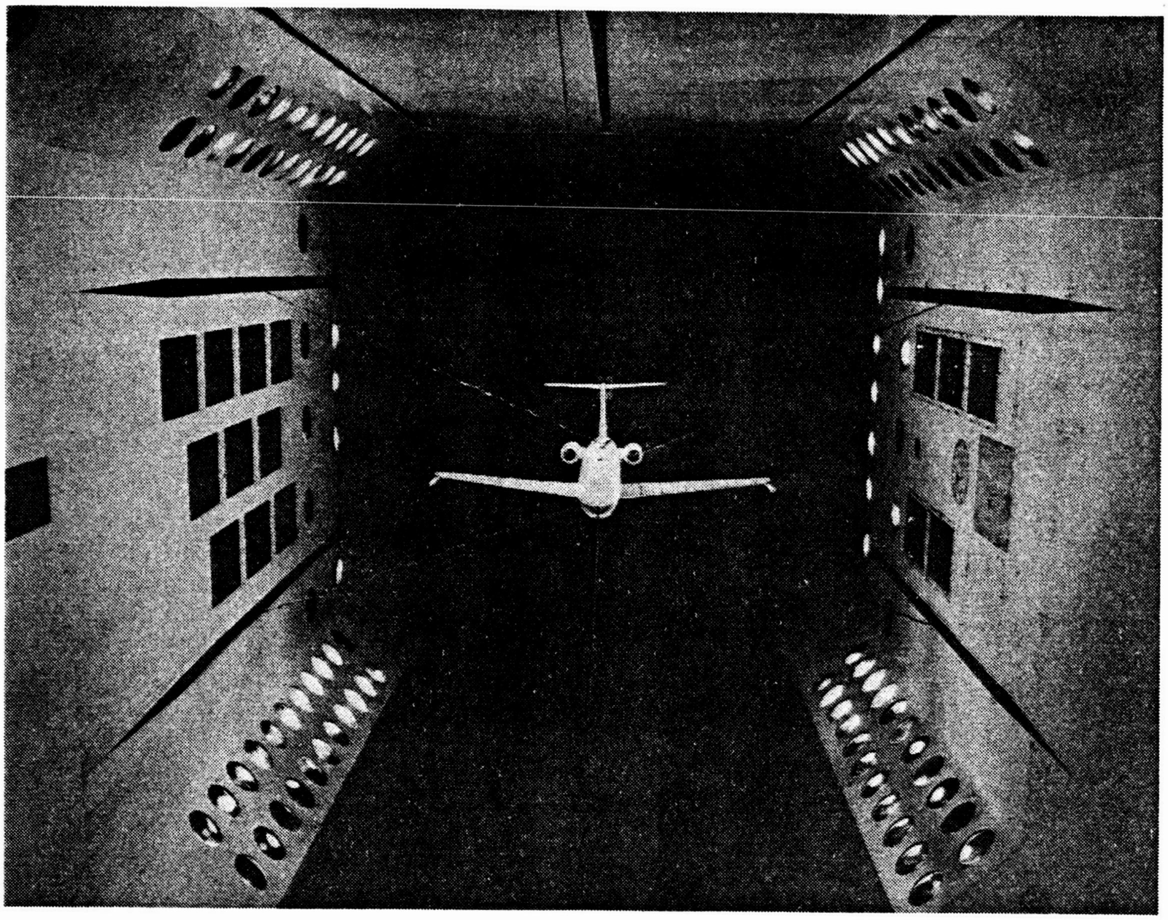

Figure 3. Bare Wing Model in NASA Langley Transonic Dynamics Tunnel

ORIGINAL PAGE IS
OF POOR QUALITY

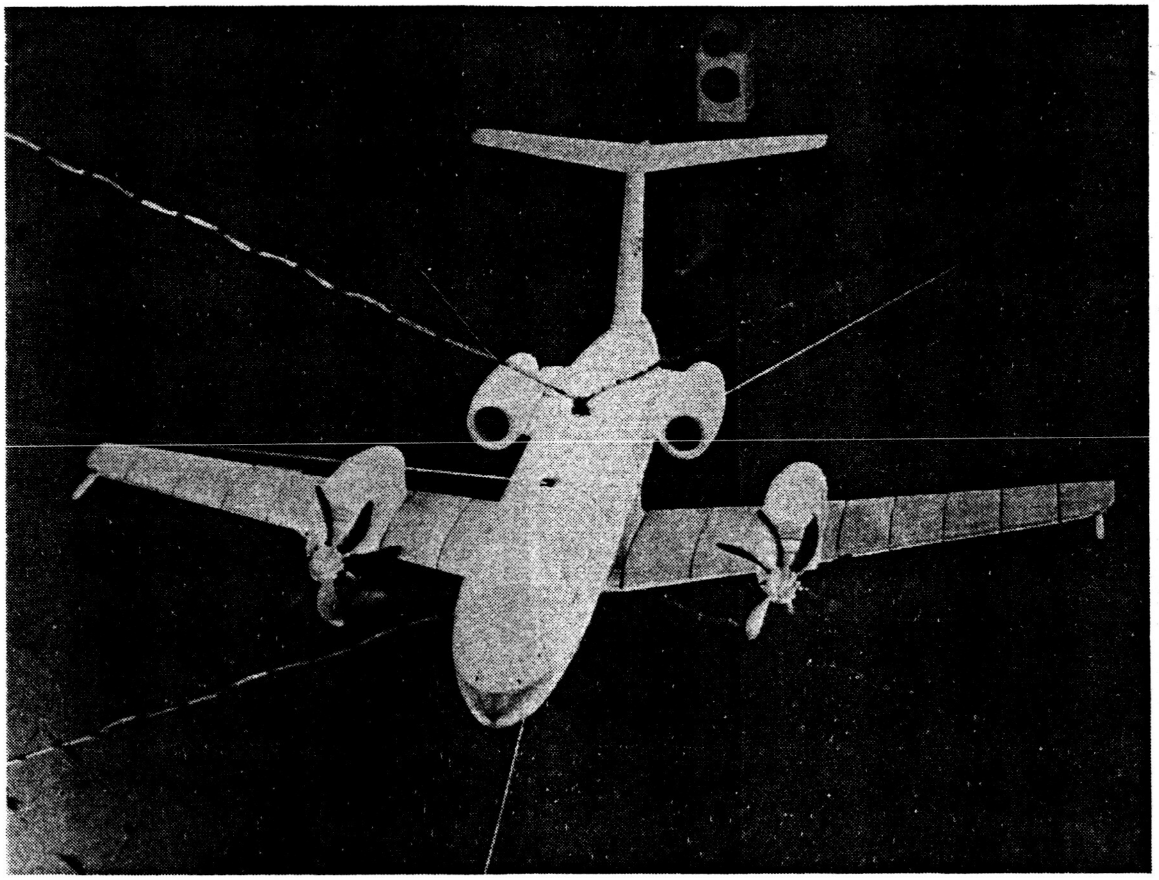

Figure 4. Twin Propfan Model with Windmilling Props

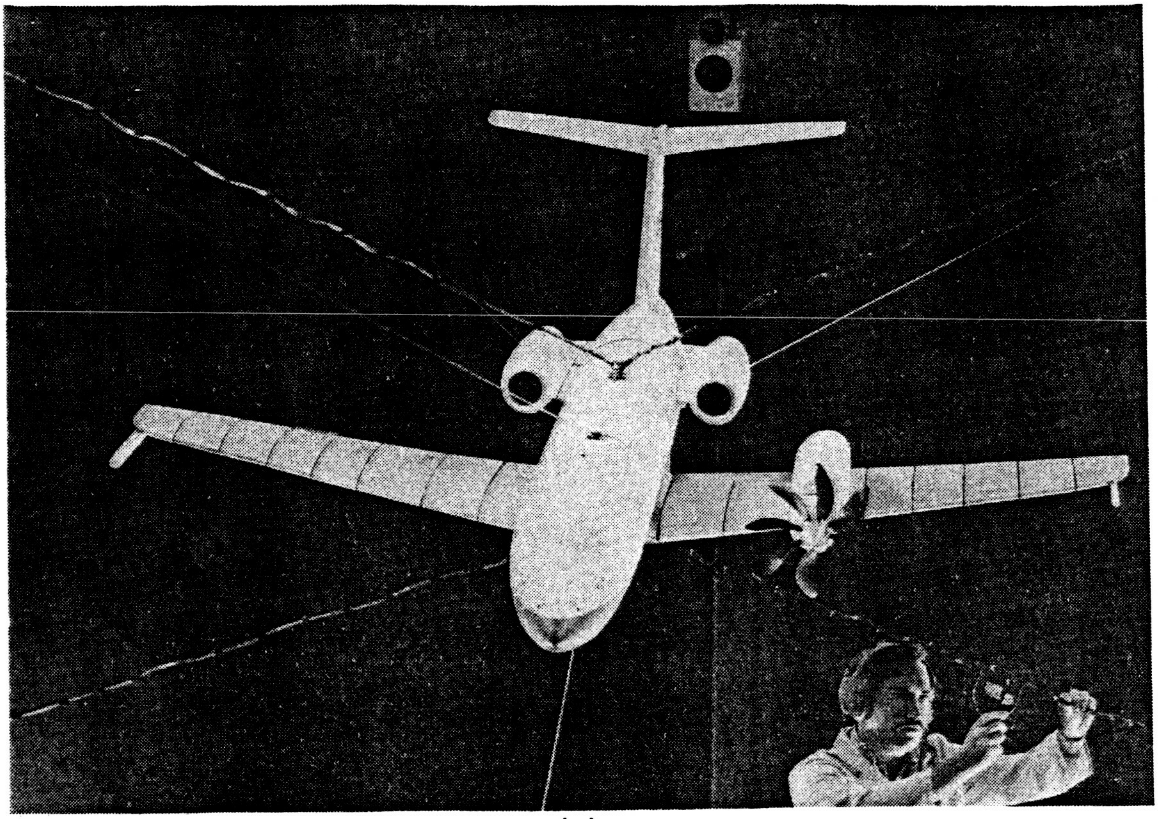

(a)

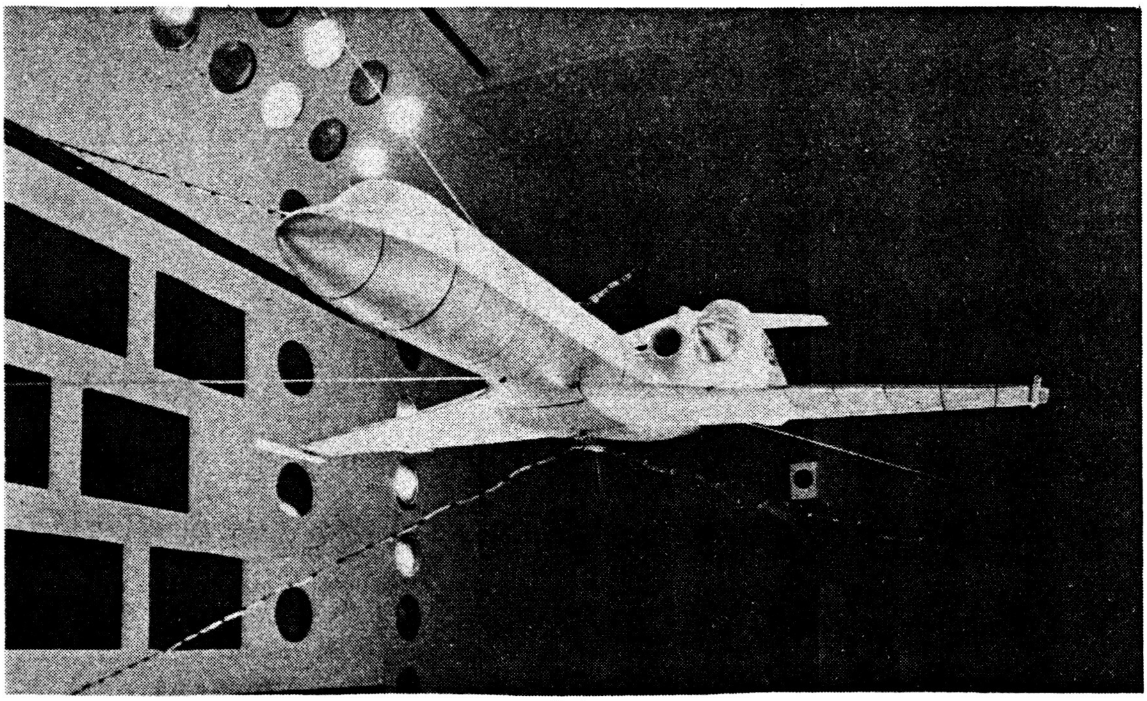

(b)

Figure 5. Single Propfan Model with (a) Windmilling Prop
(b) Weighted Spinner

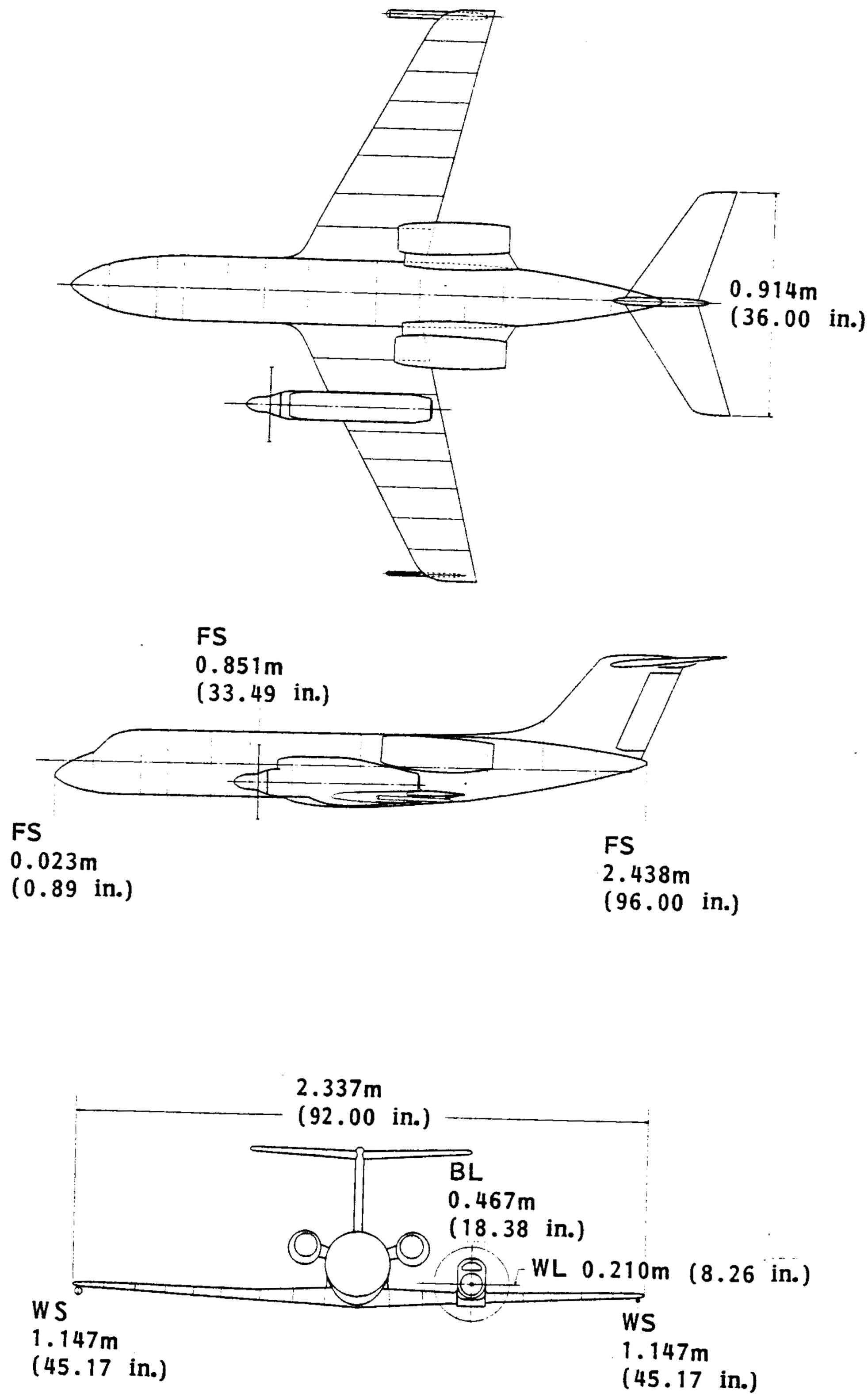

Figure 6. Single Propfan Model General Arrangment

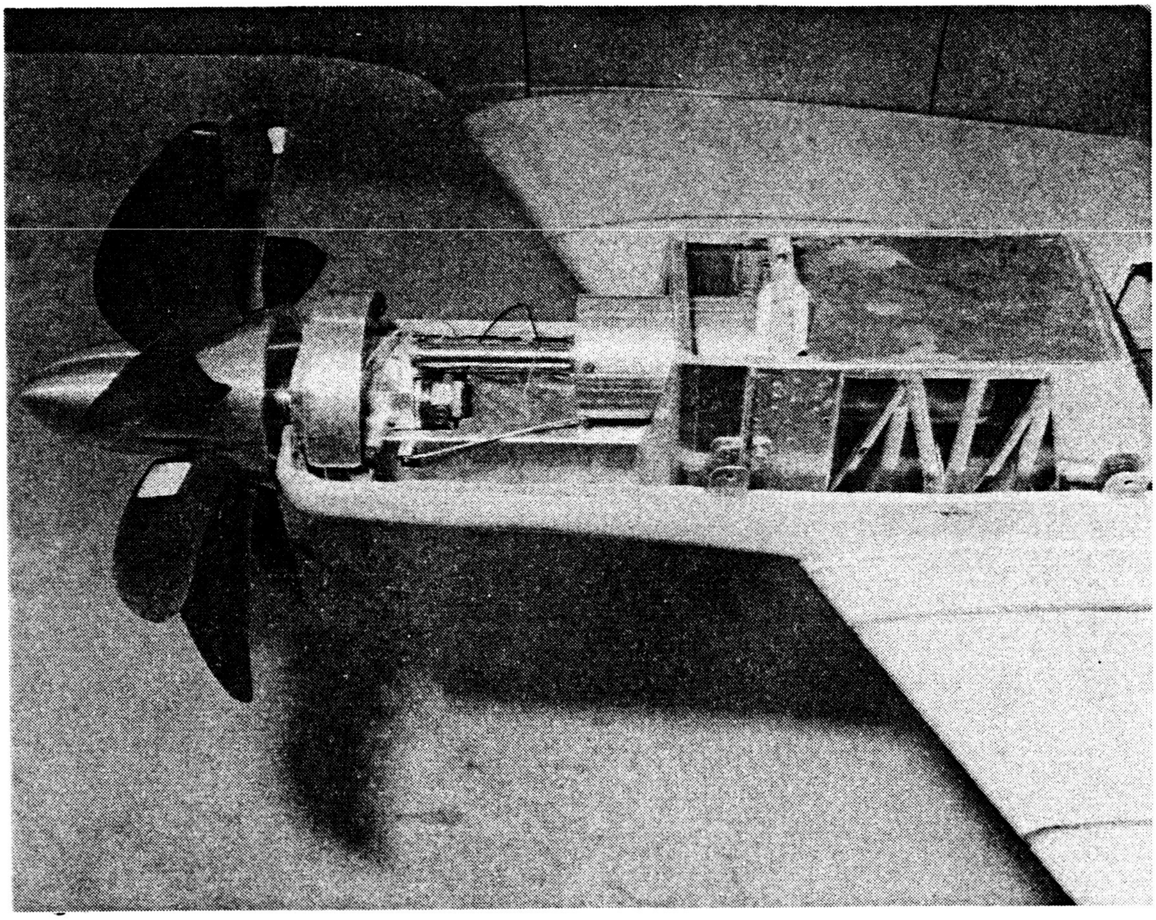

Figure 7. Model Propfan Powerplant Simulation

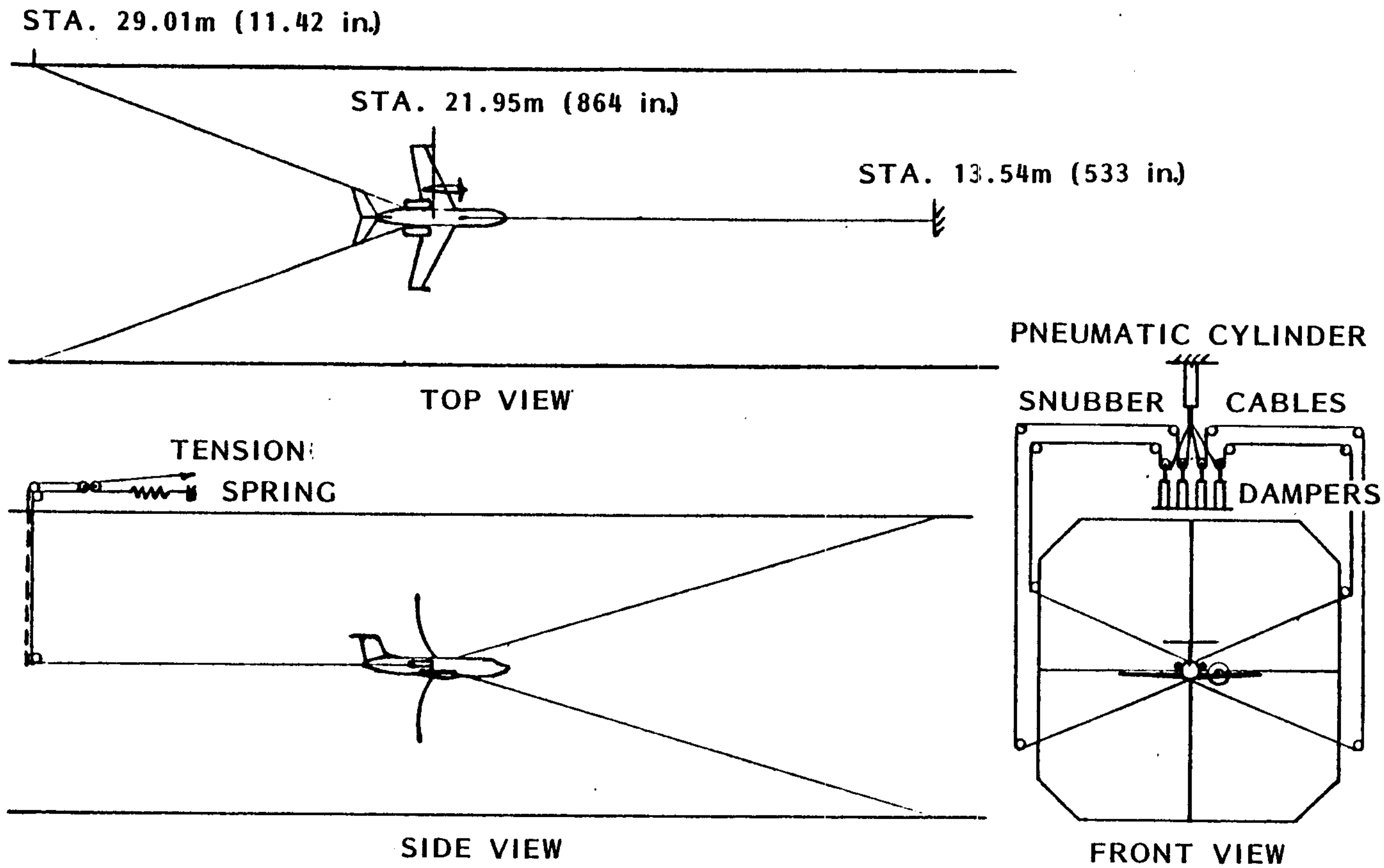

Figure 8. Model Cable Mount System Schematic

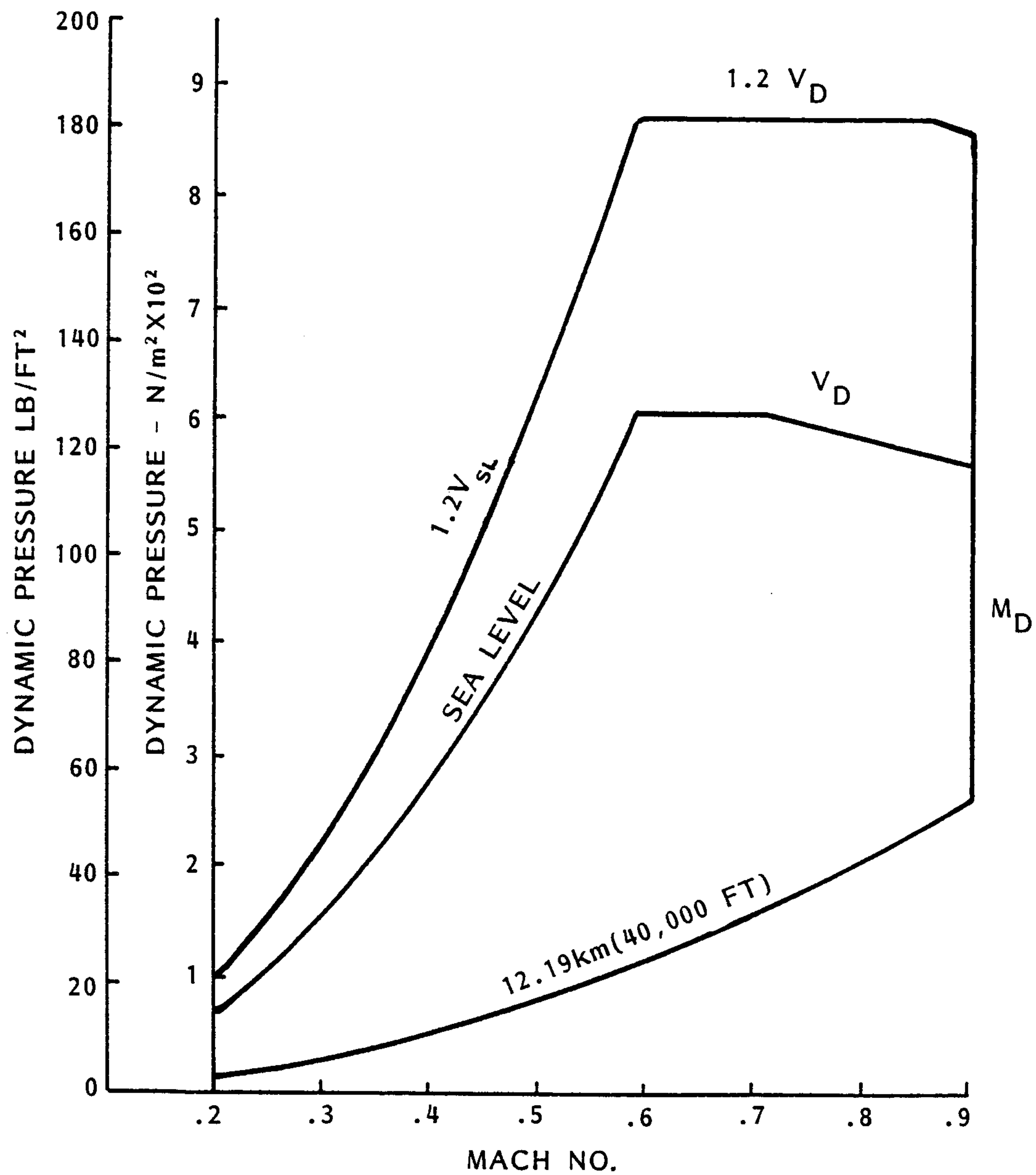

Figure 9. Model Test Envelope

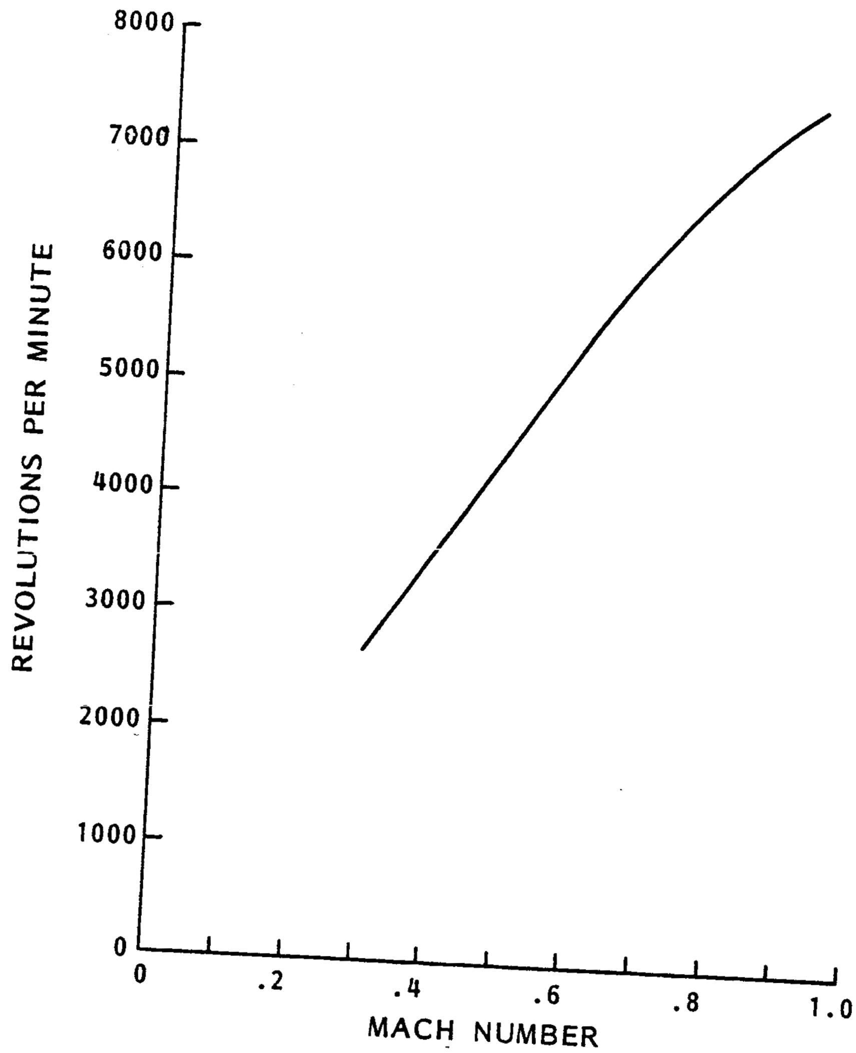

Figure 10. Model Propfan Windmilling Speed for 52.5° Blade Pitch Angle

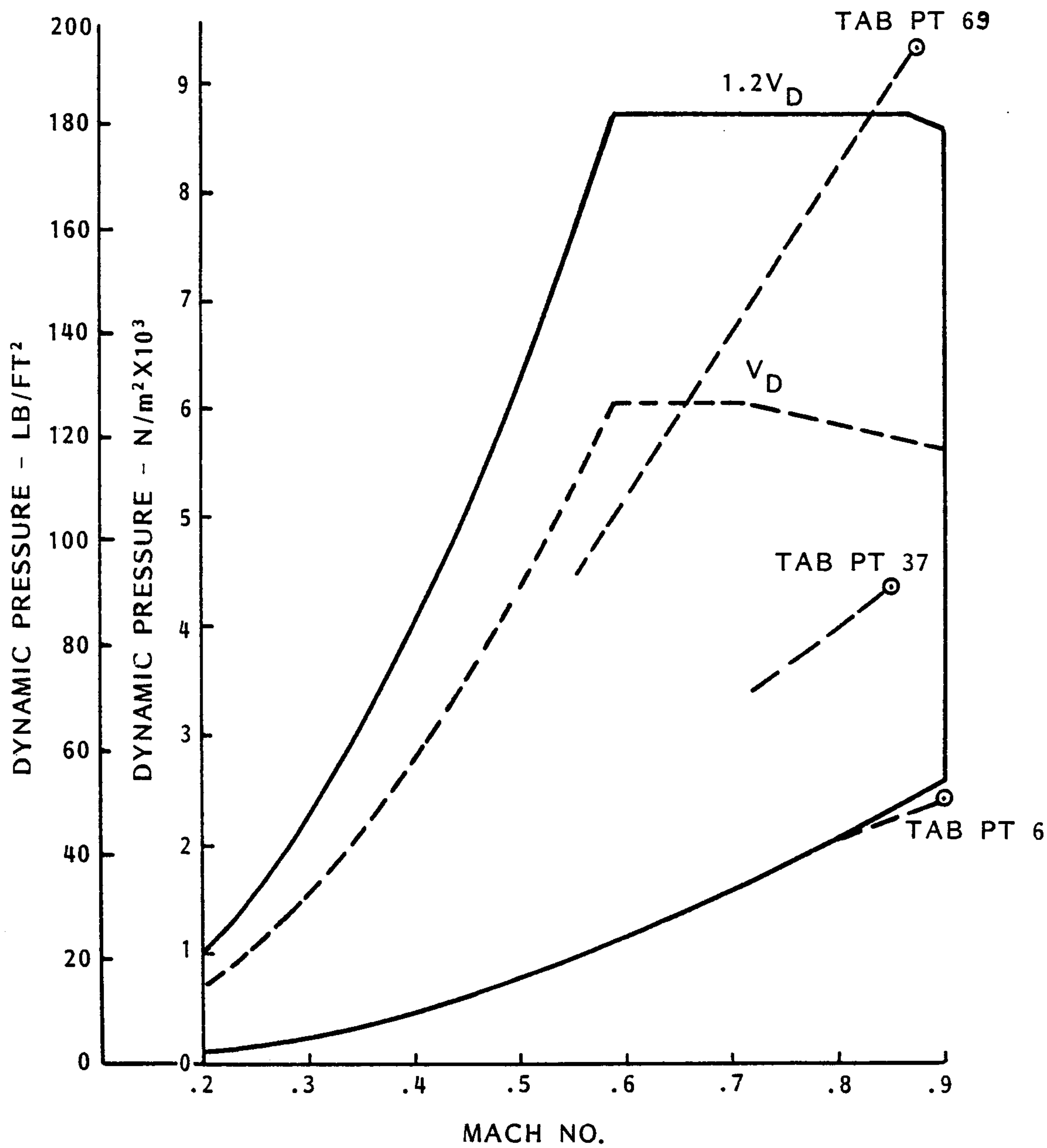

Figure 11. Test Conditions for Test Number 1

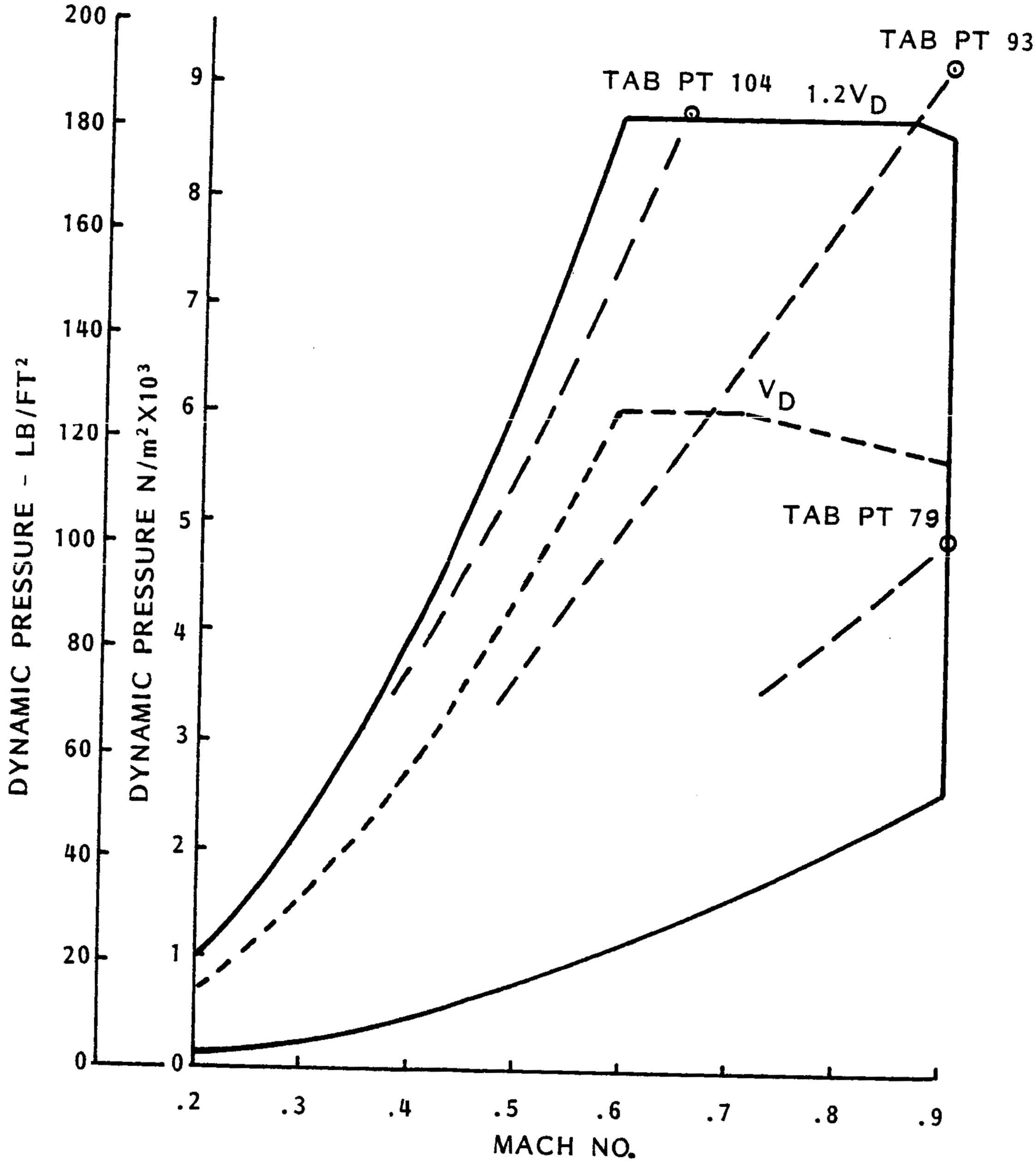

Figure 12. Test Conditions for Test Number 2

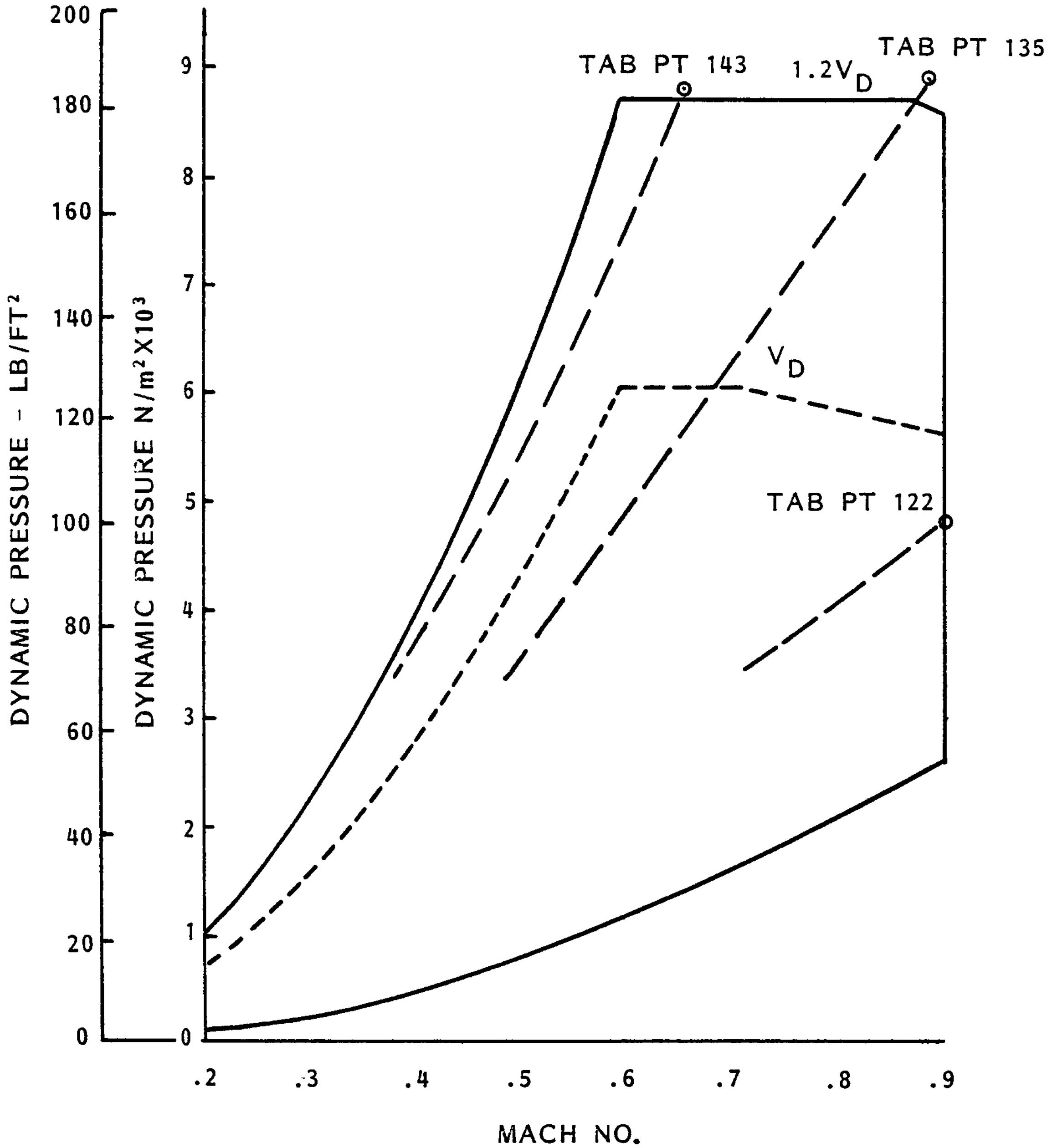

Figure 13. Test Conditions for Test Number 3

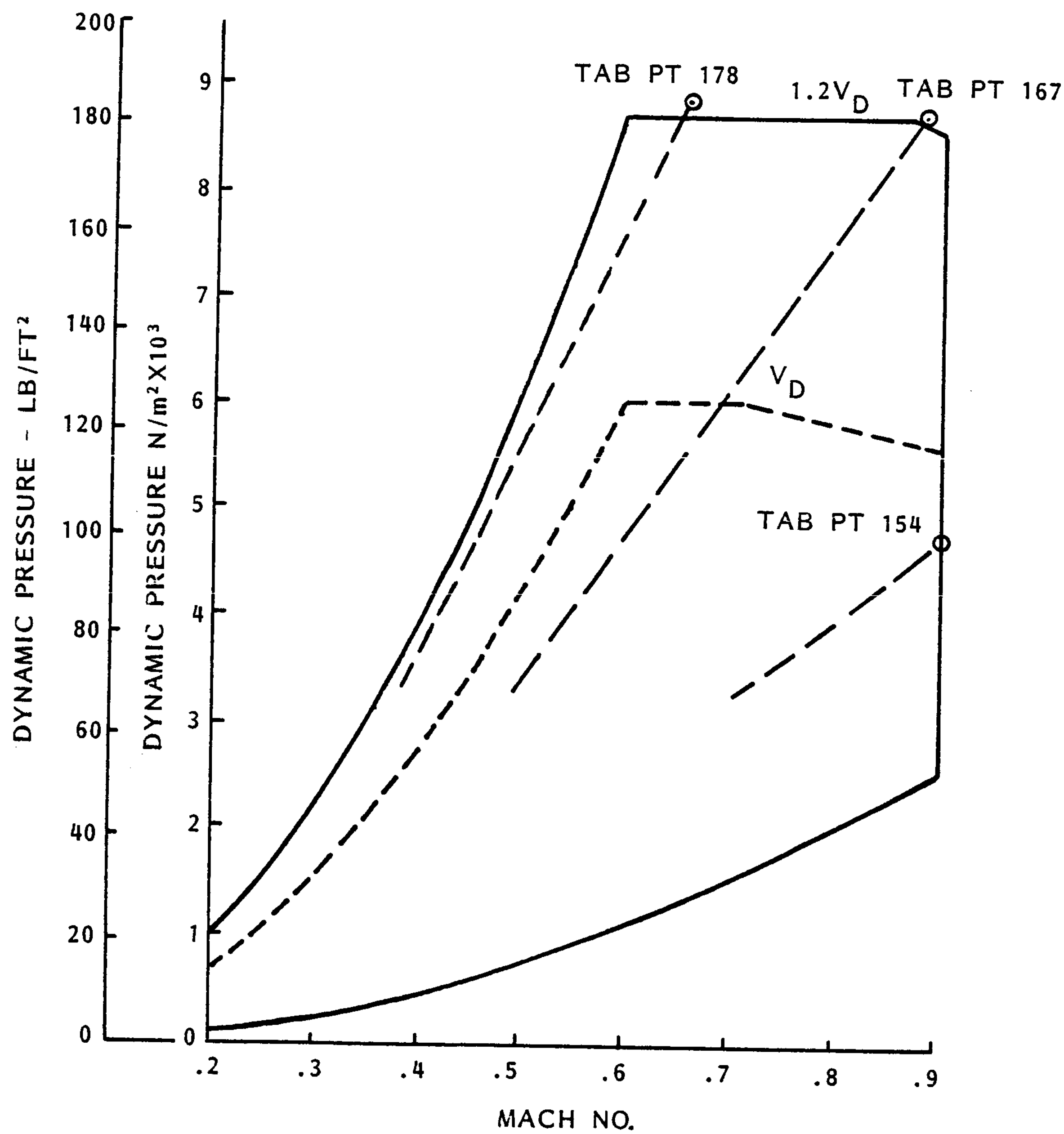

Figure 14, Test Conditions for Test Number 4

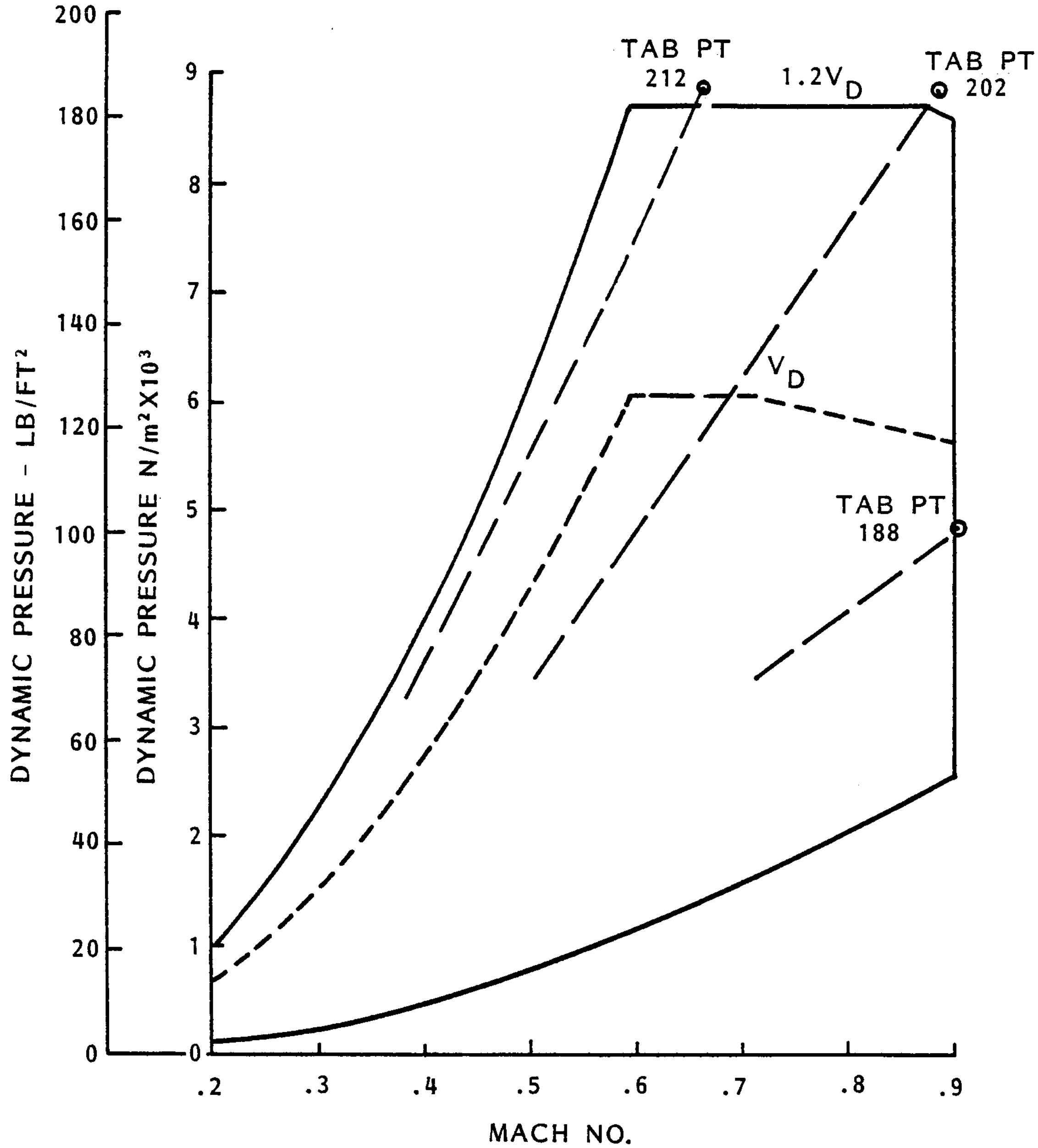

Figure 15. Test Conditions for Test Number 5

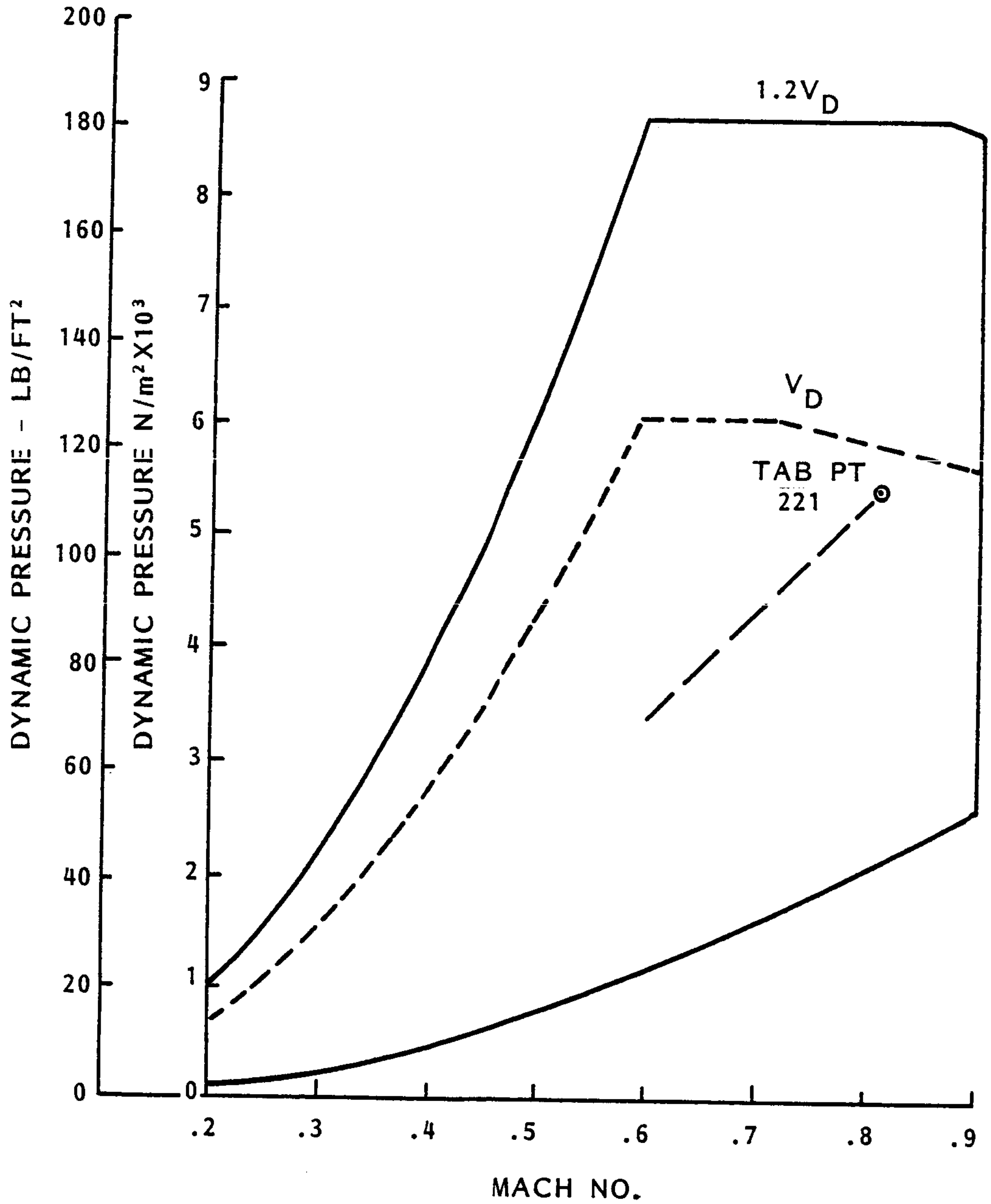

Figure 16. Test Conditions for Test Number 6

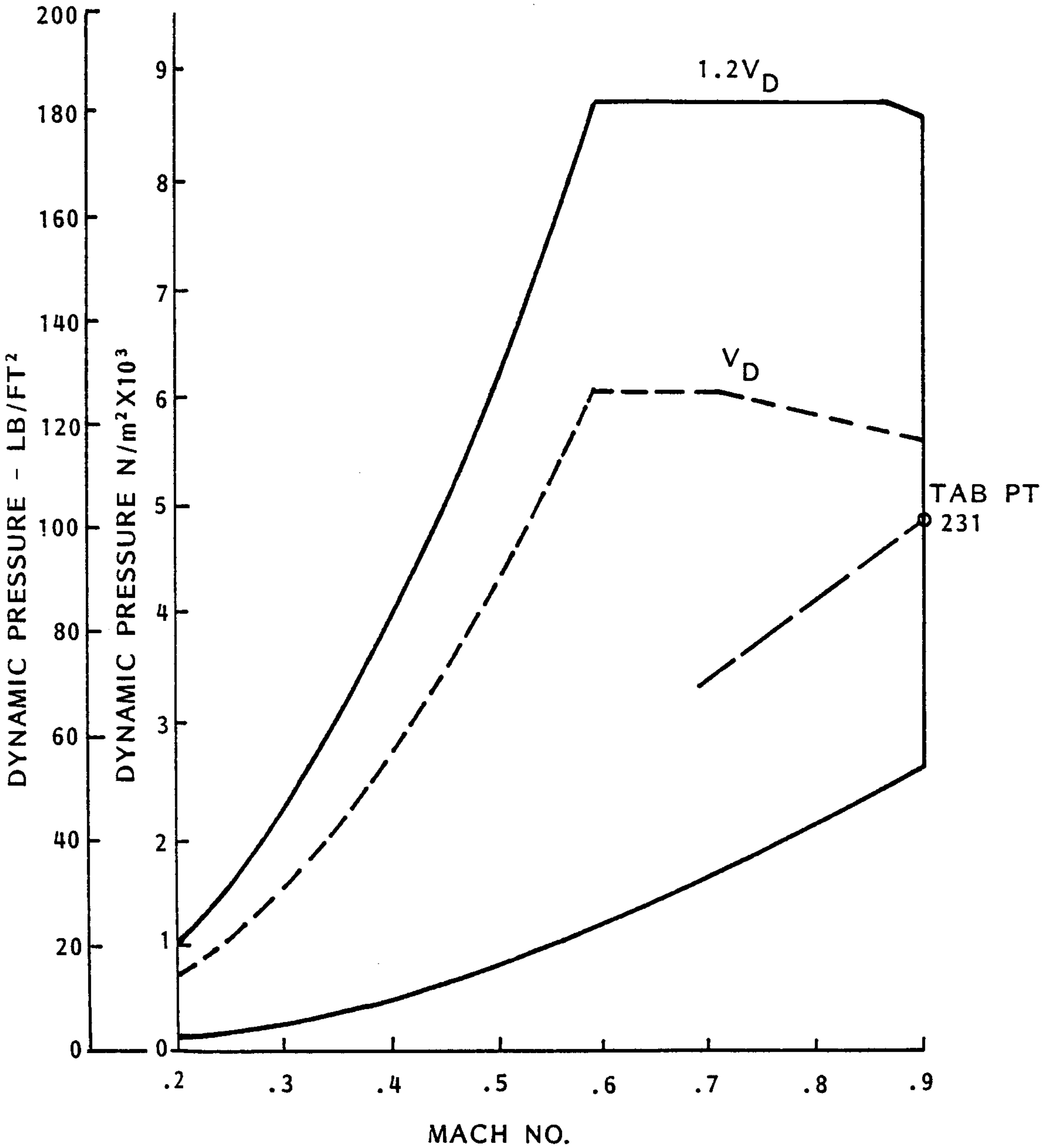

Figure 17. Test Conditions for Test Number 7

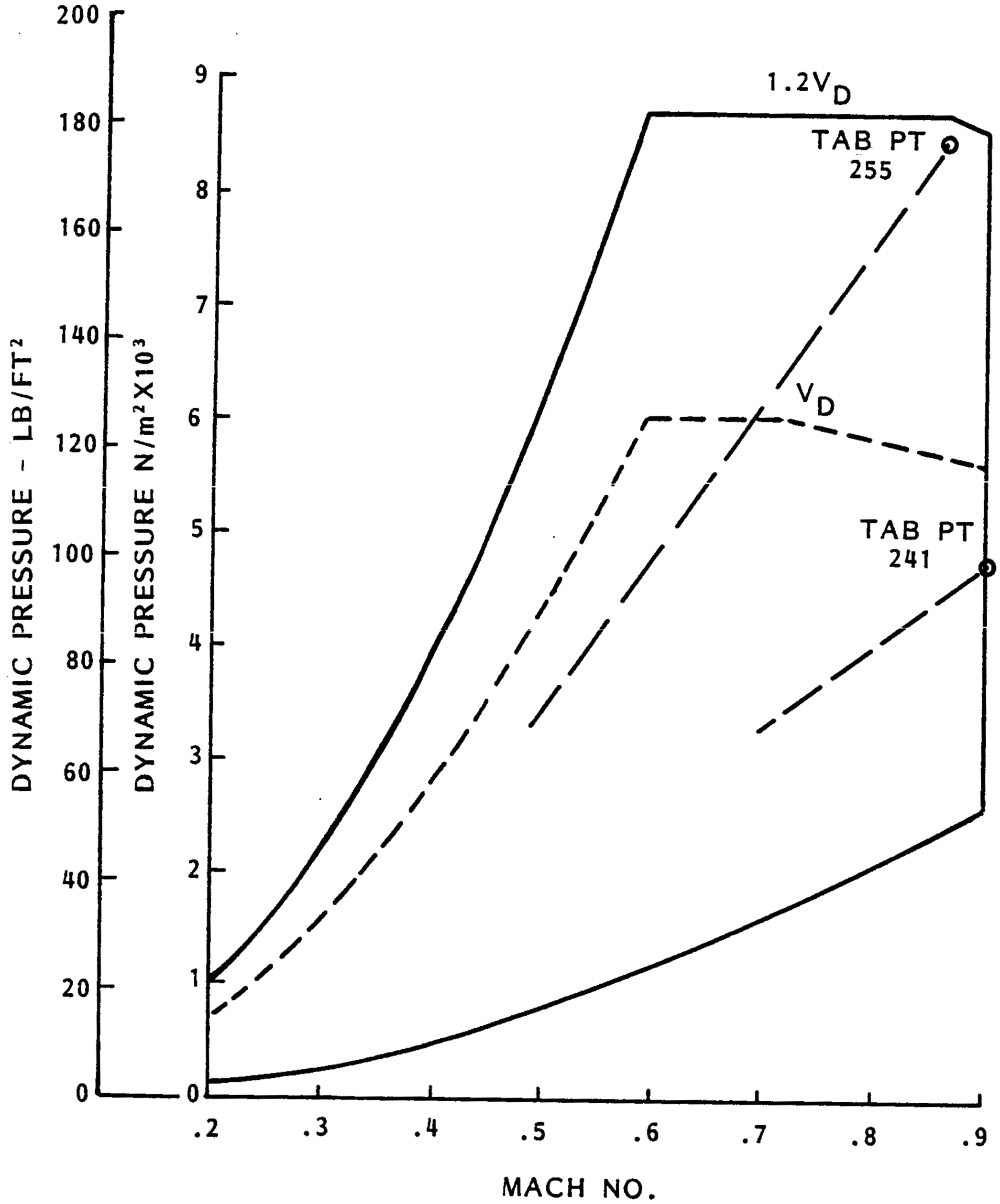

Figure 18. Test Conditions for Test Number 8

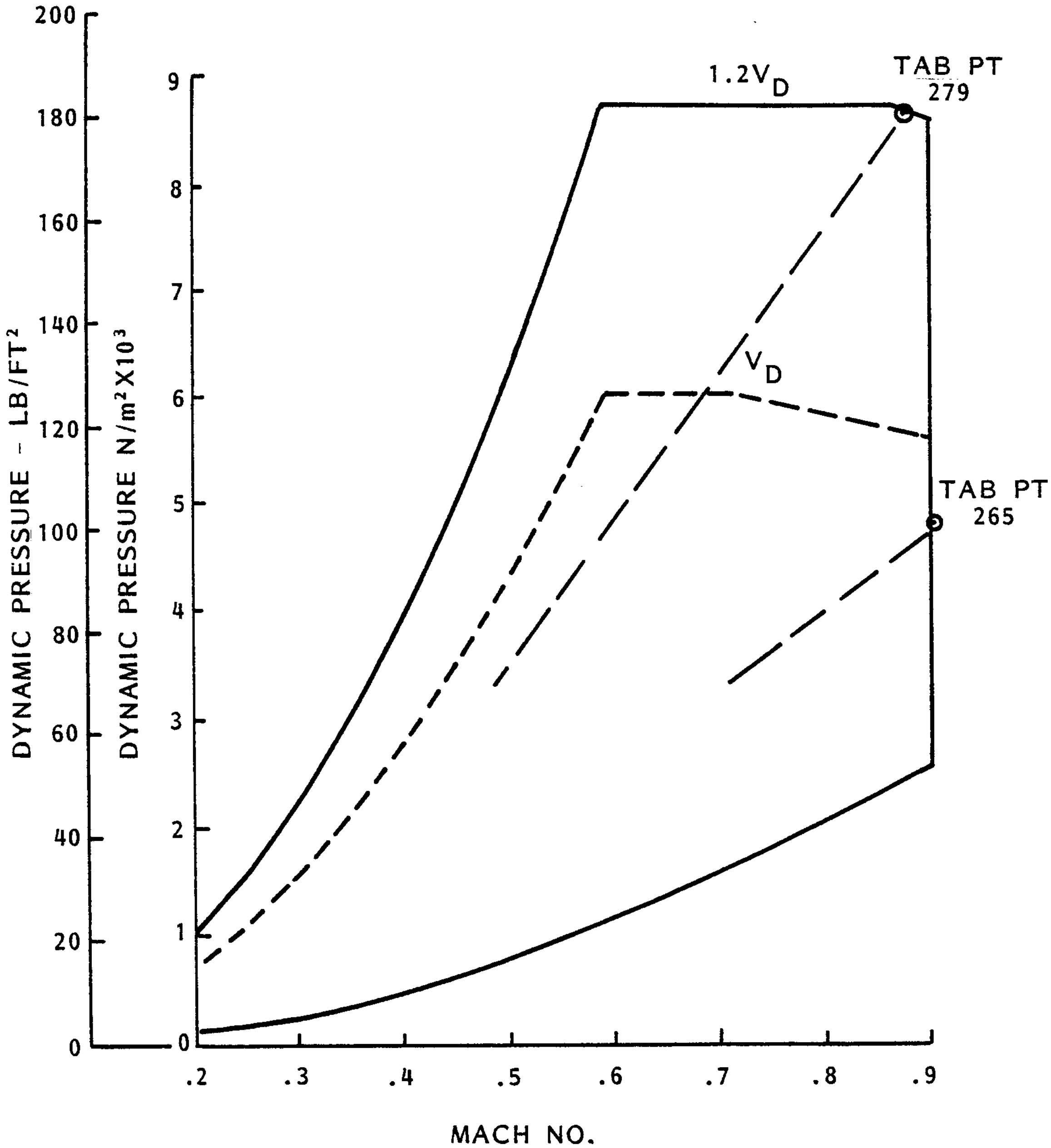

Figure 19. Test Conditions for Test Number 9

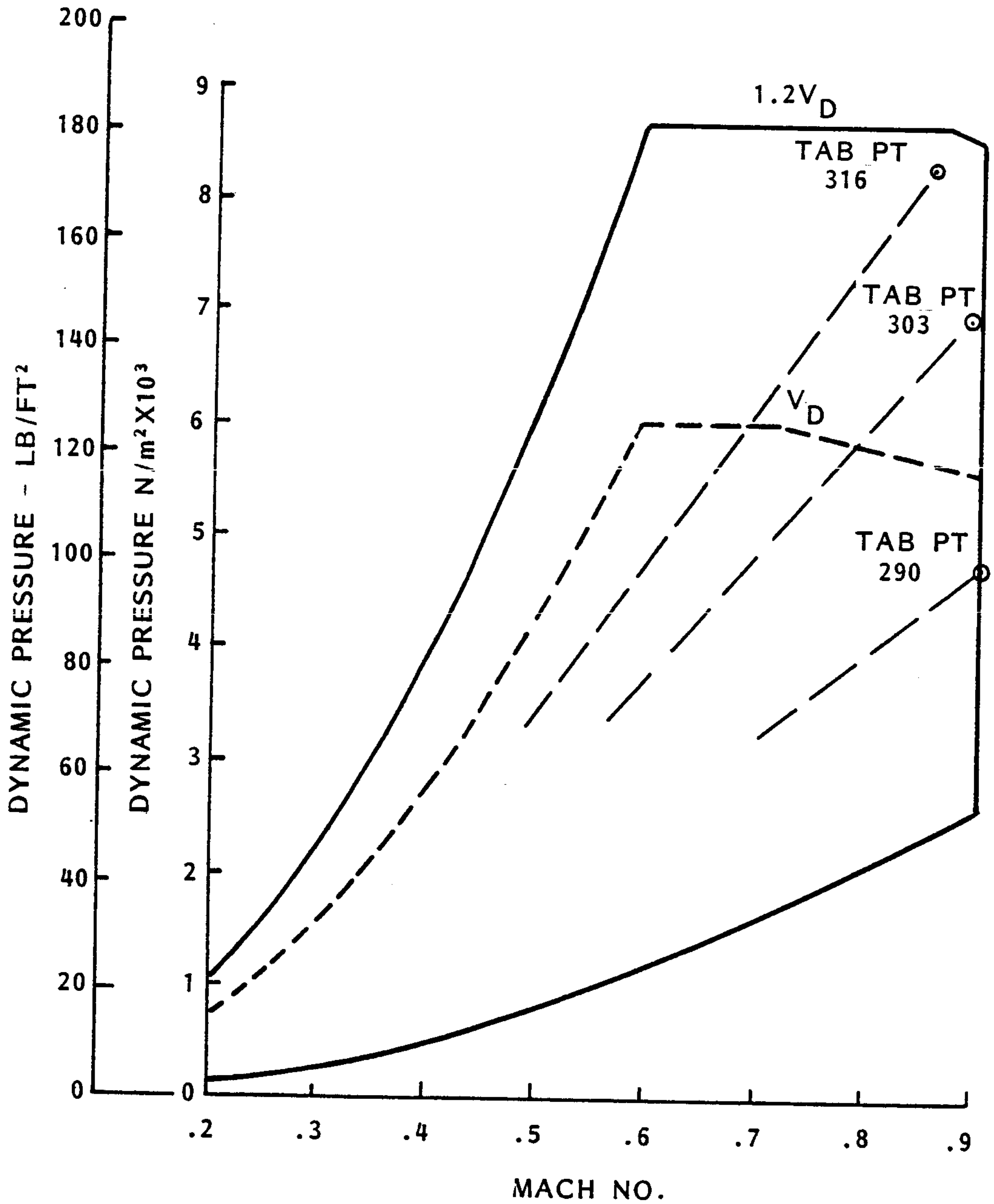

Figure 20. Test Conditions for Test Number 10

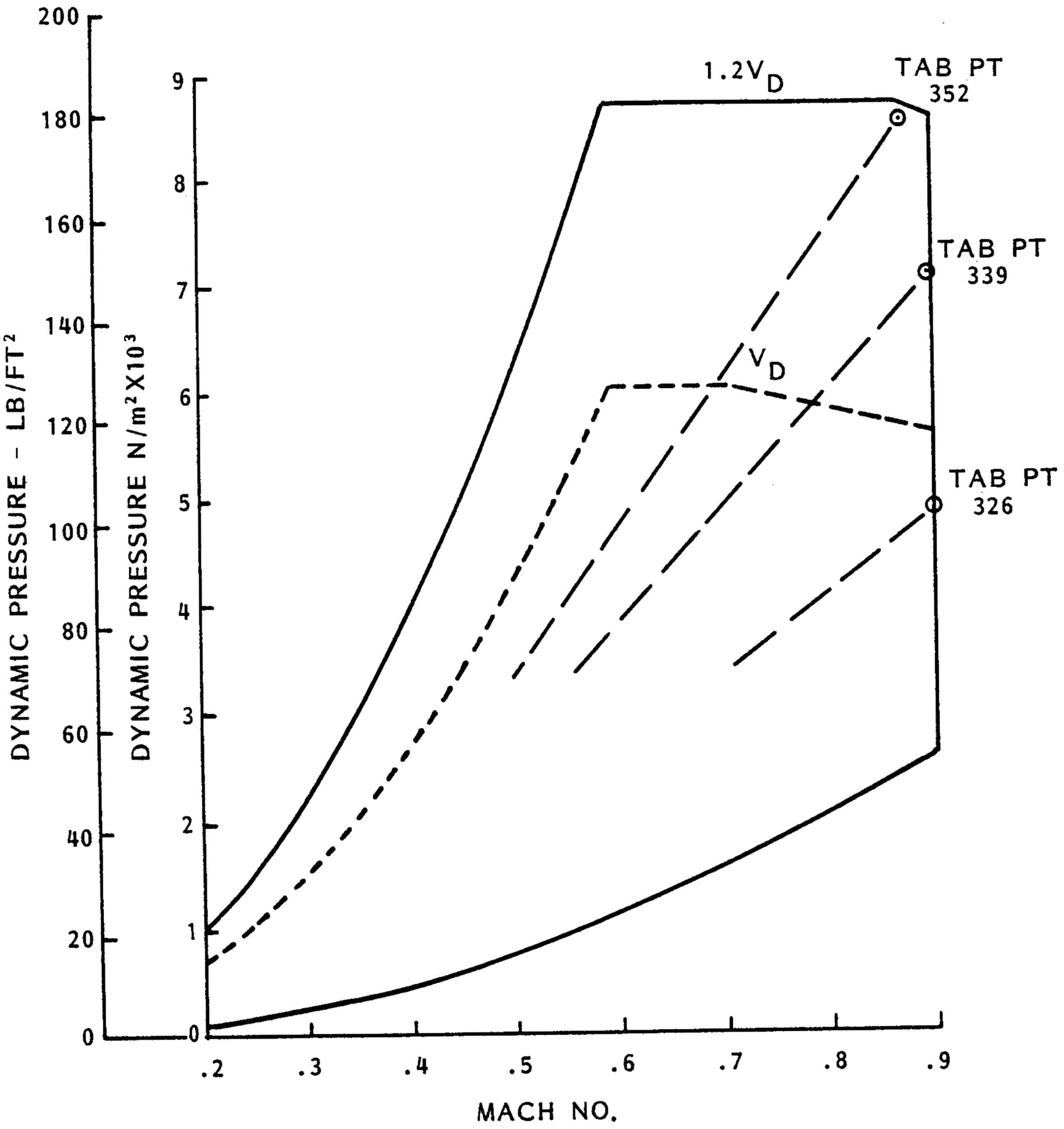

Figure 21. Test Conditions for Test Number 11

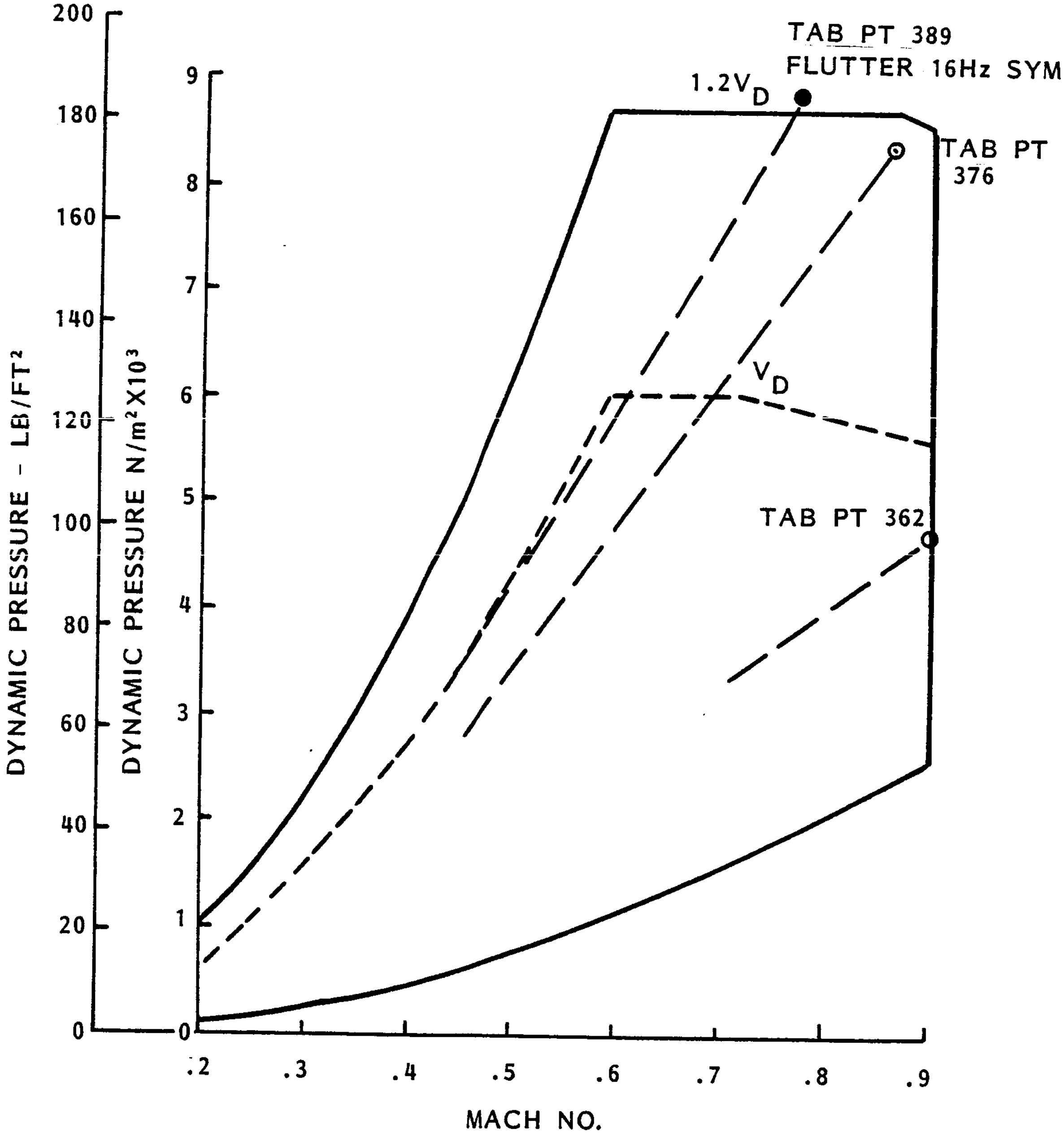

Figure 22. Test Conditions for Test Number 12

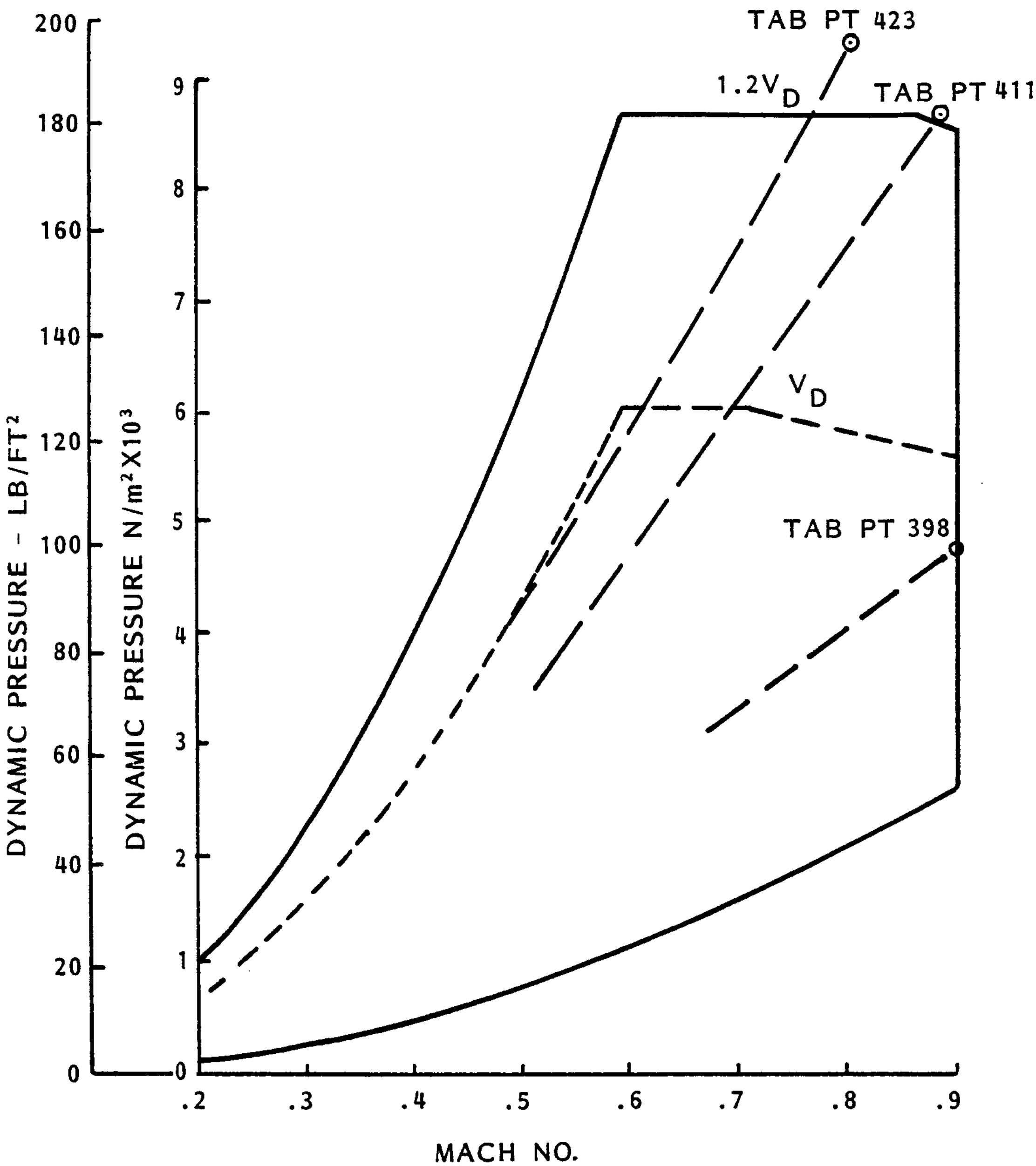

Figure 23. Test Conditions for Test Number 13

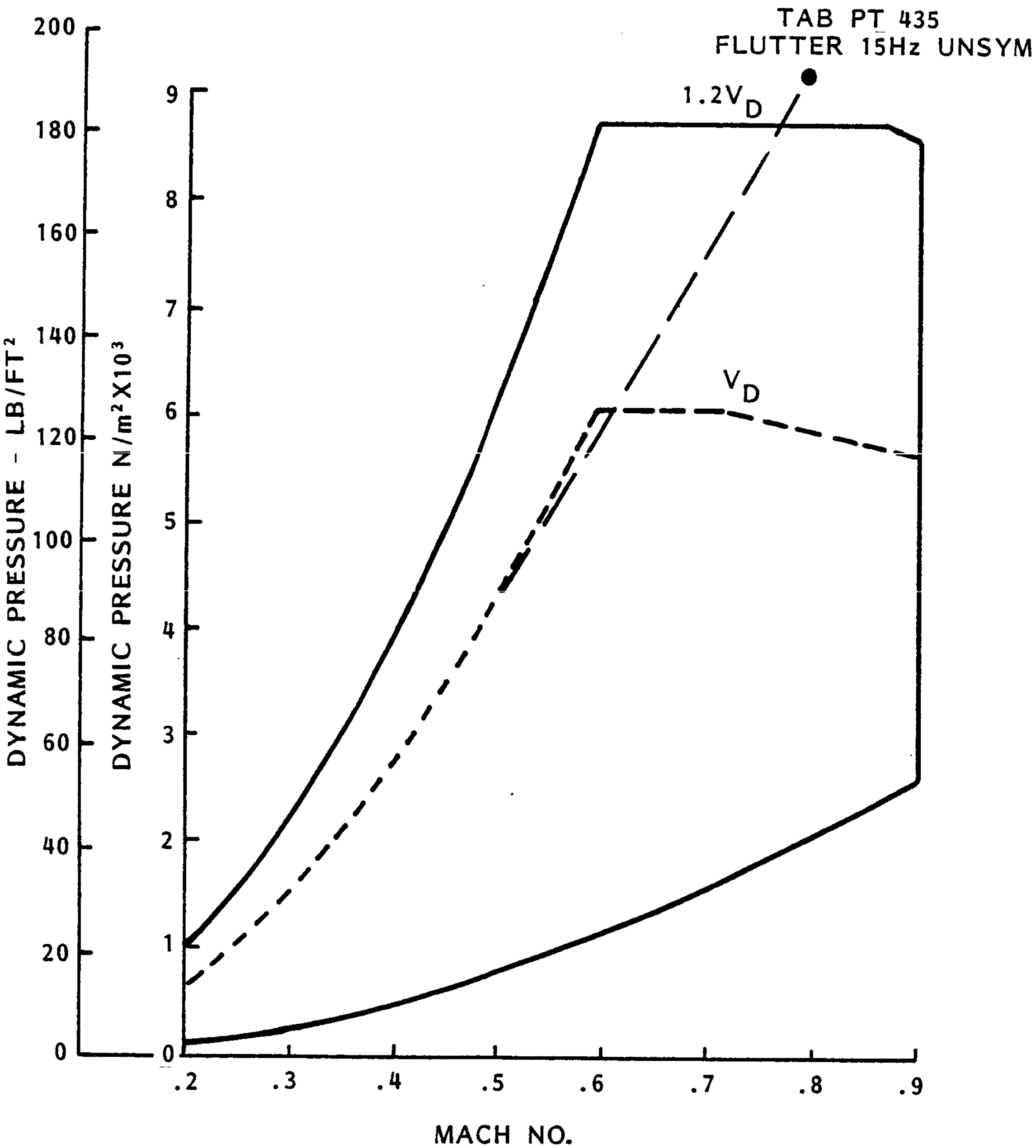

Figure 24, Test Conditions for Test Number 14

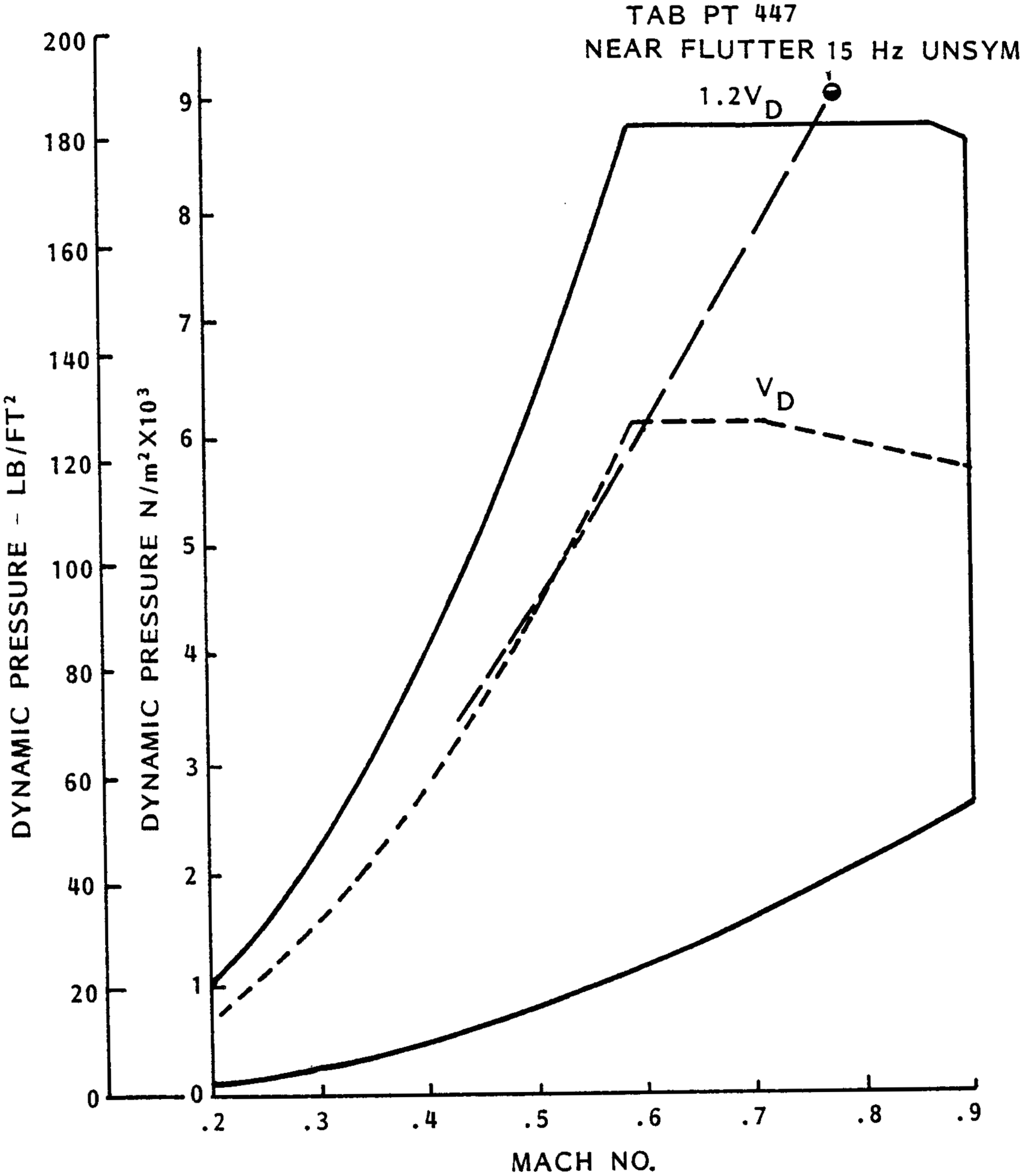

Figure 25. Test Conditions for Test Number 15

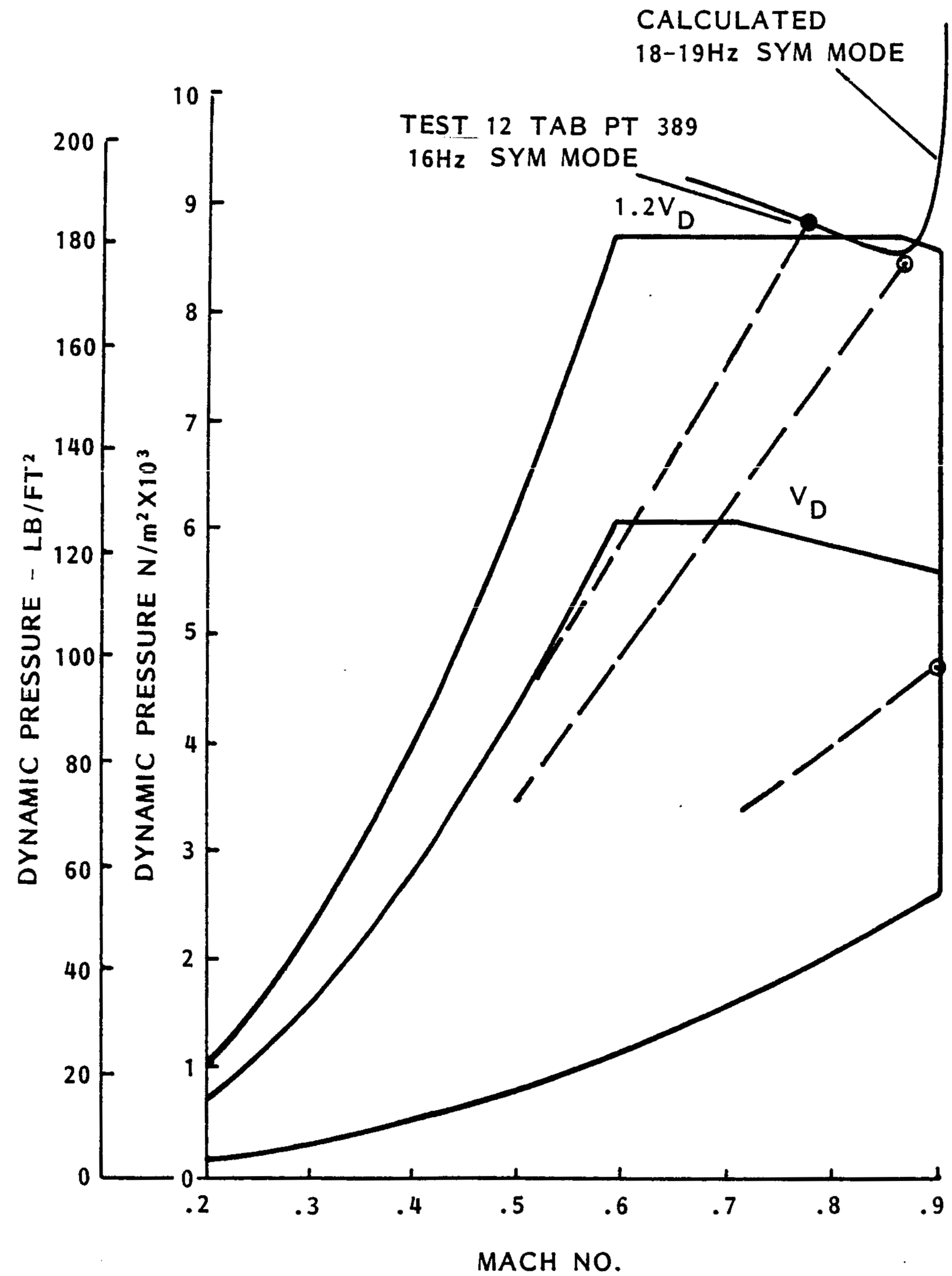

Figure 26. Calculated versus Measured Flutter Boundary - Twin Propfan Configuration with Destabilizing Booms

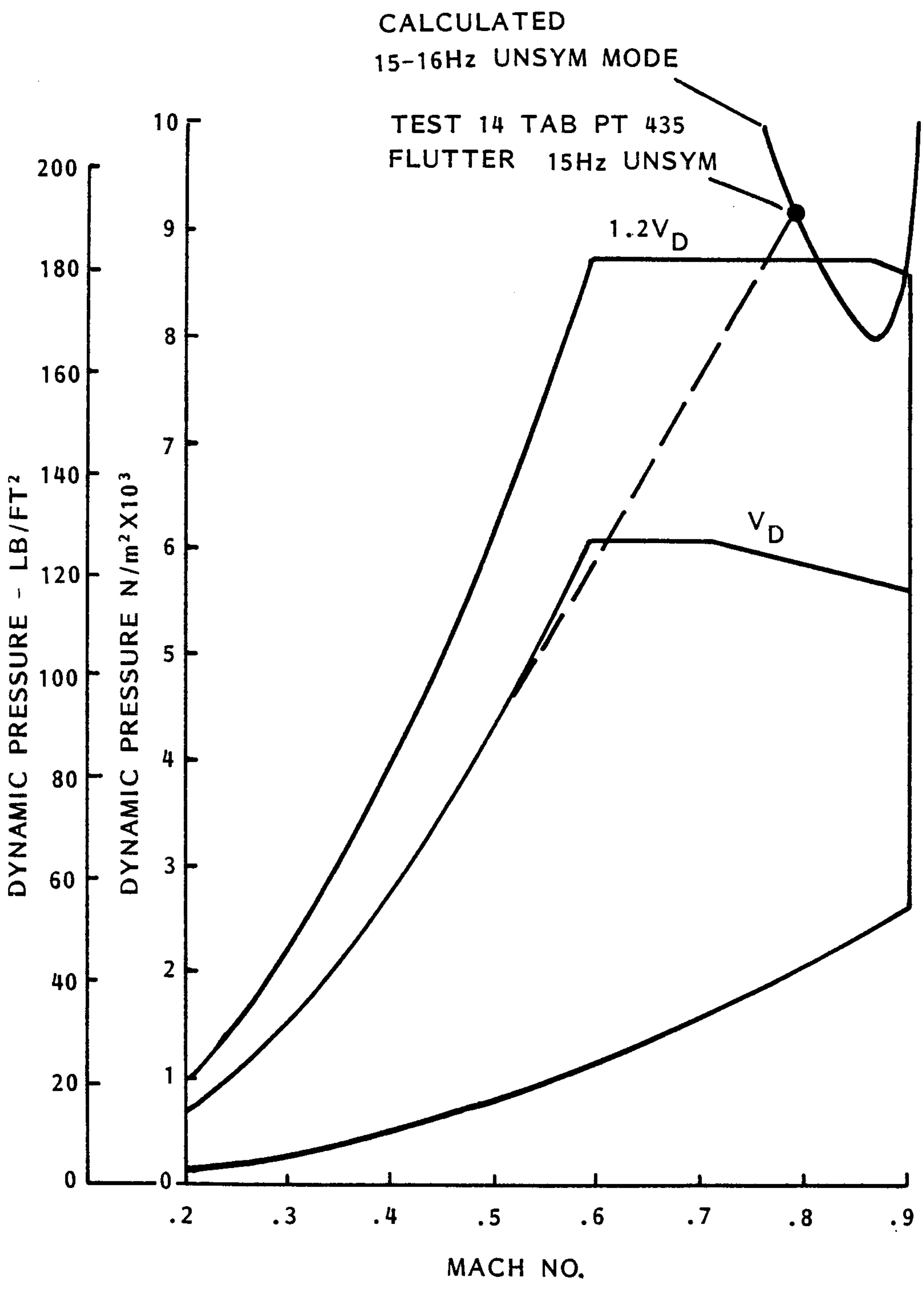

Figure 27. Calculated versus Measured Flutter Boundary - Single Propfan Configuration with Destabilizing Booms and Spinner

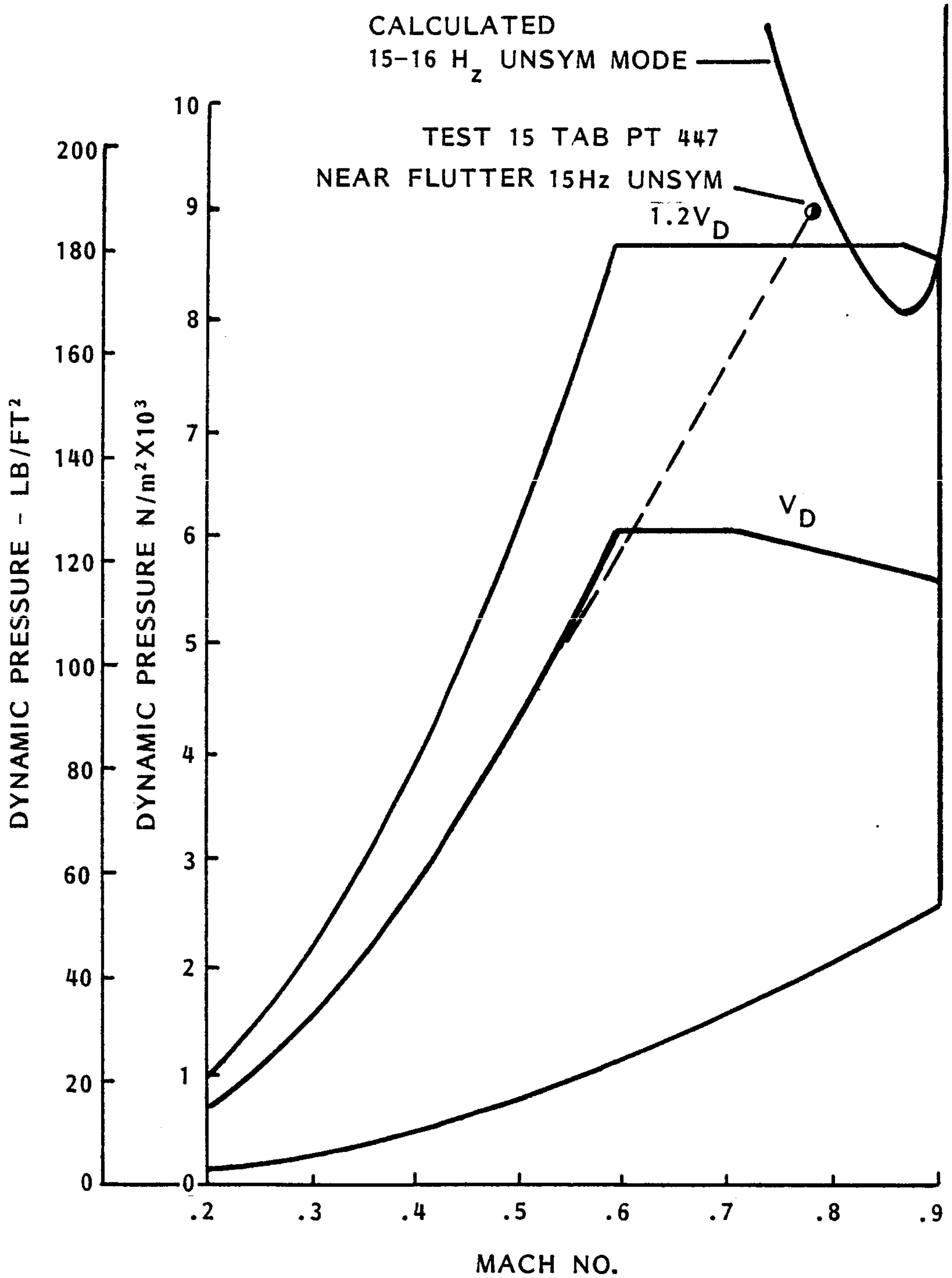

Figure 28. Calculated versus Measured Flutter Boundary - Single Propfan Configuration with Destabilizing Boom and Propfan

TABLE 1.
MODEL DESIGN SCALES

QUANTITY	SYMBOL	SCALE
Geometry	bm/ba	1/9
Mach Number	Mm/Ma	1/1
Density	$\rho m/\rho a$	1/1
Velocity	Vm/Va	1/2.02
Dynamic Pressure	qm/qa	1/4.08
Frequency	$\omega m/\omega a$	4.4554/1
Weight (Mass)	Wm/Wa	1/729
Mass Moment of Inertia	Im/Ia	1/59,049
Stiffness (Beam)	EIm/EIa, GJm/GJa	1/26,772

TABLE 2.
INSTRUMENTATION FOR BARE WING CONFIGURATION

PEN RECORDER CHANNELS

CHANNEL	SENSED QUANTITY
1	Left wing root vertical bending moment - static
2	Right wing root vertical bending moment - static
3	Left stabilizer root vertical bending moment - static
4	Left jet engine pylon vertical load - static
5	Fin root lateral bending moment - static
6	Aft fuselage (FS 1.93 [75.8]) vertical bending moment - static
7	Aft fuselage (FS 1.93 [75.8]) lateral bending moment - static
8	Fuselage nose vertical acceleration - dynamic
9	Left wing root vertical bending moment - dynamic
10	Right wing root vertical bending moment - dynamic
11	Left wing root torsion moment - dynamic
12	Right wing root torsion moment - dynamic
13	Fin root lateral bending moment - dynamic
14	Left stabilizer root vertical bending moment - dynamic
15	Aft fuselage (FS 1.93 [75.8]) torsion moment - dynamic
16	Fuselage nose lateral acceleration - dynamic

TAPE RECORDER CHANNELS

CHANNEL	SENSED QUANTITY
1	Left wing root vertical bending moment - dynamic
2	Right wing root vetical bending moment - dynamic
3	Left wing root torsion moment - dynamic
4	Right wing root torsion moment - dynamic
5	Fin root lateral bending moment - dynamic
6	Left stabilizer root vertical bending moment - dynamic
7	Aft fuselage (FS 1.93 [75.8]) torsion moment - dynamic
8	Fuselage nose lateral acceleration - dynamic
9	Fuselage nose vertical acceleration - dynamic
10	Aft fuselage (FS 1.93 [75.8]) vertical bending moment - dynamic
11	Aft fuselage (FS 1.93 [75.8]) lateral bending moment - dynamic
12	Left wing root vertical bending moment - static
13	Right wing root vertical bending moment - static
14	Time code

TABLE 3.

INSTRUMENTATION FOR SINGLE PROPFAN CONFIGURATION

PEN RECORDER CHANNELS

CHANNEL	SENSED QUANTITY
1	Left wing root vertical bending moment - static
2	Right wing root vertical bending moment - static
3	Propfan nacelle vertical bending moment - static
4	Propfan nacelle lateral bending moment - static
5	Fin root lateral bending moment - static
6	Aft fuselage (FS 1.93 [75.8]) vertical bending moment - static
7	Aft fuselage (FS 1.93 [75.8]) lateral bending moment - static
8	Left jet engine pylon vertical bending moment - static
9	Left wing root vertical bending moment - dynamic
10	Right wing root vertical bending moment - dynamic
11	Left wing root torsion moment - dynamic
12	Right wing root torsion moment - dynamic
13	Fin root lateral bending moment - dynamic
14	Aft fuselage (FS 1.93 [75.8]) vertical bending moment - dynamic
15	Propfan gearbox lateral acceleration - dynamic
16	Propfan gearbox vertical acceleration - dynamic

TAPE RECORDER CHANNELS

CHANNEL	SENSED QUANTITY
1	Left wing root vertical bending moment - dynamic
2	Right wing root vertical bending moment - dynamic
3	Left wing root torsion moment - dynamic
4	Right wing root torsion moment - dynamic
5	Fin root lateral bending moment - dynamic
6	Propfan rotation speed
7	Aft fuselage (FS 1.93 [75.8]) torsion moment - dynamic
8	Propfan nacelle vertical bending moment - dynamic
9	Propfan nacelle lateral bending moment - dynamic
10	Aft fuselage (FS 1.93 [75.8]) vertical bending moment - dynamic
11	Aft fuselage (FS 1.93 [75.8]) lateral bending moment - dynamic
12	Left wing root vertical bending moment - static
13	Right wing root vertical bending moment - static
14	Time code

TABLE 4.
INSTRUMENTATION FOR TWIN PROPFAN CONFIGURATION

PEN RECORDER CHANNELS

CHANNEL	SENSED QUANTITY
1	Left wing root vertical bending moment - static
2	Right wing root vertical bending moment - static
3	Left propfan nacelle vertical bending moment - static
4	Left propfan nacelle lateral bending moment - static
5	Left wing root torsion moment - static
6	Aft fuselage (FS 1.93 [75.8]) vertical bending moment static
7	Aft fuselage (FS 1.93 [75.8]) lateral bending moment - static
8	Left jet engine pylon vertical bending moment - static
9	Left wing root vertical bending moment - dynamic
10	Right wing root vertical bending moment - dynamic
11	Left wing root torsion moment - dynamic
12	Right wing root torsion moment - dynamic
13	Aft fuselage (FS 1.93 [75.8]) lateral bending moment - dynamic
14	Aft fuselage (FS 1.93 [75.8]) vertical bending moment - dynamic
15	Right propfan gearbox vertical acceleration - dynamic
16	Left propfan gearbox vertical acceleration - dynamic

TAPE RECORDER CHANNELS

CHANNEL	SENSED QUANTITY
1	Left wing root vertical bending - dynamic
2	Right wing root vertical bending - dynamic
3	Left wing root torsion moment - dynamic
4	Right wing root torsion moment - dynamic
5	Right propfan rotation speed
6	Left propfan rotation speed
7	Aft fuselage (FS 1.93 [75.8]) torsion
8	Left propfan nacelle vertical bending - dynamic
9	Left propfan nacelle lateral bending - dynamic
10	Aft fuselage (FS 1.93 [75.8]) vertical bending moment - dynamic
11	Aft fuselage (FS 1.93 [75.8]) lateral bending moment - dynamic
12	Left propfan gearbox vertical acceleration - dynamic
13	Right propfan gearbox vertical acceleration - dynamic
14	Time code

TABLE 5.

SUMMARY OF TEST CONFIGURATIONS

TEST NO.	RUN NOS.	TAB PT NOS.	WING CONFIG	FUEL CONDITION	PROP ROTATION		WING BOOMS		COMMENTS
					LEFT	RIGHT	LEFT	RIGHT	
1	1-5	1-70	Bare	Minimum(4)	----	----	Balance	Balance	No flutter. Max q = 9340 N/m² (195 psf)
2	6-8	71-106	Single PF	Minimum	Spinner	----	Flutter	Balance	No flutter. Max q = 9240 N/m² (193 psf)
3	9-11	107-146	Single PF	Minimum	CCW	----	Flutter	Balance	No flutter. Max q = 8950 N/m² (187 psf)
4	12	147-181	Single PF	Intermed(5)	CCW	----	Flutter	Balance	No flutter. Max q = 8950 N/m² (187 psf)
5	13	182-214	Single PF	Intermed	Spinner	----	Flutter	Balance	No flutter. Max q = 8880 N/m² (185 psf)
6	14	215-222	Single PF	Intermed	CCW	----	Flutter	Balance	Engine-gearbox connection removed. No flutter. Engine mount failure at q = 5410 N/m² (113 psf)
7	15	223-233	Twin PF	Minimum(4)	CCW	CCW	Flutter	Flutter	No flutter. Excessive left roll Maximum q = 4980 N/m² (104 psf)
8	16	234-257	Twin PF	Minimum	Spinner	Spinner	Flutter	Flutter	No flutter. max q - 8330 N/m² (174 psf)
9	17	258-281	Twin PF	Minimum	Spinner	Spinner	None	None	No flutter. Max q = 8620 (180 psf)
10	18	284-318	Twin PF	Minimum	Spinner	Spinner	Destab(1)	Destab(1)	No flutter. Large 18 Hz response. Max q = 8330 N/m² (174 psf)
11	19	319-354	Twin PF	Minimum	Spinner	Spinner	Destab(2)	Destab(2)	No flutter. Moderate 18 Hz response Max q - 8523 N/m² (178 psf)
12	20	355-391	Twin PF	Minimum	Spinner	Spinner	Destab(3)	Destab(3)	Flutter at M = .77 , q = 8860 N/m² (185 psf) 16 Hz symmetric mode
13	21	392-425	Single PF	Minimum	CCW	----	None	Balance	No flutter. Max q = 9390 N/m² (196 psf)
14	22	426-437	Single PF	Minimum	Spinner	----	Destab(3)	Balance	Flutter at M = .79, q = 9190 N/m² (192 psf) 14.9 Hz unsymmetric cmode
15	23	438-449	Single PF	Minimum	CCW	----	Destab(3)	Balance	Near flutter at M = .77, q = 9000 N/m² (188 psf) 14.9 Hz unsymmetric mode, 6540 RPM

(1) Reversed flutter booms (2) Increased weight reversed flutter booms (3) Large destabilizing booms (4) Approximately 12½% capacity fuel (1135 kg or 2500 lb) built into wing sections (5) Approximately 4535 kg (10,000 lb)

TABLE 6.
TEST CONDITIONS FOR SELECTED TAB POINTS

TEST	TAB PT	M	q(N/M²)	q(lb/ft²)	V(m/s)	V(ft/sec)	ρ(kg/m³)	ρ(sl/ft³x10³)	RNx10^{-6})	REMARKS
1	6	.898	2408	50.3	135.0	443.0	.262	0.509	.894	No flutter
	37	.850	4328	90.4	128.9	422.8	.517	1.004	1.658	No flutter, Excess. left roll
	69	.871	9327	194.8	132.6	435.1	1.052	2.042	3.504	No flutter
2	79	.899	4869	101.7	138.2	453.5	.508	0.986	1.734	No flutter
	93	.896	9250	193.2	135.8	445.7	.995	1.931	3.422	No flutter
	104	.651	8767	183.1	99.5	326.6	1.750	3.397	4.343	No flutter
3	122	,901	4855	101.4	135.8	445.4	.523	1.016	1.821	No flutter. Prop RPM = 7440
	135	.879	8934	186.6	133.2	437.1	.999	1.939	3.372	No flutter. Prop RPM = 7200
	143	.656	8829	184.4	100.1	328.4	1.744	3.384	4.362	No flutter. Prop RPM = 5700
4	154	.902	4769	99.6	136.0	446.3	.512	0.994	1.784	No flutter. Prop RPM = 7380
	167	.880	8820	184.2	133.0	436.3	.989	1.919	3.340	No flutter. Prop RPM = 7200
	178	.654	8944	186.8	99.5	326.5	1.785	3.465	4.455	No flutter. Prop RPM - 5700
5	188	.904	4850	101.3	135.7	445.1	.522	1.014	1.784	No flutter
	202	.886	8891	185.7	133.6	438.2	.984	1.910	3.273	No flutter
	212	.660	8920	186.3	100.2	328.8	1.743	3.382	4.275	No flutter
6	221	.810	5425	113.3	122.0	400.3	.721	1.400	2.200	Engine mt.failure. Prop RPM = 6780
7	231	.904	4960	103.6	135.5	444.6	.535	1.039	1.827	Excessive left roll. Prop RPM=7380
8	241	.878	4496	93.9	132.0	433.2	.512	0.993	1.691	No flutter
	255	.866	8484	177.2	130.7	428.7	.981	1.904	3.181	No flutter
9	263	.856	4453	93.0	128.5	421.6	.534	1.037	1.724	No flutter
	279	.873	8638	180.4	131.7	432.2	.983	1.908	3.220	No flutter
10	290	.904	4783	99.9	136.0	446.2	.513	0.996	1.749	No flutter
	303	.891	7014	146.5	134.3	440.5	.770	1.494	2.580	No flutter
	316	.854	8331	174.0	129.0	423.2	.989	1.920	3.165	No flutter. Large 18 Hz response

TABLE 6. (CONTINUED)

TEST	TAB PT	M	q(N/m²)	q(lb/ft²)	V(m/s)	V(ft/sec)	ρ(kg/m³)	ρ(sl/ft³x10³)	RNx10^{-6}	REMARKS
11	326	.900	4884	102.0	135.7	445.3	.525	1.021	1.789	No flutter
	339	.896	7101	148.3	135.6	444.8	.765	1.484	2.573	No flutter
	352	.870	8542	178.4	131.9	432.7	.971	1.884	3.167	No flutter. Moderate 18 Hz response
12	362	.898	4711	98.4	135.3	443.8	.511	0.991	1.732	No flutter
	376	.864	8470	176.9	130.8	429.1	.978	1.898	3.175	No flutter. Strong 17 Hz response
	389	.770	8858	185.0	116.8	383.2	1.279	2.483	3.684	Flutter. 16 Hz sym. mode
13	398	.900	4764	99.5	135.6	445.0	.997	0.997	1.741	No flutter. Prop RPM = 7440
	411	.882	8705	181.8	134.0	439.7	1.955	1.859	3.174	No flutter. Prop RPM = 7200
	423	.801	9385	196.0	122.0	400.4	1.243	2.412	3.725	No flutter. Prop RPM = 6720
14	435	.787	9174	191.6	121.5	398.5	1.227	2.382	3.635	Flutter. 15 Hz unsym. mode
15	447	.774	8997	187.9	57.3	187.9	1.248	2.422	3.644	Near flutter. 15 Hz unsym. mode Prop RPM = 6540

TABLE 7.
COMPARISON OF CALCULATED AND MEASURED NORMAL MODE FREQUENCIES – TWIN PROPFAN CONFIGURATION

SYMMETRIC MODES

Calculated Freq. (Hz)	Measured Freq. (Hz)	Calc/Meas. Freq.	Mode Description
14.04	14.01	1.00	Wing 1st vertical bending
21.50	21.48	1.00	Wing 1st torsion, propfan nacelle vertical bending
22.96	22.70	1.01	Propfan nacelle lateral bending
28.88	29.38	0.98	Fuselage vert. bend., jet engine vertical
30.47	30.50	1.00	Propfan powerplant yawing
31.34	31.50	0.99	Propfan powerplant pitching
36.99	36.28	1.02	Jet engines vertical

ANTISYMMETRIC MODES

Calculated Freq. (Hz)	Measured Freq. (Hz)	Calc/Meas. Freq.	Mode Description
14.94	15.10	.99	Aft fuselage lateral bending, torsion
17.65	18.09	.98	Wing 1st vertical bending, aft fuselage lateral bending
22.42	22.70	.99	Propfan nacelle lateral bending
24.57	24.41	1.01	Jet engine vertical
28.82			Propfan powerplant pitching, jet engine vertical
30.31	30.64	.99	Propfan powerplant yawing
32.11			Aft fuselage torsion, fin torsion
34.35	33.85	1.01	Fin torsion, fwd. fuselage lateral bending
39.03			Propfan powerplant pitching, wind 2nd torsion
39.20	40.50	.97	Fwd. fuselage lateral bend., fin lateral bending

TABLE 8.

COMPARISON OF CALCULATED AND MEASURED NORMAL MODE FREQUENCIES-SINGLE PROPFAN CONFIGURATION

CALCULATED FREQ. (Hz)	MEASURED FREQ. (Hz)	CALC/MEAS. FREQ.	MODE DESCRIPTION
8.40	8.38	1.00	Right Wing 1st Vertical Bending
14.36	14.41	1.00	Aft Fuselage Lateral Bending, Torsion, Left Wing Vertical Bending
17.33	17.50	.99	Left Wing 1st Vertical Bending, Right Wing 1st Torsion
19.90	19.75	1.01	Right Wing Torsion, Left Wing Torsion
22.15	22.70	.98	Propfan Nacelle Lateral, Right Wing Fore and Aft Bending
23.95	--	--	Propfan Nacelle Lateral, Left Wing 1st Torsion
24.50	24.17	1.01	Right Wing Fore-and-Aft Bending, Propfan Nacelle Lateral
28.24	29.22	.97	Fuselage Vertical Bending, Jet Engine Pylon Vertical Bending
29.47	31.40	.94	Propfan Powerplant Pitching, Jet Engine Pylon Vertical
30.30	30.50	.99	Propfan Powerplant Yawing
33.14	--	--	Fin Torsion, Jet Engine Vertical
34.79	36.52	.95	Right Jet Engine Vertical, Aft Fuselage Vertical

APPENDIX - MODEL BASIC DATA

Model geometric, mass, stiffness, and resonance data are presented in Figures 29 through 44 and Tables 9 through 22. The model "actual" data were determined almost entirely by tests. The "desired" data represent the aircraft preliminary design as of June 1985. The desired wing mass data include $12\frac{1}{2}$ percent of the Gulfstream II capacity fuel distribution because the model wings could not be made light enough to simulate the empty aircraft wings. In most cases, the "actual" data agree very closely with the desired characteristics. Some of the actual spar stiffness data differ significantly from the desired data over short distances. However, the net effect of these local differences on the model normal modes is much less significant because of the effective "integrations" involved.

Measured normal modes for the bare wing, twin propfan, and single propfan configurations are presented in Figures 42, 43, and 44, respectively. The resonant frequency and node (zero motion) lines for each mode are shown on an isometric view of the model.

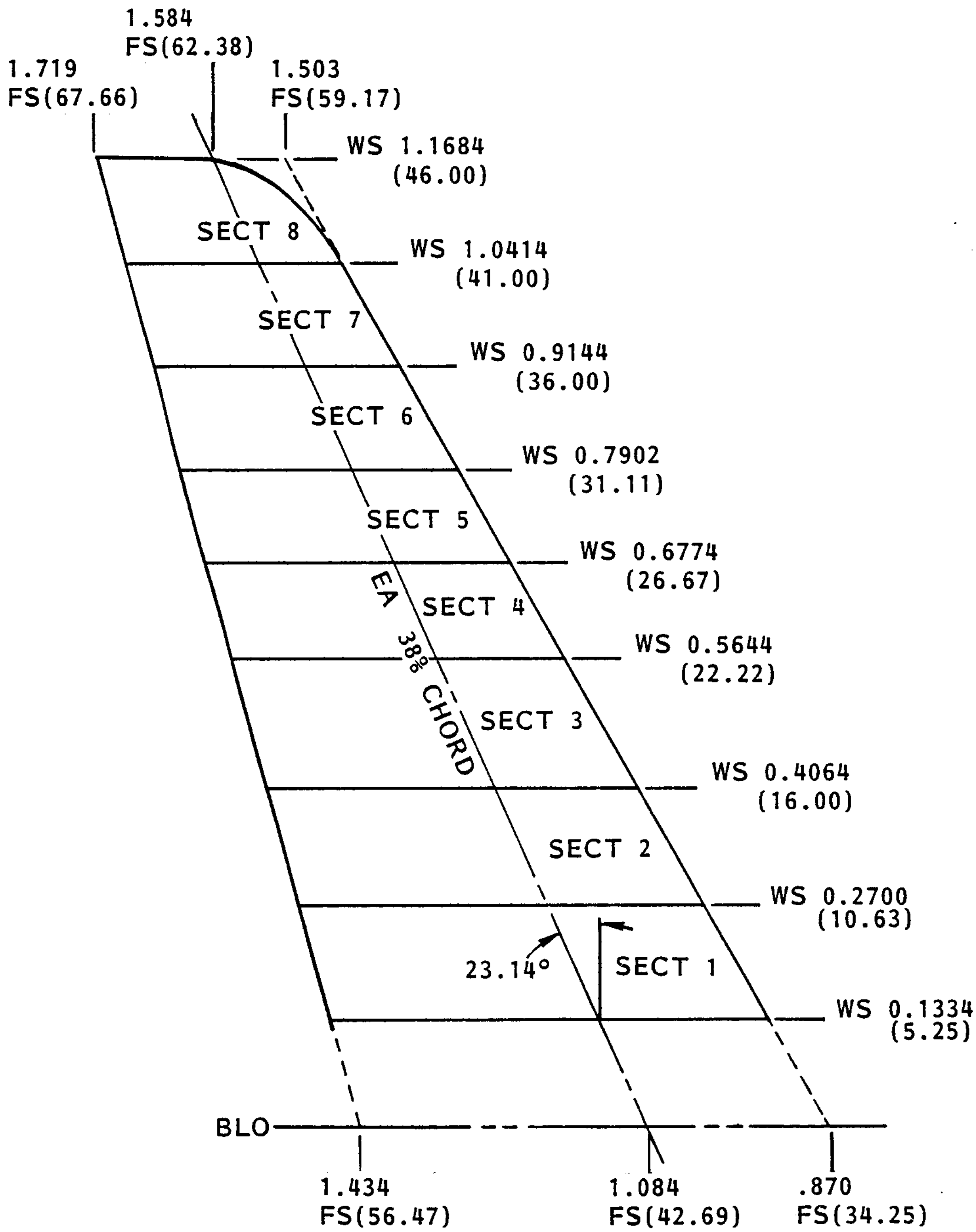

Figure 29. Wing Geometry

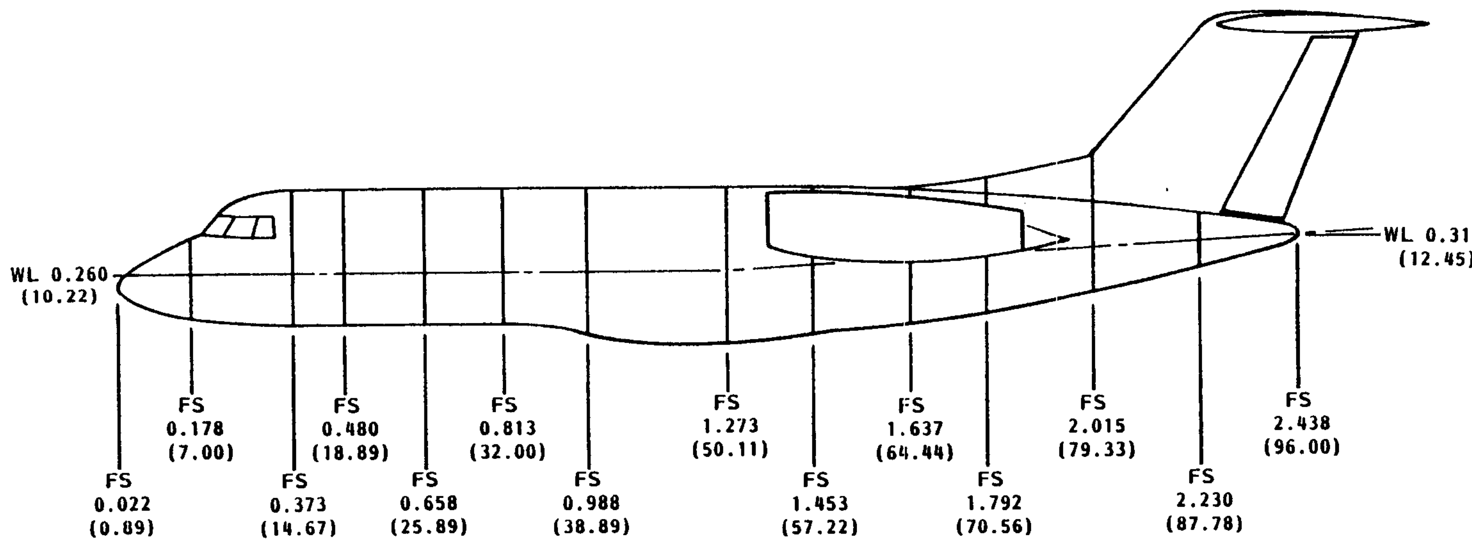

Figure 30. Fuselage Geometry

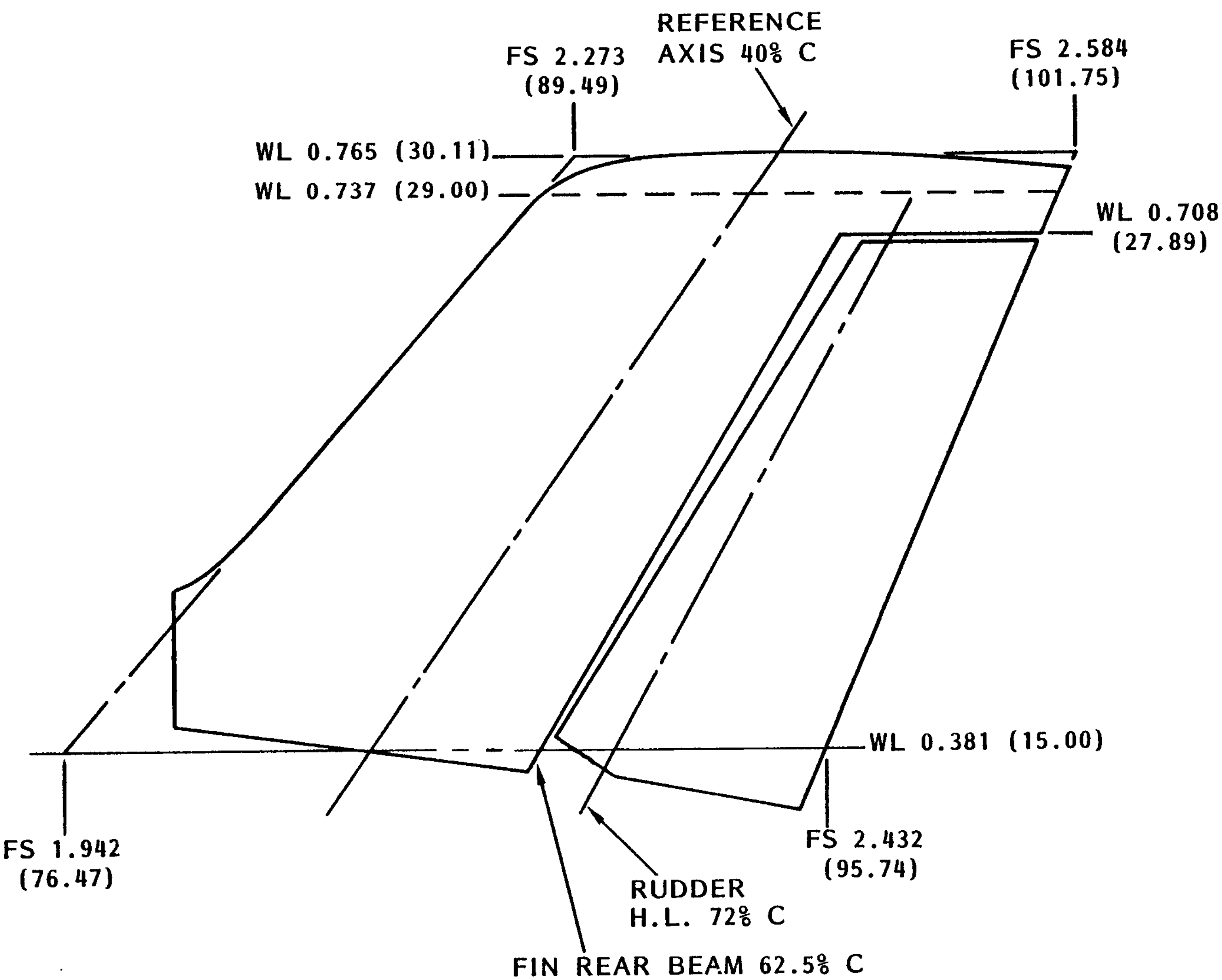

Figure 31. Vertical Stabilizer Geometry

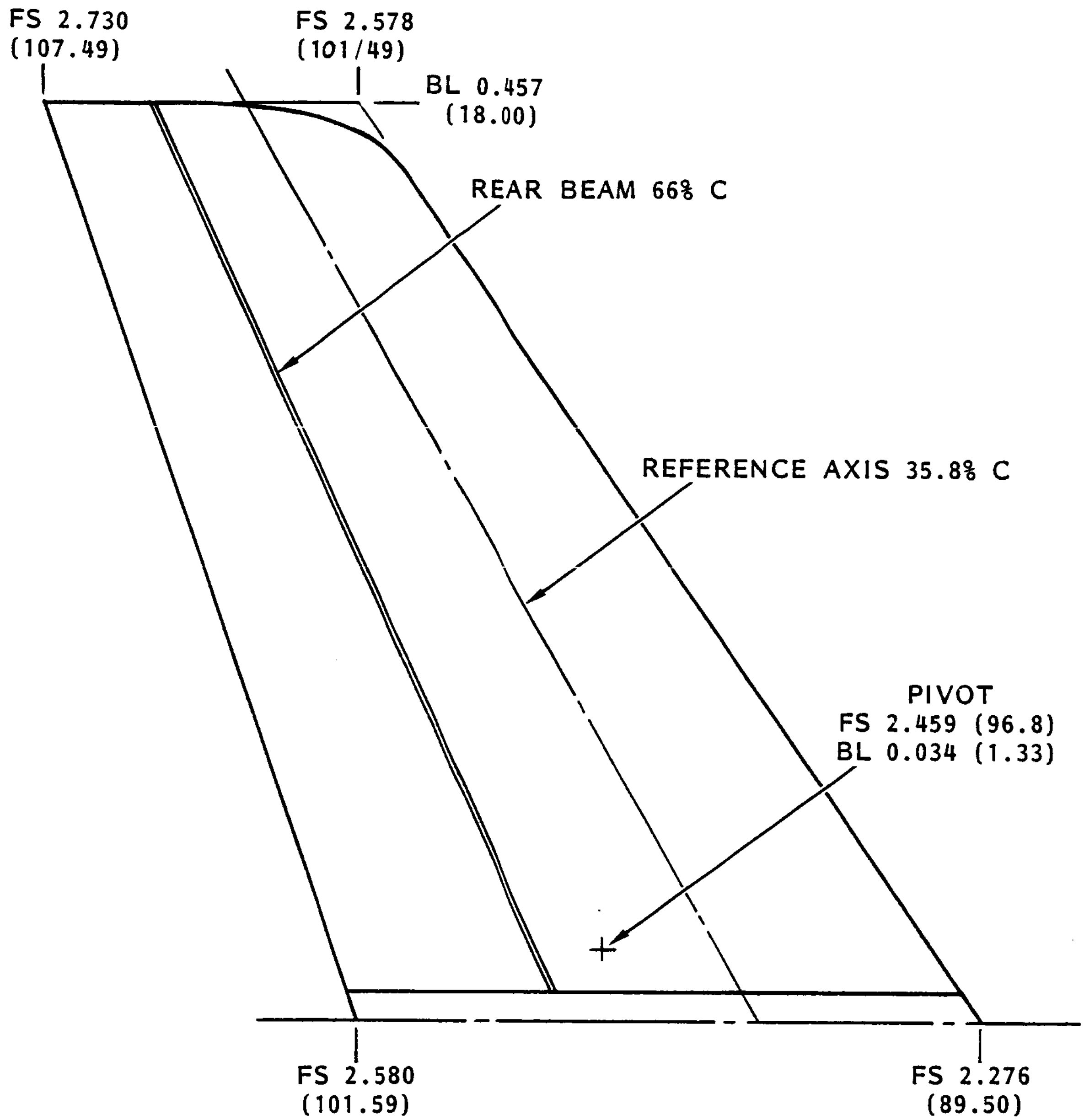

Figure 32. Horizontal Stabilizer Geometry

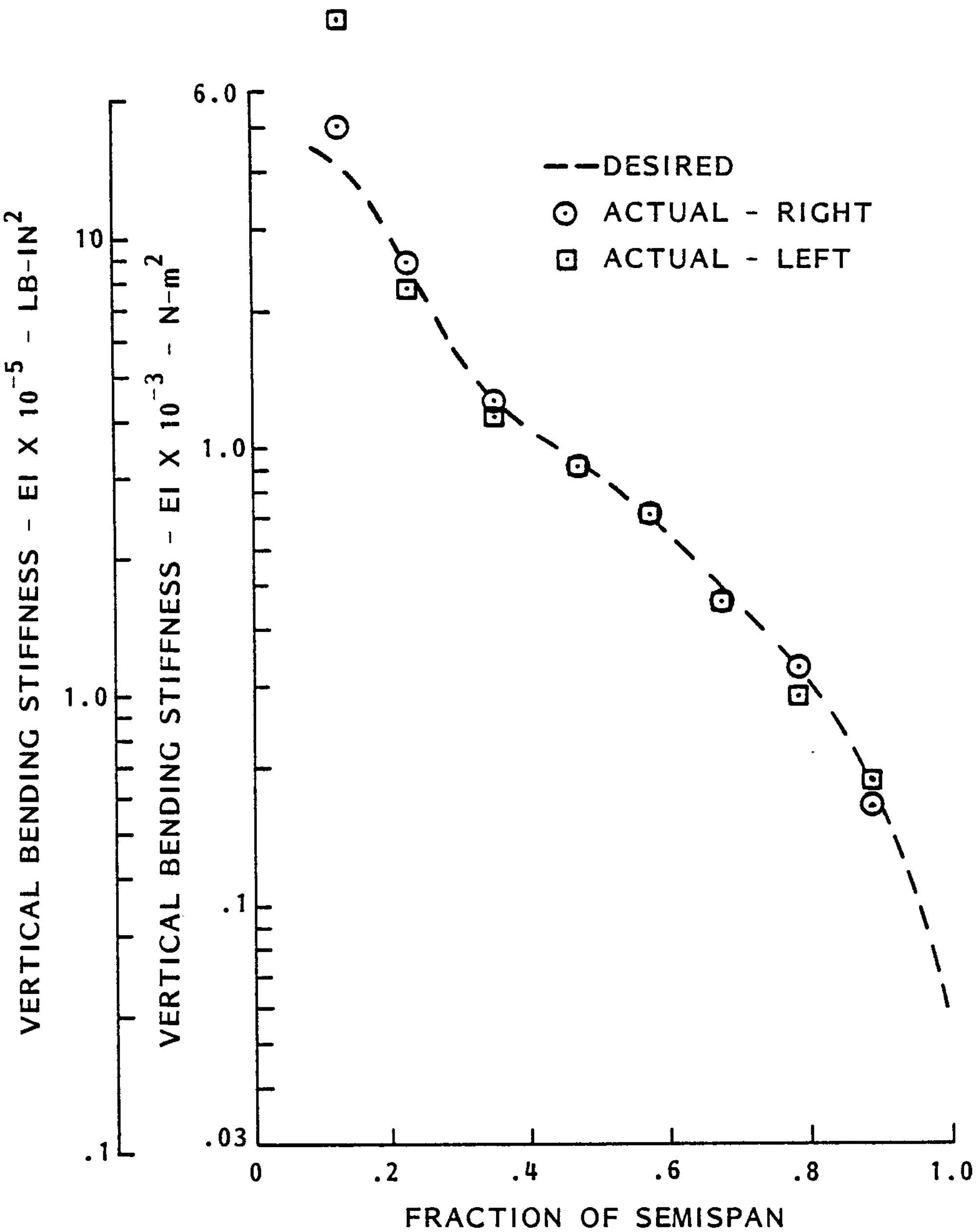

Figure 33. Bare Wing Vertical Bending Stiffness

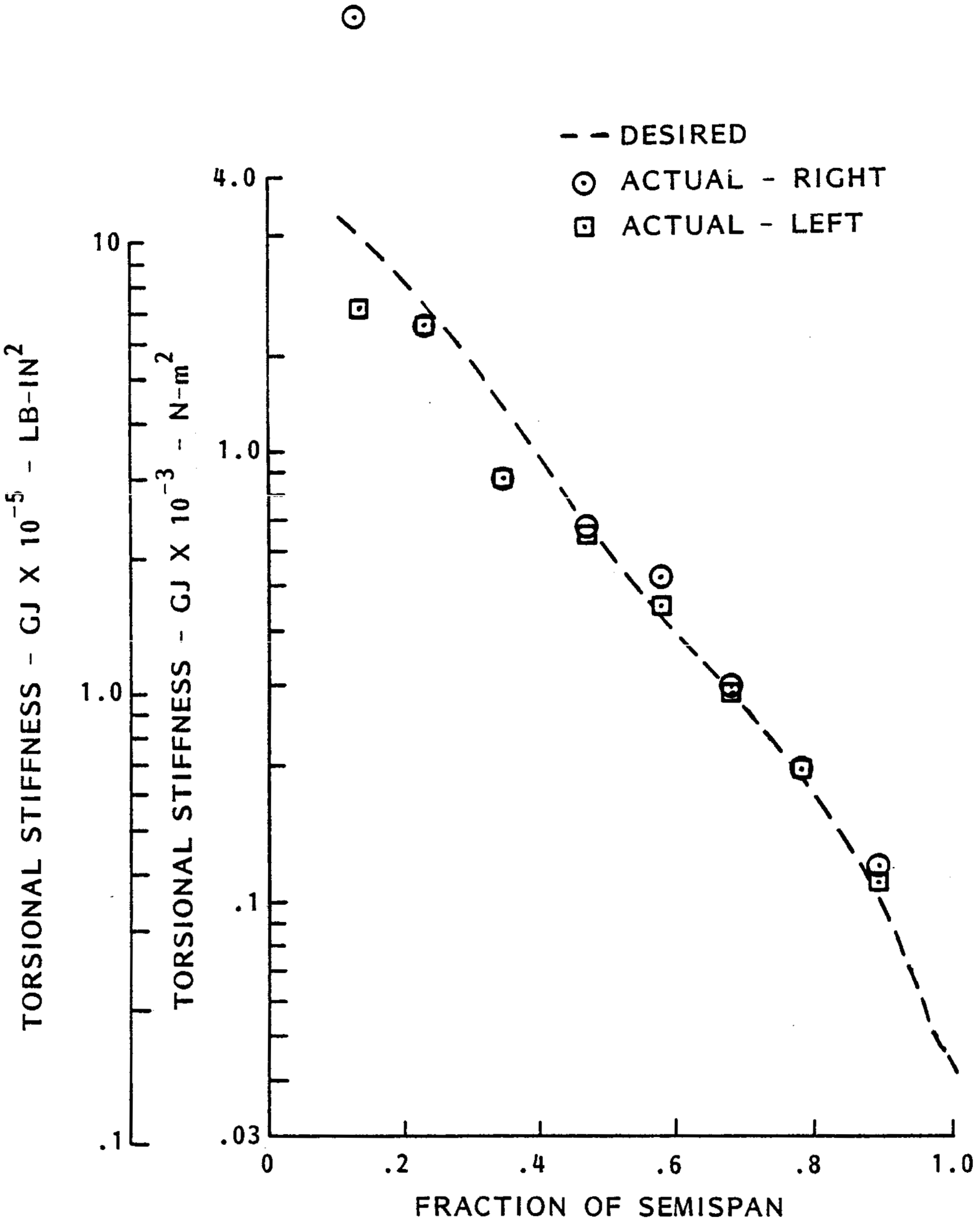

Figure 34, Bare Wing Torsional Stiffness

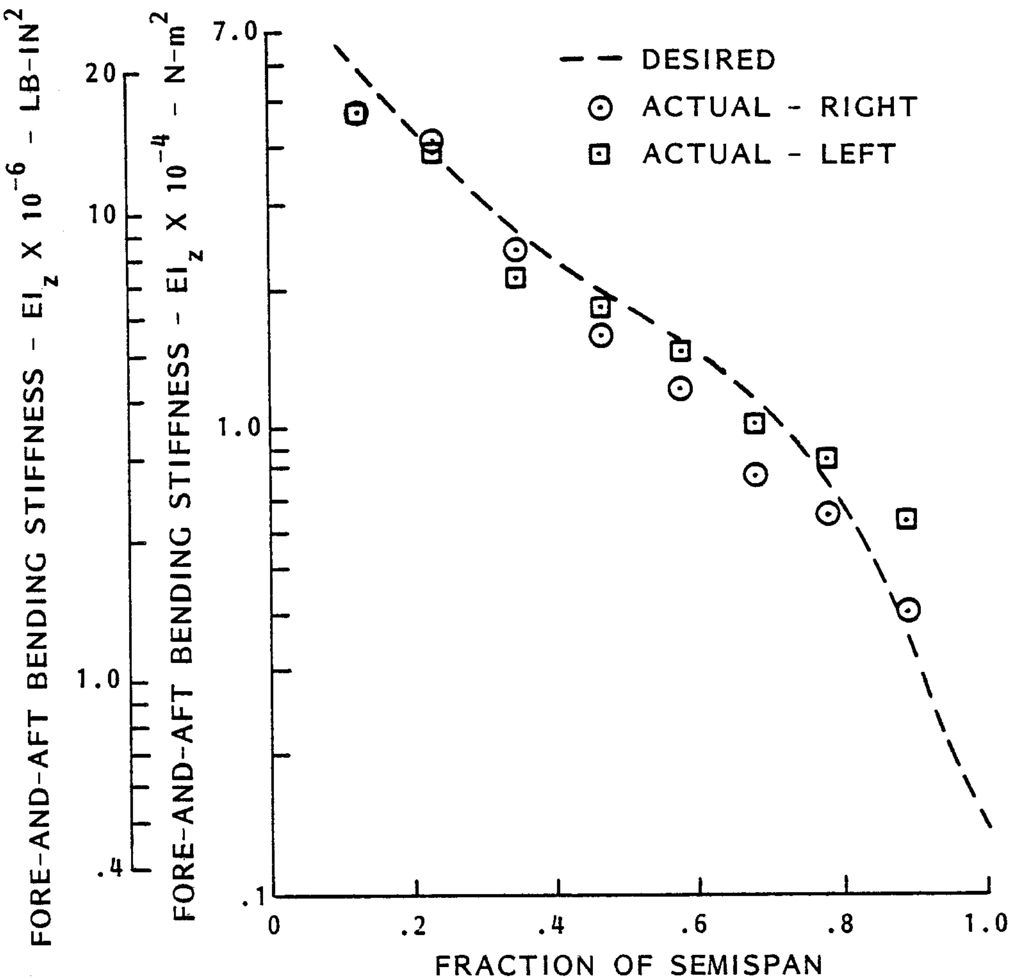

Figure 35. Bare Wing Fore-and-Aft Stiffness

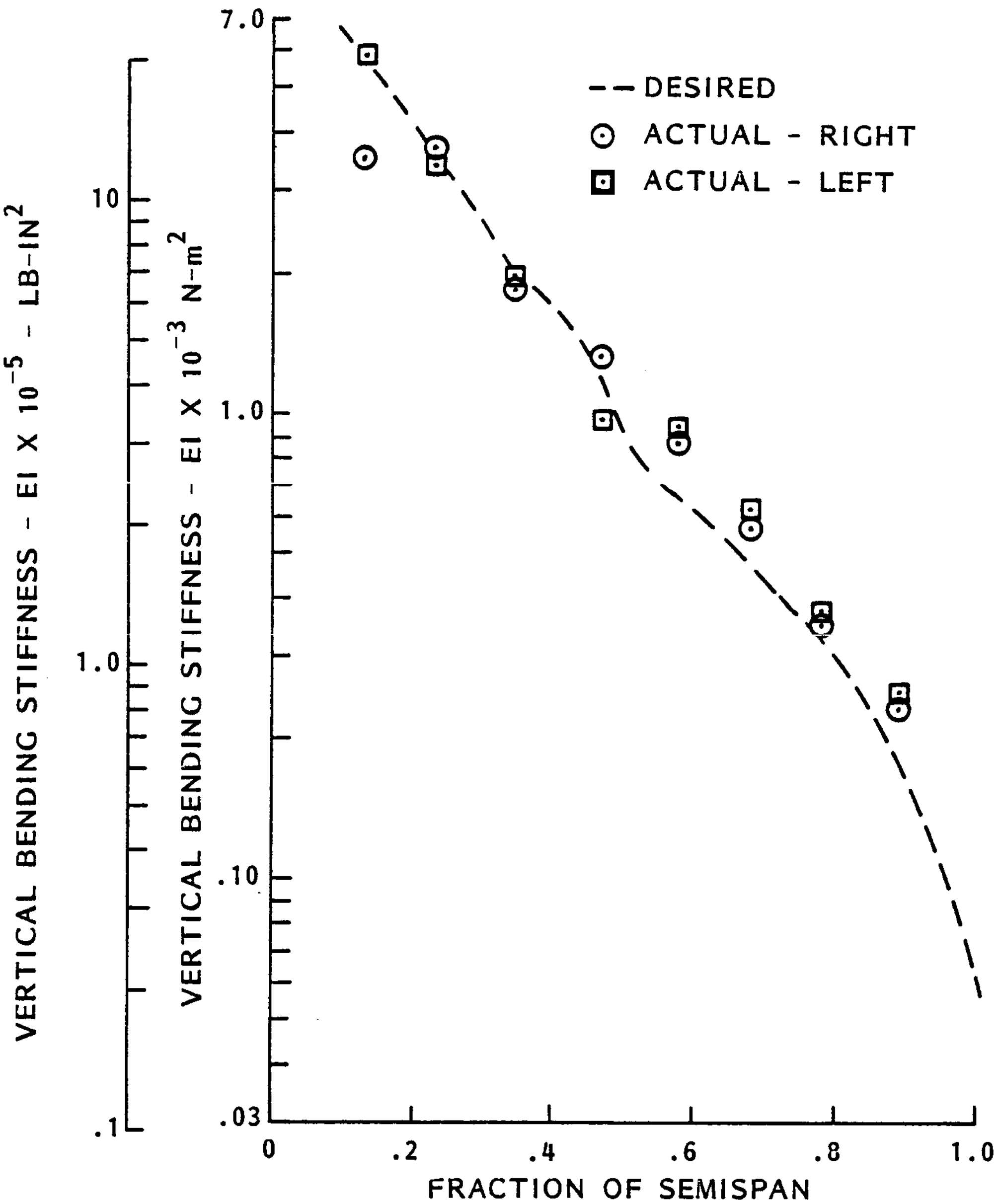

Figure 36. Propfan Wing Vertical Bending Stiffness

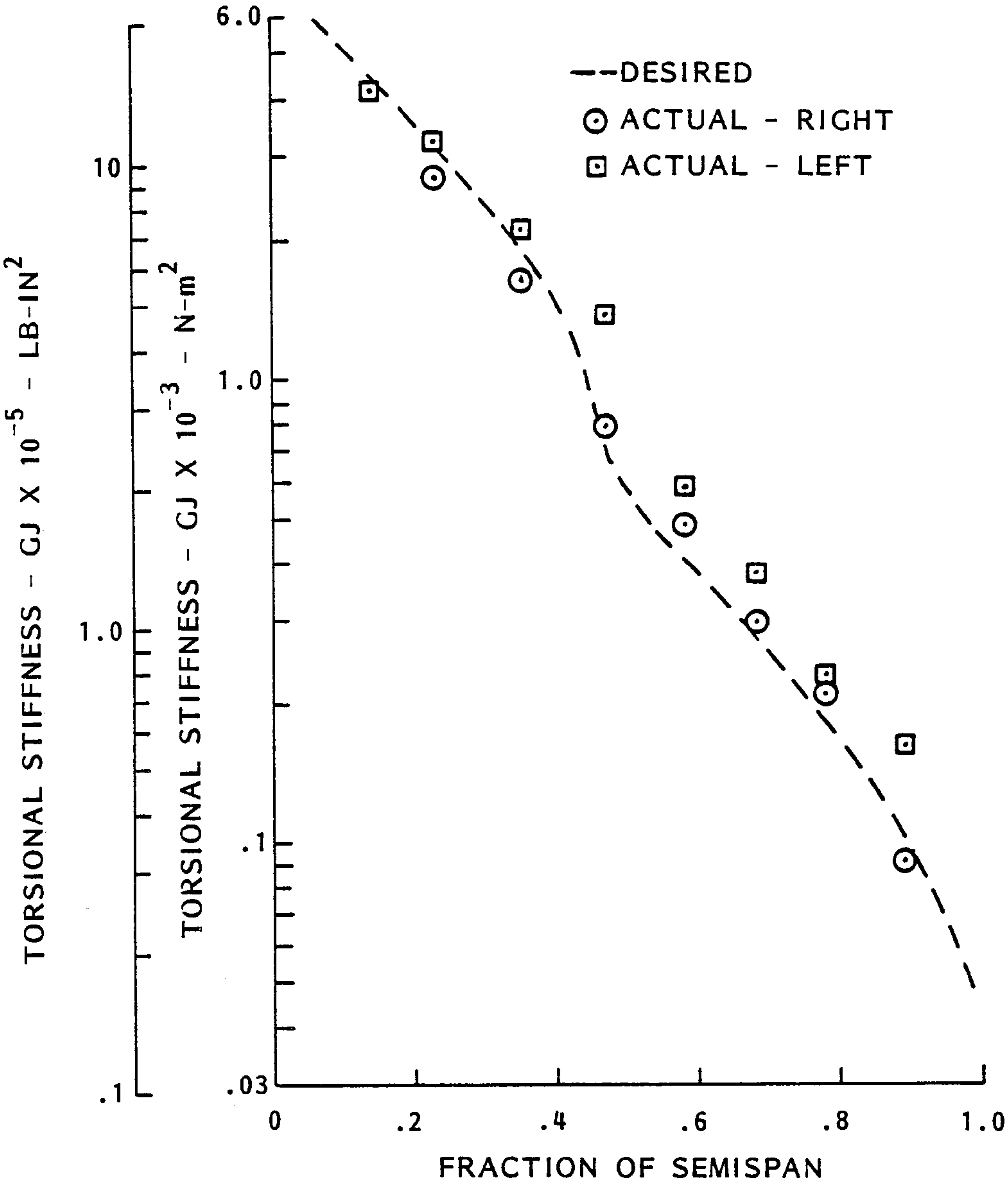

Figure 37. Propfan Wing Torsional Stiffness

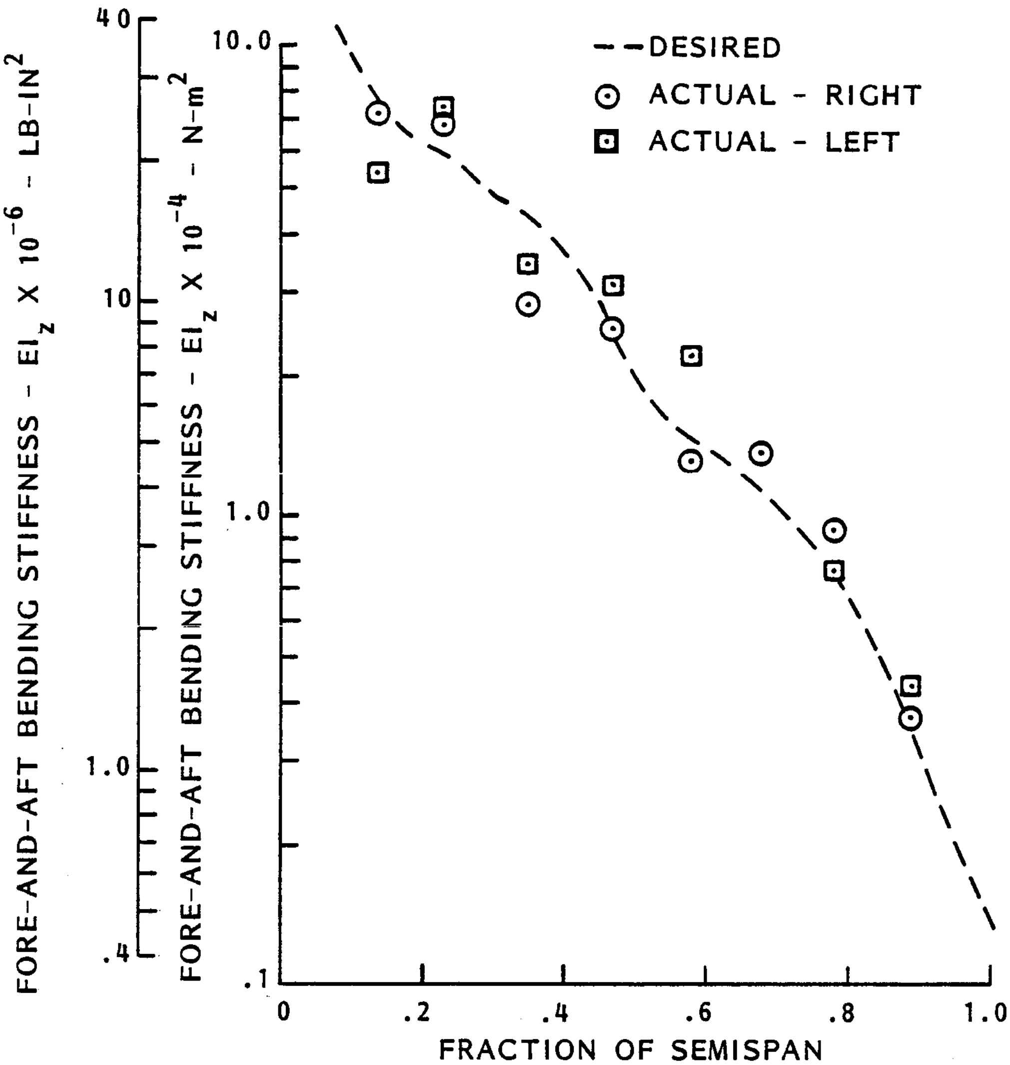

Figure 38. Propfan Wing Fore-and-Aft Bending Stiffness

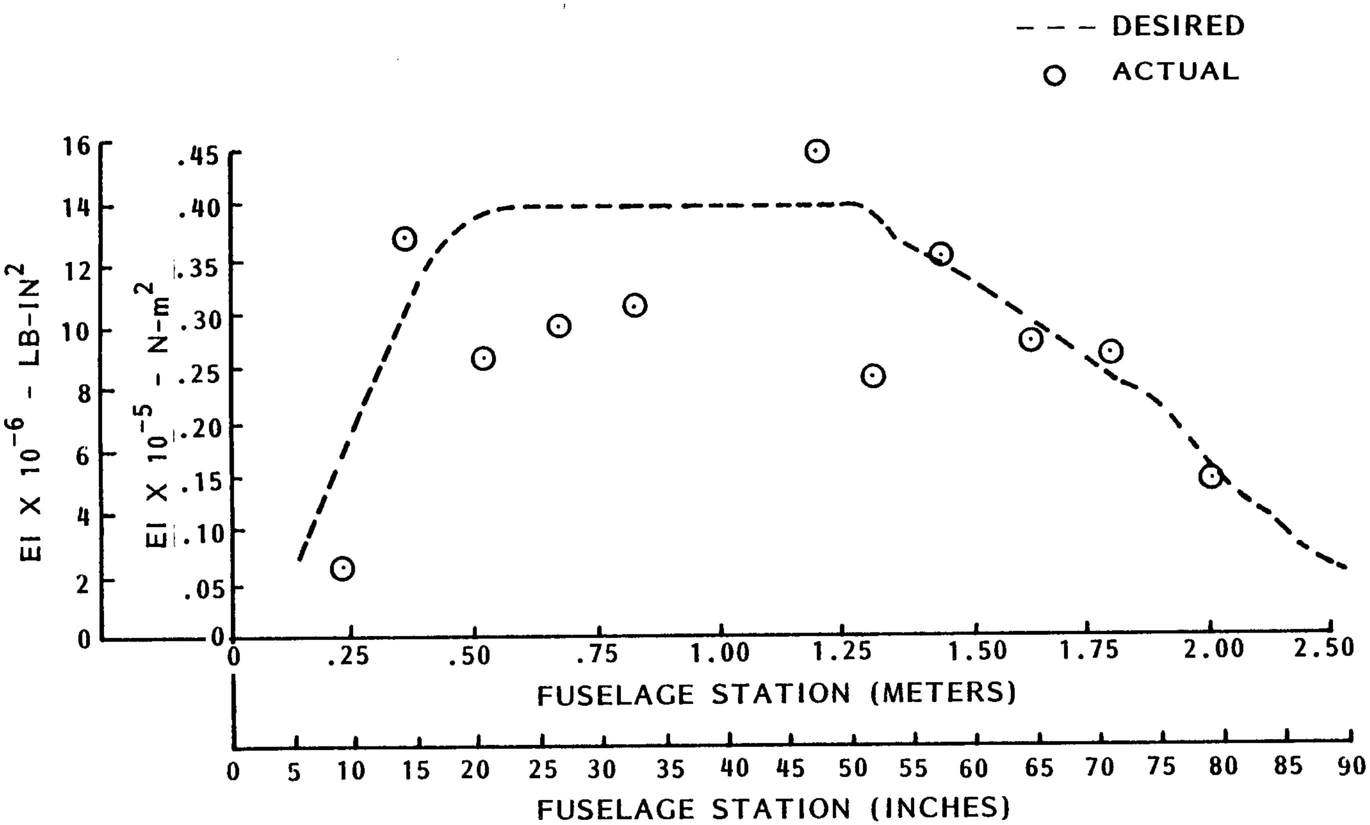

Figure 39. Fuselage Vertical Bending Stiffness

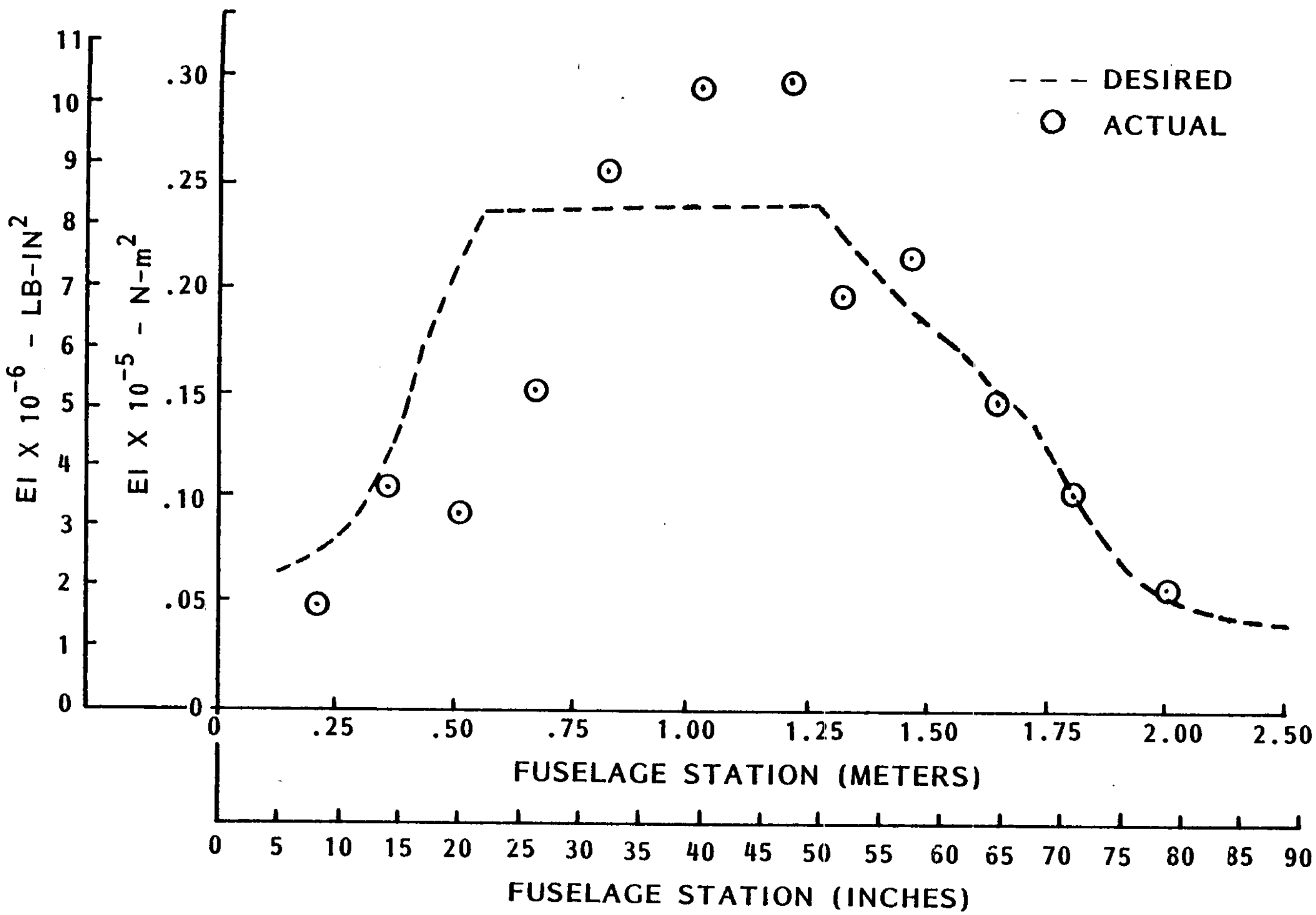

Figure 40. Fuselage Lateral Bending Stiffness

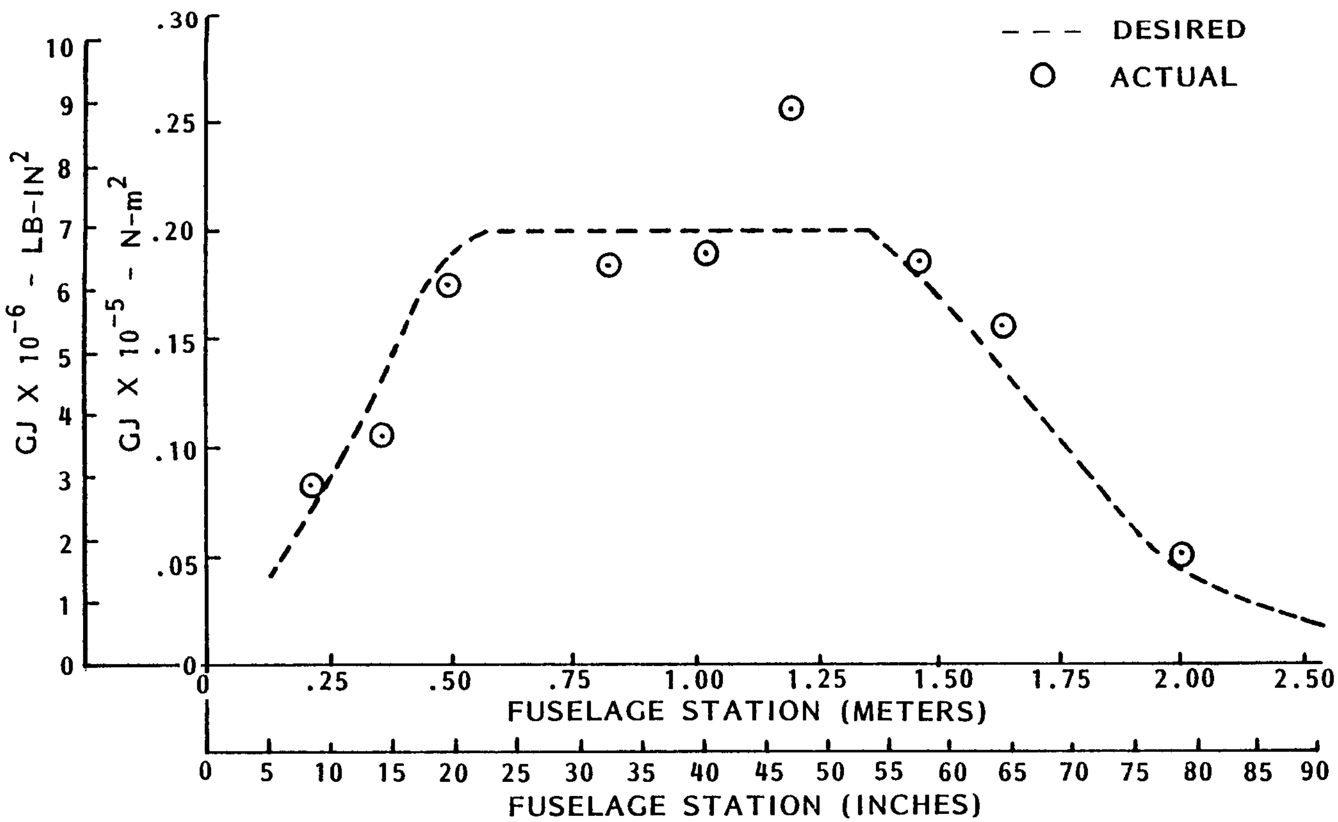

Figure 41. Fuselage Torsional Stiffness

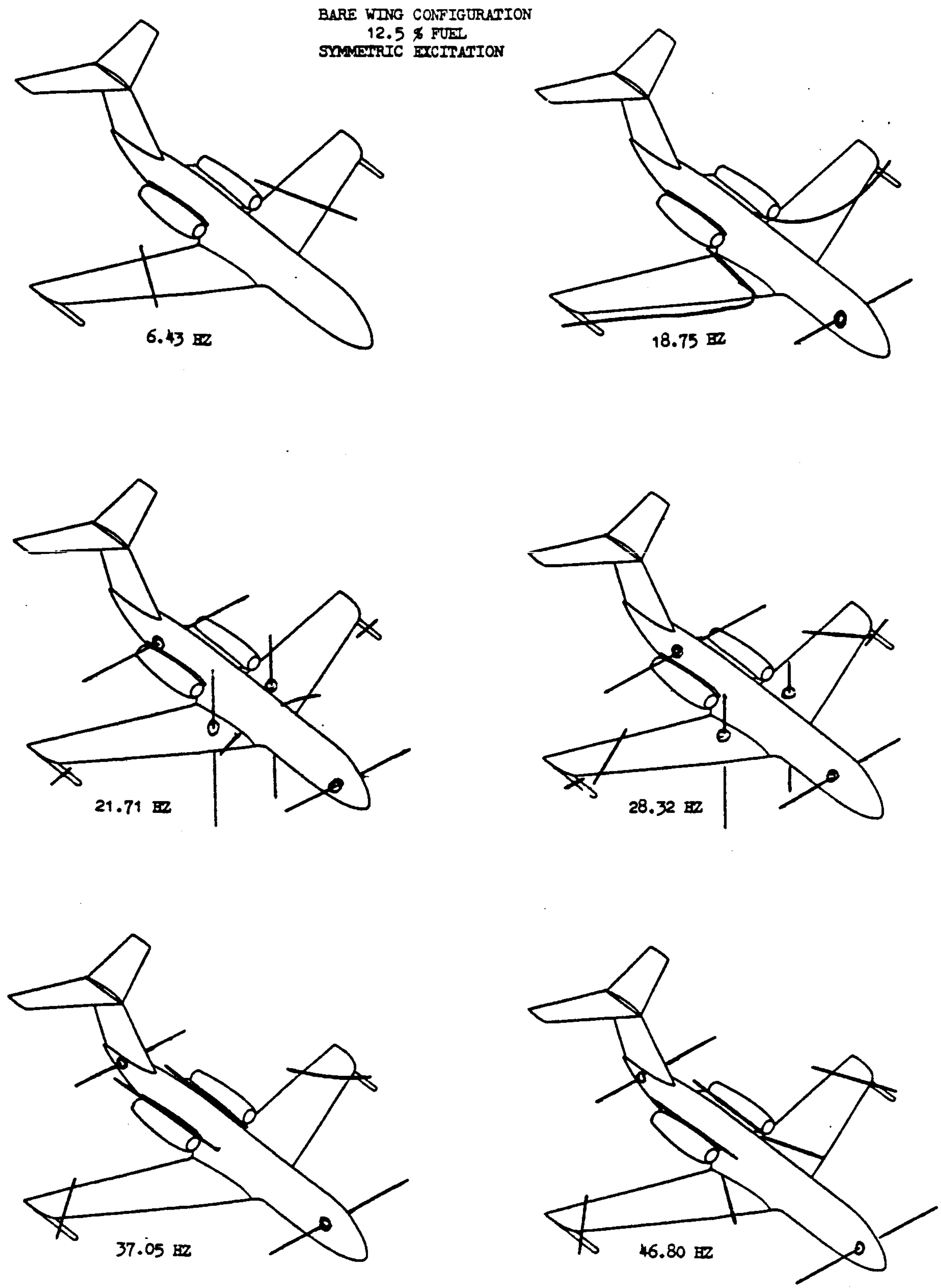

Figure 42. Measured Normal Modes - Bare Wing Configuration (1 of 2)

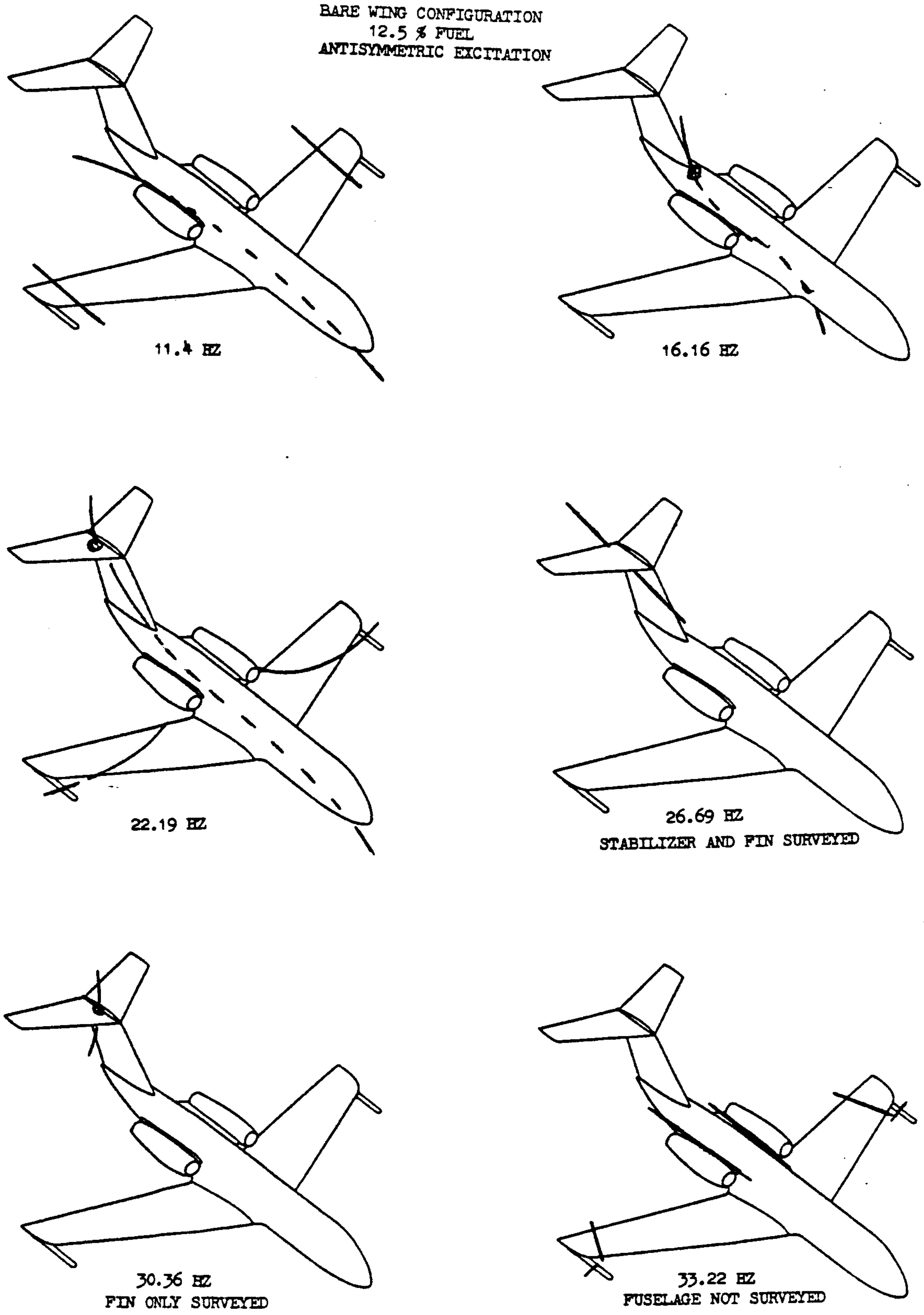

Figure 42. Measured Normal Modes - Bare Wing Configuration (2 of 2)

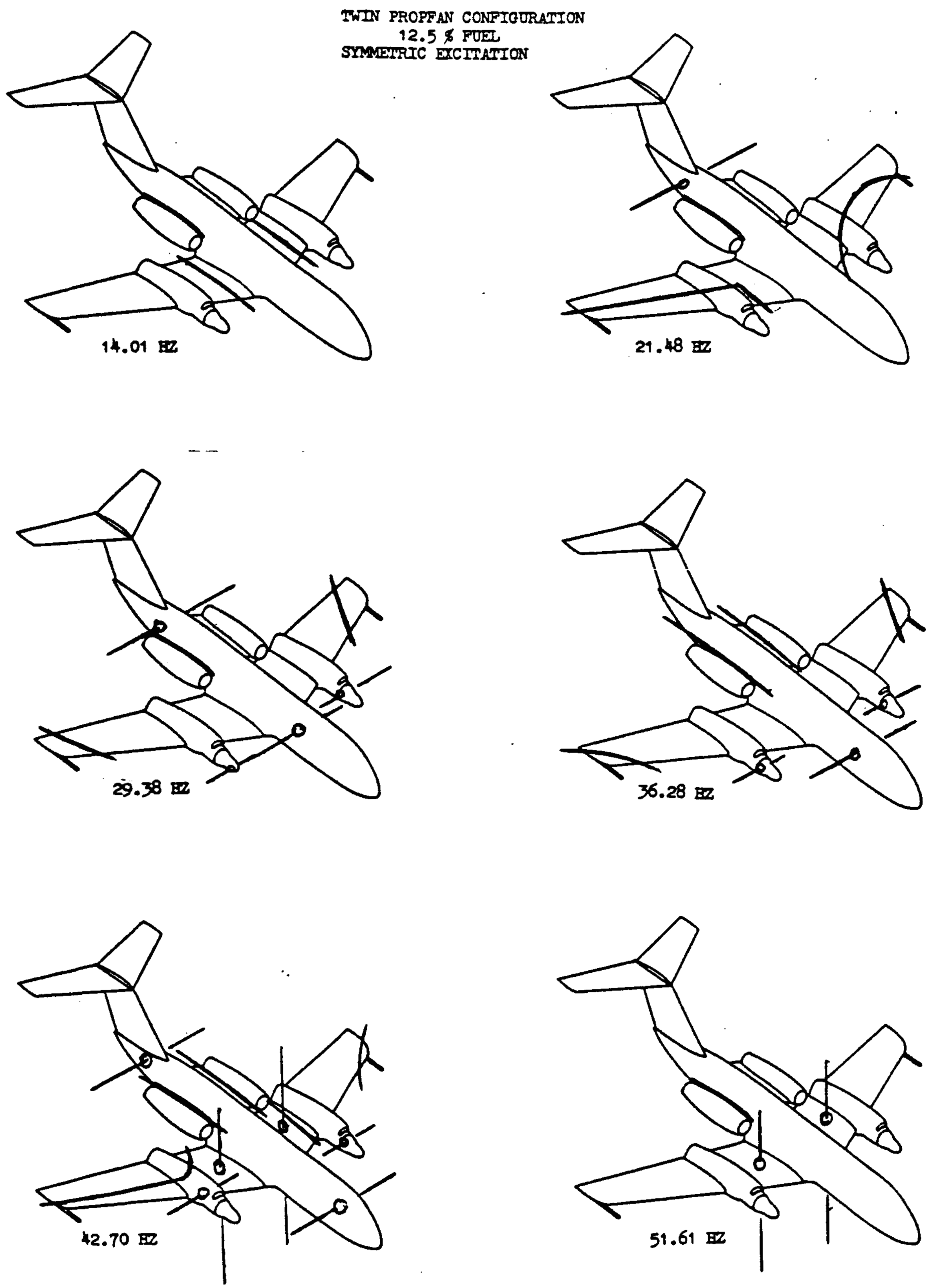

Figure 43. Measured Normal Modes - Twin Propfan Configuration (1 of 2)

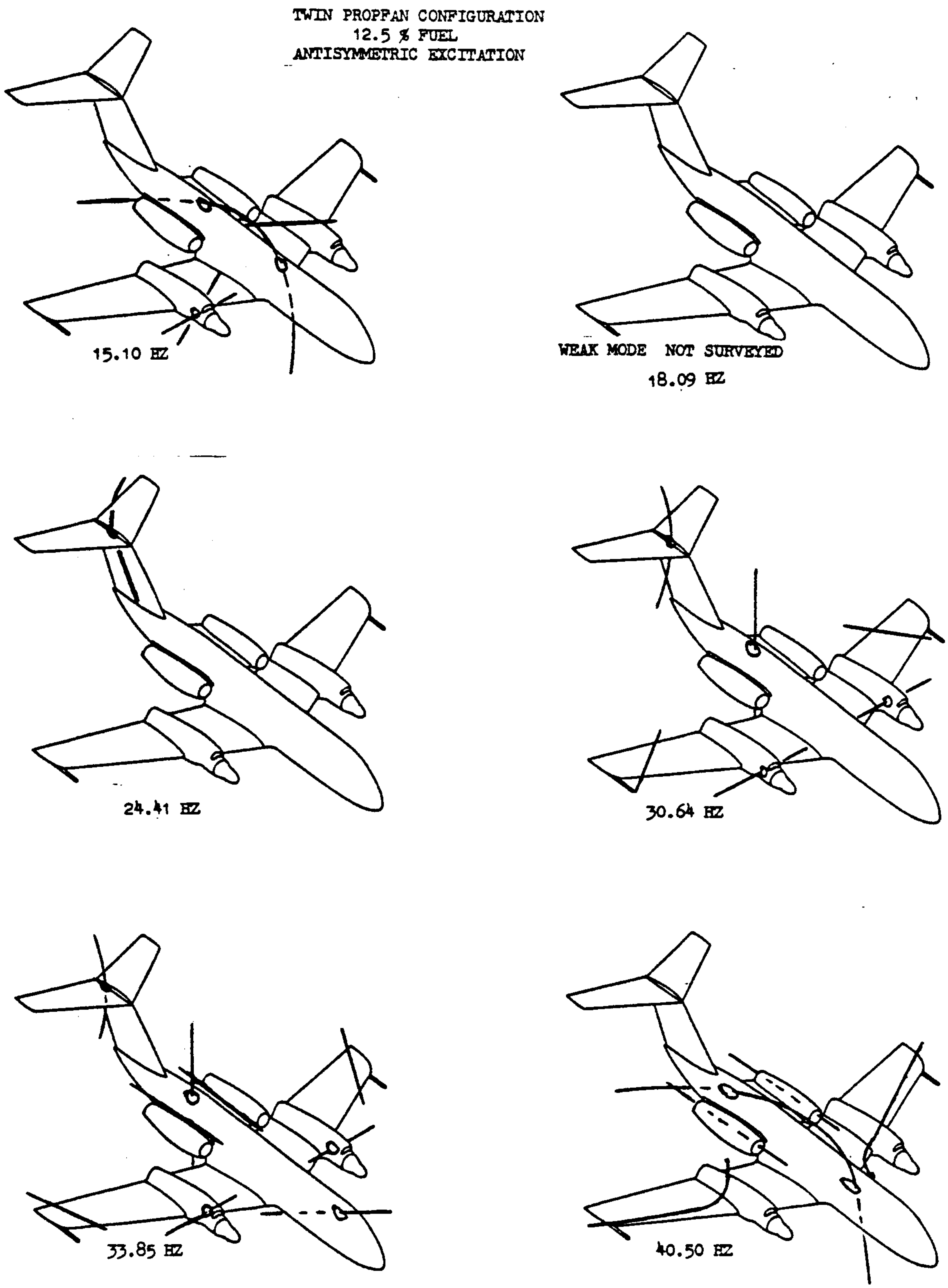

Figure 43. Measured Normal Modes - Twin Propfan Configuration (2 of 2)

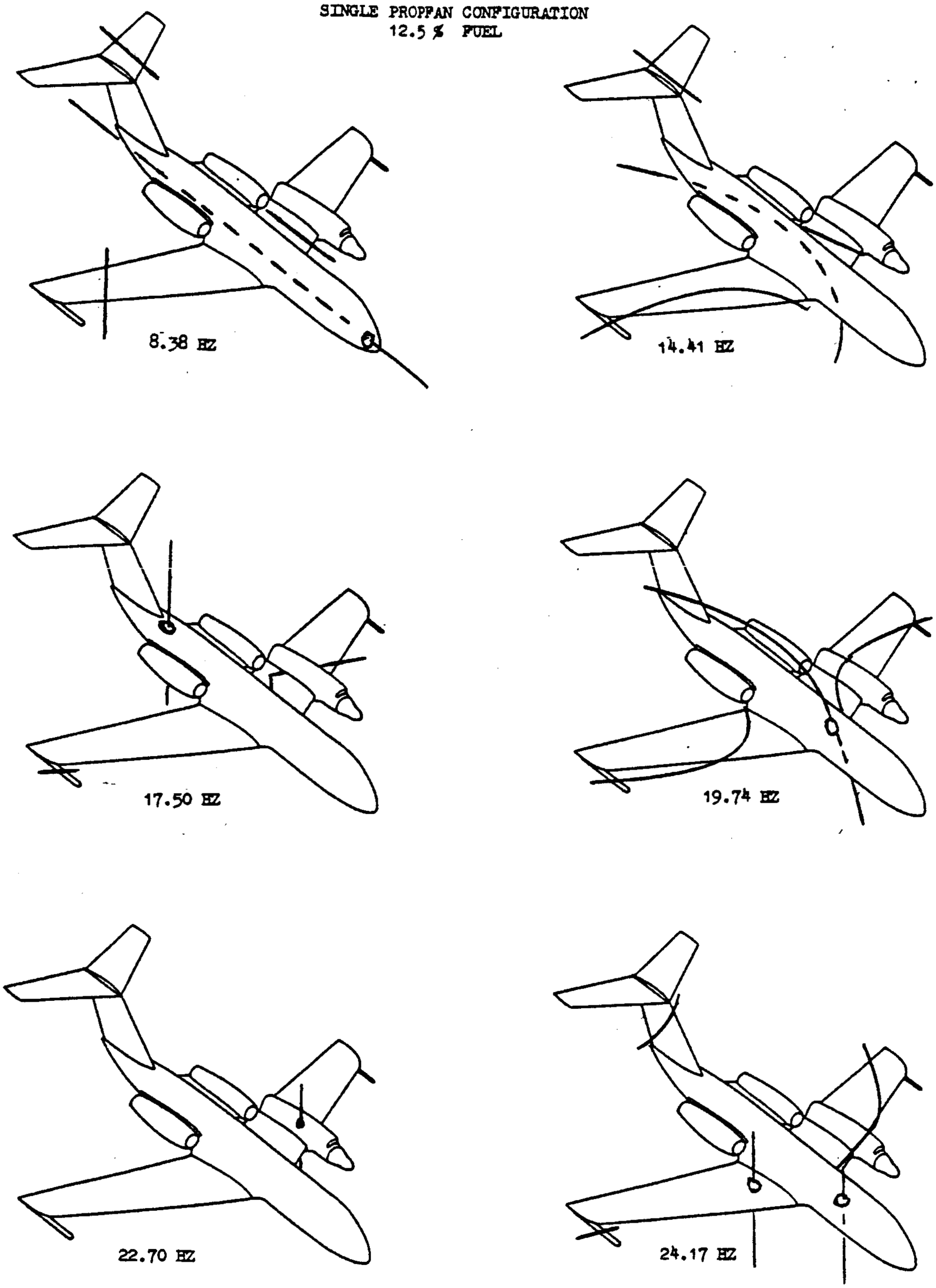

Figure 44. Measured Normal Modes - Single Propfan Configuration (1 of 2)

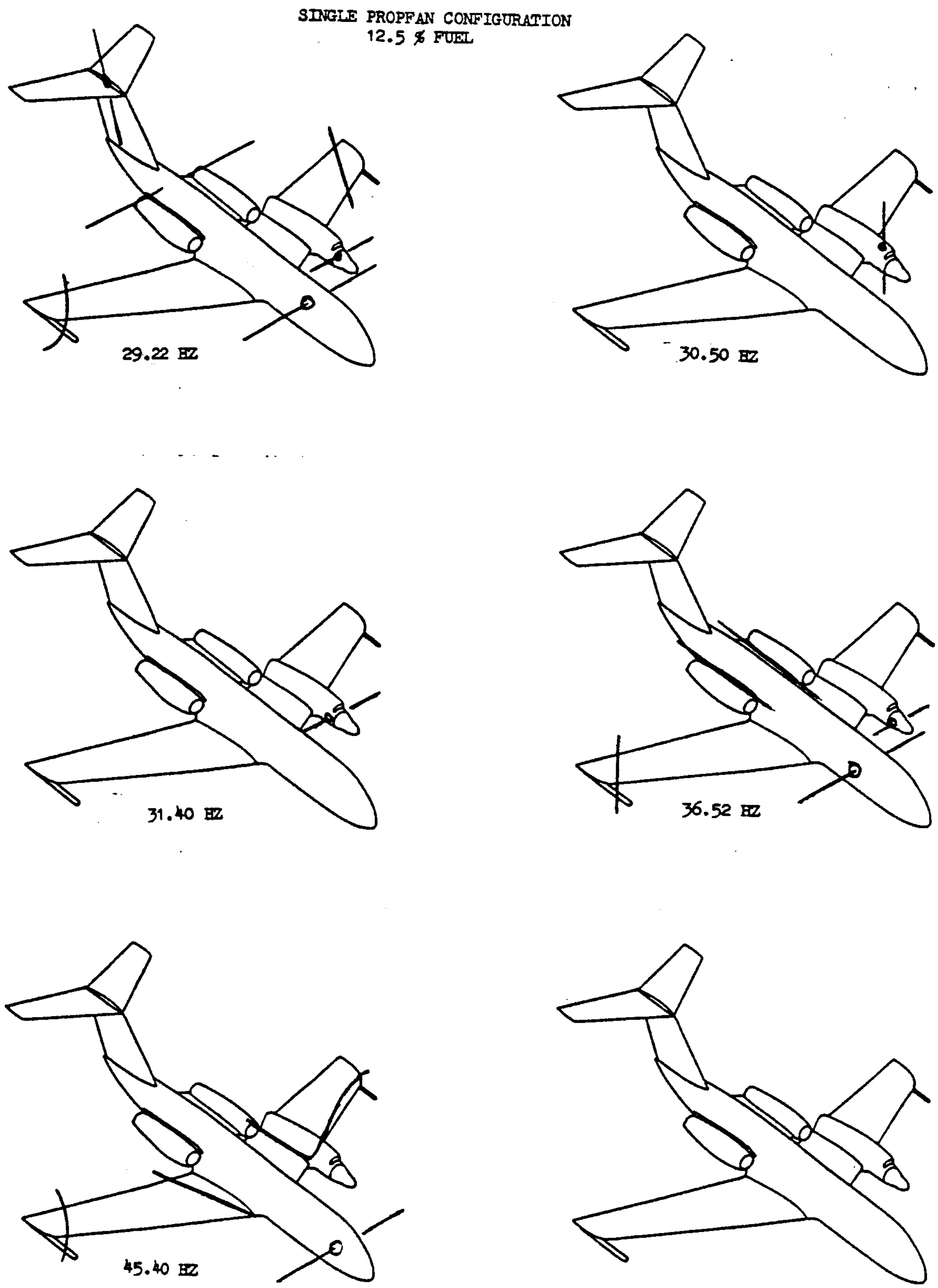

Figure 44. Measured Normal Modes - Single Propfan Configuration (2 of 2)

TABLE 9.
BARE WING MODEL MASS DATA SUMMARY

COMPONENT	MASS (kg x 10^{-3})		$\bar{x}$ - FS (m)		$\bar{x}$ - FS (in)	
	DESIRED	ACTUAL	DESIRED	ACTUAL	DESIRED	ACTUAL
Left Wing	2522	2656	1.347	1.339	53.03	52.7
Right Wing	2522	2692	1.347	1.339	53.03	52.7
Fuselage	16964	23789*	1.074	.960*	42.30	37.8*
Left Jet Engine	2333	2236	1.590	1.593	62.61	62.7
Right Jet Engine	2333	2257	1.590	1.588	62.61	62.5
Vertical Fin	590	907	2.306	2.299	90.78	90.5
Horizontal Stabilizer	641	787	2.498	2.464	98.36	97.0
Left Balance Boom	1556	1556	1.411	1.415	55.55	55.7
Right Balance Boom	1556	1556	1.411	1.415	55.55	55.7
TOTAL	31017	38436	1.283	1.186	50.51	46.7

*Includes 5.443kg ballast at FS .229m (9.0 in) for stability

TABLE 10.
SINGLE PROPFAN MODEL MASS DATA SUMMARY

COMPONENT	MASS (kg x 10^{-3})		x - FS (m)		x - FS (in)	
	DESIRED	ACTUAL	DESIRED	ACTUAL	DESIRED	ACTUAL
Left Wing	4052	4172	1.283	1.283	50.51	50.5
Right Wing	2522	2692	1.347	1.339	53.03	52.7
Fuselage	16964	22772*	1.074	.993*	42.30	39.1
Left Jet Engine	2333	2236	1.590	1.593	62.61	62.7
Right Jet Engine	2333	2257	1.590	1.588	62.61	62.5
Propfan Powerplant**	2133	2200	.975	.970	38.39	38.2
Vertical Fin	590	907	2.306	2.299	90.78	90.5
Horizontal Stabilizer	641	787	2.498	2.464	98.36	97.0
Balance Boom	1556	1556	1.415	1.415	55.55	55.7
Flutter Boom***	187	189	1.468	1.445	56.36	56.9
TOTAL	33311	39768	1.253	1.191	49.34	46.9

*Includes 4.427kg ballast at FS .229m (9.0 in) for stability

**Includes propfan hub with blades

***Used for all tests of this configuration except Nos. 13, 14 and 15

TABLE 11.
TWIN PROPFAN MODEL MASS DATA SUMMARY

COMPONENT	(MASS (kg x 10^{-3}) DESIRED	ACTUAL	x - FS (m) DESIRED	ACTUAL	x - FS (in) DESIRED	ACTUAL
Left Wing	4052	4172	1.283	1.282	50.51	50.49
Right Wing	4052	4170	1.283	1.278	50.51	50.31
Fuselage	16964	21848*	1.074	1.026*	42.30	40.4*
Left Jet Engine	2333	2236	1.590	1.593	62.61	62.7
Right Jet Engine	2333	2257	1.590	1.588	62.61	62.5
Left Propfan Power-Plant**	2133	2200	.975	.970	38.39	38.2
Right Propfan Power-Plant**	2133	2214	.975	.970	38.39	38.2
Vertical Fin	590	907	2.306	2.299	90.78	90.5
Horizontal Stabilizer	641	787	2.498	2.464	98.36	97.0
Left Flutter Boom***	187	189	1.432	1.445	56.36	56.9
Right Flutter Boom***	187	189	1.432	1.445	56.36	56.9
TOTAL	35605	41169	1.227	1.194	48.32	47.0

*Includes 3.502 kg ballast at FS .229 m (9.0 in) for stability

**Includes propfan hub and blades

***Used for all tests of this configuration except Nos. 9 - 12

TABLE 12.

BARE WING PLUS 12½% FUEL MASS DATA - SI UNITS

SECTION NUMBER	SECTION LIMITS WS (m)	MASS(kg x 10^{-3})			$\bar{x}$ - F.S. (m)			$\bar{y}$ - W.S. (m)			I_{yy_0} (kg-m² x 10^{-3})		
		Des'd	R. Act.	L. Act.	Des'd	R. Act.	L. Act.	Des'd	R. Act.	L. Act.	Des'd	R. Act.	L. Act.
1	.1334 - .2700	691.0	725.9	722.8	1.2456	1.2301	1.2306	.2017	.2017	.2014	9.272	9.554	9.337
2	.2700 - .4064	481.0	505.4	509.2	1.2634	1.2680	1.2685	.3383	.3383	.3383	6.357	5.622	5.841
3	.4064 - .5644	408.0	424.2	425.6	1.3261	1.3226	1.3249	.4851	.4851	.4851	4.610	3.890	3.955
4	.5644 - .6774	240.8	255.4	257.6	1.3879	1.3680	1.3711	.6210	.6210	.6210	2.430	1.608	1.711
5	.6744 - .7902	197.0	251.3	211.1	1.4315	1.4244	1.4148	.7338	.7297	.7338	1.703	1.390	1.351
6	.7902 - .9144	207.5	216.8	216.7	1.4877	1.4773	1.4750	.8524	.8524	.8524	1.229	1.292	1.328
7	.9144 - 1.0414	160.4	170.7	171.8	1.5347	1.5187	1.5128	.9779	.9779	.9779	.802	.709	.681
8	1.0414 - 1.1684	135.9	142.8	141.7	1.5895	1.5761	1.5814	1.1049	1.1156	1.1011	.459	.490	.470
TOTAL		2521.6	2692.5	2656.5	1.3470	1.3396	1.3381	.4524	.5110	.5075	---	---	---

TABLE 13.

BARE WING PLUS 12½% FUEL MASS DATA - ENGLISH UNITS

SECTION NUMBER	SECTION LIMITS WS(in)	MASS (gm)			$\bar{x}$ - F.S. (in)			$\bar{y}$ - W.S. (in)			I_{yy_0} (gm - in²)		
		Des'd	R. Act.	L. Act.	Des'd	R. Act.	L. Act.	Des'd	R. Act.	L. Act.	Des'd	R. Act.	L. Act.
1	5.25 - 10.63	691.0	725.9	722.8	49.04	48.43	48.45	7.94	7.94	7.93	14,372	14,808	14,472
2	10.63 - 16.00	481.0	505.4	509.2	49.74	49.92	49.91	13.32	13.32	13.32	9,854	8,714	9,052
3	16.00 - 22.22	408.0	424.2	425.6	52.21	52.07	52.16	19.10	19.10	19.10	7,145	6,029	6,130
4	22.22 - 26.67	240.8	255.4	257.6	54.64	53.86	53.98	24.45	24.45	24.45	3,766	2,493	2,652
5	26.67 - 31.11	197.0	251.3	211.1	56.36	56.08	55.70	28.89	28.73	28.89	2,640	2,155	2,094
6	31.11 - 36.00	207.5	216.8	216.7	58.51	58.16	58.07	33.56	33.56	33.56	1,905	2,002	2,058
7	36.00 - 41.00	160.4	170.7	171.8	60.42	59.79	59.56	38.50	38.50	38.50	1,243	1,099	1,055
8	41.00 - 46.00	135.9	142.8	141.7	62.58	62.05	62.26	43.50	43.92	43.35	712	760	728
TOTAL		2521.6	2692.5	2656.5	53.03	52.74	52.68	17.81	20.12	19.98	---	---	---

TABLE 14.
PROPFAN WING PLUS 12½% FUEL MASS DATA - SI UNITS

SECTION NUMBER	SECTION LIMITS WS (m)	MASS (kg x 10^{-3})			x - F.S. (m)			y - W.S. (m)			I_{yyo} (kg-m² x 10^{-3})		
		Des'd	R. Act.	L. Act.	Des'd	R. Act.	L. Act.	Des'd	R. Act.	L. Act.	Des'd	R. Act.	L. Act.
1	.1334 - .2700	755.8	791.2	795.2	1.2476	1.2329	1.2357	.2014	.2014	.2014	10.379	11.151	9.980
2	.2700 - .4064	533.9	558.3	558.7	1.2649	1.2700	1.2675	.3383	.3383	.3383	6.814	6.047	6.355
3*	.4064 - .5644	1820.2	1820.6	1820.2	1.2047	1.2047	1.2144	.4854	.4854	.4854	49.724	51.599	54.185
4	.5644 - .6774	240.8	255.1	257.4	1.3876	1.3602	1.3640	.6210	.6210	.6160	2.432	1.539	1.557
5	.6774 - .7902	197.0	213.1	209.9	1.4315	1.4148	1.4079	.7338	.7338	.7338	1.718	1.048	1.115
6	.7902 - .9144	207.5	216.1	217.4	1.4874	1.4661	1.4694	.8524	.8524	.8524	1.230	1.227	1.186
7	.9144 - 1.0414	160.4	171.3	170.7	1.5342	1.5098	1.5116	.9779	.9779	.9779	.803	.608	.601
8	1.0414 - 1.1684	135.9	144.7	142.0	1.5885	1.5786	1.5781	1.1125	1.1125	1.1067	.462	.475	.453
TOTAL		4051.5	4170.4	4171.5	1.2830	1.2779	1.2824	.4925	.4938	.4925	---	---	---

*Includes propfan nacelle structure and fairing

TABLE 15.
PROPFAN WING PLUS 12½% FUEL MASS DATA - ENGLISH UNITS

SECTION NUMBER	SECTION LIMITS WS (in)	MASS (gm)			x - F.S. (in)			y - W.S. (in)			I_{yy_0} (gm-in²)		
		Des'd	R. Act.	L. Act.	Des'd	R. Act.	L. Act.	Des'd	R. Act.	L. Act.	Des'd	R. Act.	L. Act.
1	5.25 - 10.63	755.8	791.2	795.2	49.12	48.54	48.65	7.93	7.93	7.93	16.087	17,284	15,469
2	10.63 - 16.00	533.9	558.3	558.7	49.80	50.00	49.90	13.32	13.32	13.32	10,561	9,373	9,851
3*	16.00 - 22.22	1820.2	1820.6	1820.2	47.43	47.43	47.81	19.11	19.11	19.11	77,073	79,979	83,987
4	22.22 - 26.67	240.8	255.1	257.4	54.63	53.55	53.70	24.45	24.45	24.25	3,770	2,385	2,413
5	26.67 - 31.11	197.0	213.1	209.9	56.36	55.70	55.49	28.89	28.89	28.89	2,663	1,624	1,729
6	31.11 - 36.00	207.5	216.1	217.4	58.56	57.72	57.85	33.56	33.56	33.56	1.906	1,902	1,839
7	36.00 - 41.00	160.4	171.3	170.7	60.40	59.44	59.51	38.50	38.50	38.50	1,244	943	931
8	41.00 - 46.00	135.9	144.7	142.0	62.54	62.15	62.13	43.80	43.86	43.57	716	736	702
TOTAL		4051.5	4170.4	4171.5	50.51	50.31	50.49	19.39	19.44	19.39	---	---	---

*Includes propfan nacelle structure and fairing

TABLE 16.
WING FUEL MASS DATA

WING SECTION NO.	SECTION LIMITS - W.S. m	in	MASS (kg x 10^{-3}) Desired	R. Actual	L. Actual
1	.1334 - .2700	5.25 - 10.63	547	552	552
2	.2700 - .4064	10.63 - 16.00	418	421	421
3	.4064 - .5644	16.00 - 22.22	332	307	307
4	.5644 - .6774	22.22 - 26.67	91	132	132
TOTAL			1388	1412	1412

NOTE: Quantities shown are in addition to the 12½ percent fuel built into wing sections.

TABLE 17.
WING TIP BOOM MASS DATA

BOOM	MASS(kg x 10^{-3})	$\bar{x}$-FS(m)	$\bar{x}$-FS(in)	$\bar{z}$-WL(m)	$\bar{z}$-WL(in)	I_{yy_o}(kg-m²)	I_{yy_o}(gm-in)
Flutter-Desired	186.6	1.432	56.36	.1676	6.60	1.388	2,152
Right Flutter-Actual	189.3	1.445	56.88	.1676	6.60	1.474	2,285
Left Flutter-Actual	189.3	1.445	56.88	.1676	6.60	1.474	2,285
Balance-Desired	1,556	1.411	55.55	.1570	6.18	7.432	11,520
Right Balance-Actual	1,556	1.415	55.7	.1575	6.2	9.806	15,200
Left Balance-Actual	1,556	1.415	55.7	.1575	6.2	9.806	15,200
Rt. Rev. Flutter-Actual	189.3	1.702	67.02	.1676	6.6	1,474	2,285
Lt. Rev. Flutter-Actual	189.3	1.702	67.02	.1676	6.6	1,474	2,285
Rt. Hvy. Rev. Flutter -Actual	322.5	1.699	66.90	.1676	6.6	1.398	2,167
Lt. Hvy. Rev. Flutter -Actual	323.4	1.701	66.95	.1676	6.6	1.352	2,095
Rt. Large Destab. -Actual	363.6	1.744	68.67	.1562	6.15	4.851	7,519
Lt. Large Destab. -Actual	361.0	1.743	68.62	.1562	6.15	4.563	7,073

NOTE: All booms attached at WS 1.147m (45.17 in)

TABLE 18.
FUSELAGE MASS DATA

SECTION NUMBER	SECTION LIMITS FS(m)	SECTION LIMITS FS(in)	MASS (kg x 10^{-3}) DESIRED	ACTUAL	$\bar{x}$ - FS (m) DESIRED	ACTUAL	$\bar{x}$ - FS (in) DESIRED	ACTUAL
1	.023 - .178	0.89 - 7.00	152	388	.145	.145	5.7	5.7
2	.178 - .373	7.00 - 14.67	1393	1464	.279	.279	11.0	11.0
3	.373 - .480	14.67 - 18.89	1012	734	.427	.427	16.8	16.8
4	.480 - .658	18.89 - 25.89	574	1122	.569	.569	22.4	22.4
5	.658 - .813	25.89 - 32.00	479	1557	.742	.762	29.2	30.0
6	.813 - .988	32.00 - 38.89	1027	1073	.909	.909	35.8	35.8
7	.988 - 1.273	38.89 - 51.00	7428	5044	1.074	1.207	42.3	47.5
8	1.273 - 1.453	50.11 - 57.22	1475	1182	1.364	1.364	53.7	53.7
9	1.453 - 1.637	57.22 - 64.44	2050	2071	1.562	1.577	61.5	62.1
10	1.637 - 1.792	64.44 - 70.56	610	1409	1.692	1.692	66.6	66.5
11	1.792 - 2.015	70.56 - 79.33	476	1040	1.887	1.887	74.3	74.3
12	2.015 - 2.230	79.33 - 87.78	234	1011	2.134	2.134	84.0	84.0
13	2.230 - 2.438	87.78 - 96.00	54	250	2.296	2.296	90.4	90.4
TOTAL			16964	18345	1.074	1.178	42.3	46.4

NOTE: Mass required for cable mount stability was located at FS .229m (9.0 in) as follows: Bare wing configuration, 5.443 kg; Single Propfan configuration, 4.427 kg; Twin Propfan configuration, 3.502 kg.

TABLE 19.
JET ENGINE MASS DATA

	MASS kg x 10^{-3}	$\bar{x}$-FS		$\bar{y}$-BL		$\bar{z}$-WL		I_{xx_o}		I_{yy_o}		I_{zz_o}	
		m	in	m	in	m	in	kg-m²	gm-in²	kg-m²	gm-in²	kg-m²	gm-in²
Desired	2,333	1.590	62.61	.216	8.49	.338	13.30	5.31	8,230	43.922	68,080	43.839	67,950
RH Actual	2,257	1.586	62.45	.213	8.4	.345	13.6	7.596	11,774	49.862	77,287	45.974	72,260
LH Actual	2,236	1.592	62.66	.213	8.4	.345	13.6	7.382	11,442	48,239	74,770	45.076	69,868

NOTE: Includes engine and nacelle only. Pylon mass included in fuselage Section 7.

TABLE 20.
EMPENNAGE MASS DATA

COMPONENT	MASS kg x 10^{-3}	$\bar{x}$-FS m	$\bar{x}$-FS in	$\bar{z}$-WL m	$\bar{z}$-WL in	I_{xx_O}, kg-m²	I_{xx_O}, gm-in²	I_{yy_O}, kg-m²	I_{yy_O}, gm-in²	I_{zz_O}, kg-m²	I_{zz_O}, gm-in²
Hor. Stab. Desired	641	2.498	98.36	.737	29.01	30.18	46,790	8.57	9,771	36.48	56,550
Hor. Stab. Actual	787	2.464	97.0	.737	29.01	43.21	66,980	8.88	13,290	50.48	78,240
Vert. Fin Desired	590	2.306	90.78	.567	22.34	8.07	12,500	17.83	27,630	9.76	15,130
Vert. Fin Actual	907	2.299	90.52	.546	21.50	18.65	28,915	39.58	61,350	25.05	38,820

TABLE 21.
PROPFAN POWERPLANT MASS DATA - SI UNITS

	Mass ($kg\times10^{-3}$)		x-FS (m)		z-WL (m)		I_{xx_0} ($kg\text{-}m^2\times10^{-3}$)		I_{yy_0} ($kg\text{-}m^2\times10^{-3}$)		I_{zz_0} ($kg\text{-}m^2\times10^{-3}$)	
	Des'd	Actual	Des'd	Actual	Des'd	Actual	Des'd	Actual	Des'd	Actual	Des'd	Actual
L. Prop/Hub	863.	795.5	.8410	.8433	.2050	.2050	1.355	1.883	1.235	1.610	1.235	1.610
L. Gearbox	368.5	524.3	.9286	.9271	.2090	.2200	.153	---	.217	---	.189	---
L. Pwr. Sect	850.8	844.8	1.1298	1.1328	.2291	.2311	.581	.862	3.343	3.529	3.143	3.273
L. Torque-meter/Struts	50.4	29.4	.9962	.9957	.2283	.2311	.005	---	.026	---	.026	---
L. Total	2132.7	2200.0	.9751	.9693	.2159	.2189	2.372	3.127	41.781	43.528	41.271	43.394
R. Prop/Hub	863.	791.0	.8410	.8433	.2050	.2050	1.355	1.887	1.235	1.568	1.235	1.568
R. Gearbox	368.5	530.3	.9286	.9271	.2090	.2200	.153	---	.217	---	.189	---
R. Pwr. Sect	850.8	863.0	1.1298	1.1328	.2291	.2311	.581	.917	3.343	3.514	3.143	3.393
R. Torque-meter/Struts	50.4	29.4	.9962	.9957	.2283	.2311	.005	---	.026	---	.026	---
R. Total	2132.7	2213.7	.9751	.9708	.2159	.2189	2.372	3.186	41.781	43.898	41.271	43.899
L. Spinner	863.	801.3	.8410	.8473	.2050	.2050	*	.649	*	.865	*	.865
R. Spinner	863.	801.3	.8410	.8473	.2050	.2050	*	.649	*	.865	*	.865

NOTE: Spinners were used in lieu of props and hubs for tests 2, 5, 8-12 and 14.
*Desired moments of inertia were not specified.

TABLE 22.
PROPFAN POWERPLANT MASS DATA - ENGLISH UNITS

	Mass-gms		x - F.S.		z - W.L.		I_{xx_O}-gm-in²		I_{yy_O}-gm-in²		I_{zz_O}-gm-in²	
	Des'd	Actual	Des'd	Actual	Des'd	Actual	Des'd	Actual	Des'd	Actual	Des'd	Actual
L. Prop/Hub	863.	795.5	33.11	33.2	8.07	8.07	2100	2919	1915	2495	1915	2495
L. Gearbox	368.5	524.3	36.56	36.5	8.23	8.66	237	---	336	---	293	---
L. Pwr. Sect	850.8	844.8	44.48	44.6	9.02	9.1	901	1336	5181	5470	4872	5073
L. Torque-meter/Struts	50.4	29.4	39.22	39.2	8.99	9.1	8	---	41	---	41	---
L. Total	2132.7	2200	38.39	38.16	8.50	8.62	36 76	4847	64,760	67,468	63,970	67,261
R. Prop/ Hub	863.	791.0	33.11	33.2	8.07	8.07	2100	2925	1915	2431	1915	2431
R. Gearbox	368.5	530.3	36.56	36.5	8.23	8.66	237	---	336	---	293	---
R. Pwr. Sect	850.8	863.0	44.48	44.6	9.02	9.1	901	1421	5181	5446	4872	5259
R. Torque-meter/Struts	50.4	29.4	39.22	39.2	8.99	9.1	8	---	41	---	41	---
R. Total	2132.7	2213.7	38.39	38.22	8.50	8.62	3676	4939	64,760	68,042	63,970	68,044
L. Spinner	863.	801.3	33.11	33.36	8.07	8.07	*	1006	*	1341	*	1341
R. Spinner	863.	801.3	33.11	33.36	8.07	8.07	*	1006	*	1341	*	1341

NOTE: Spinners were used in lieu of props and hubs for tests 2, 5, 8-12, and 14.
*Desired moments of inertia were not specified.

TABLE 23.

PROPFAN NACELLE FLEXIBILITIES

FLEXIBILITY	UNITS	DESIRED	LEFT ACTUAL	RIGHT ACTUAL
C_{ZZ}-Vert. Defl./vert/load	m/N(in/lb)	$.379 \times 10^{-5}(.664 \times 10^{-3})$	$.495 \times 10^{-5}(.867 \times 10^{-3})$	$.264 \times 10^{-5}(.464 \times 10^{-3})$
$C_{\theta Z}$-Pitch defl./vert. load	rad/N(rad/lb)	$.760 \times 10^{-5}(.338 \times 10^{-4})$	$.202 \times 10^{-4}(.899 \times 10^{-4})$	$.220 \times 10^{-4}(.980 \times 10^{-4})$
$C_{\theta\theta}$-Pitch defl./pitch mom.	rad/M-N(rad/in-lb)	$.341 \times 10^{-3}(.386 \times 10^{-4})$	$.726 \times 10^{-4}(.820 \times 10^{-5})$	$.150 \times 10^{-3}(.169 \times 10^{-4})$
C_{YY}-Lat. defl./lat. load	m/N(in/lb)	$.466 \times 10^{-5}(.817 \times 10^{-3})$	$.457 \times 10^{-5}(.800 \times 10^{-3})$	$.680 \times 10^{-6}(.119 \times 10^{-3})$
$C_{\psi Y}$-Yaw defl./lat. load	rad/N(rad/lb)	$.431 \times 10^{-5}(.192 \times 10^{-4})$	$.315 \times 10^{-4}(.140 \times 10^{-3})$	$.537 \times 10^{-4}(.239 \times 10^{-3})$
$C_{\psi\psi}$-Yaw defl./yaw mom.	rad/m-N(rad/in-lb)	$.307 \times 10^{-3}(.347 \times 10^{-4})$	$.136 \times 10^{-3}(.154 \times 10^{-4})$	$.134 \times 10^{-3}(.151 \times 10^{-4})$

NOTE: Loads applied at front engine mount location, FS .948 (37.32), WS .467 (18.37), WL .210 (8.27).
Deflections measured at front engine mount location relative to wing spar.

TABLE 24.
JET ENGINE PYLON FLEXIBILITIES

FLEXIBILITY	UNITS	DESIRED	ACTUAL (RIGHT & LEFT)
C_{ZZ}-Vert. defl./vert. load	m/N (in/lb)	1.1×10^{-5} (1.95×10^{-3})	7.08×10^{-6} (1.24×10^{-3})
$C_{\Theta\Theta}$-Pitch defl./pitch mom.	rad/m-N (rad/in-lb)	1.03×10^{-4} (1.16×10^{-5})	1.00×10^{-4} (1.13×10^{-5})

NOTE: Loads applied at engine c.g. Deflections measured at engine c.g. relative to fuselage spar.

C-2

REFERENCES

1. Bradley, E. S., et al., "Advanced Turboprop Testbed Systems Study," NASA Lewis Research Center, CR 167928 (prepared by Lockheed-Georgia Company and issued as LG81ER0202), July 1982.

2. Goldsmith, I. M., "Advanced Turboprop Testbed Systems Study," NASA Lewis Research Center, CR 167895 (prepared by McDonnell Douglas Corporation), July 1982.

3. "The Langley Transonic Dynamics Tunnel," Langley Research Center, Hampton, Virginia, LWP-799, September 1969.

4. "Wind Tunnel Model Systems Criteria," NASA Langley Research Center LHB 1710.15, September 1983, Revised January 1985.

5. Crooks, O. J., "Propfan Test Airplane Flutter Model Design Specification," Lockheed-Georgia Company, PTA 41-001, September 1984.

6. Jenness, C. M. J., "Propfan Test Assessment Testbed Aircraft Flutter Model System Safety," Lockheed-Georgia Company, PTA 41-003, July 1985.

DISTRIBUTION LIST

CR-179458 NAS3-24339
LG 85ER0187

NASA Lewis Research Center
21000 Brookpark Road
Cleveland, OH 44135

		No. of Copies
Attn:	Report Control Office, MS 60-1	1
	Library, MS 60-3	2
	Tech. Util. Office, MS 7-3	1
	B. Batthauer, MS 4-8	1
	L. Bober, MS 86-7	1
	C. Ciepluch, MS 100-5	1
	D. Cheston, MS 86-2	1
	E. Graber, MS 86-7	10
	J. Groeneweg, MS 86-7	1
	R. Hager, MS 86-7	1
	R. Hogan, MS 4-2	1
	R. Kielb, MS 23-3	1
	J. Lubomski, MS 86-7	1
	D. Reemsnyder, MS 86-7	1
	R. McKnight, MS 4-8	1
	B. Miller, MS 5-3	1
	R. Ranaudo, MS 4-8	1
	J. Rohde, MS 86-7	1
	G. Sarvay, MS 86-2	1
	J. Schaefer, MS 6-8	2
	K. Sievers, MS 86-7	1
	I. Sumner, MS 86-7	1
	J. Whitlow, MS 86-7	1
	J. Williams, MS 500-211	1
	J. Ziemianski, MS 86-1	1

NASA Headquarters
Washington, DC 20546

Attn:	RP/J. Facey	1
	RJ/J. McCarthy	1

NASA Scientific and Technical Information Facility
P. O. Box 8757
Baltimore Washington International Airport, MD 21240

Attn:	Accessioning Department	20

NASA Ames Research Center
Moffett Field, CA 94035

Attn:	D. Bencze, MS 227-6	1

PRECEDING PAGE BLANK NOT FILMED

NASA Dryden Flight Research Center
P. O. Box 273
Edwards, CA 93523

Attn:	W. Albrecht, MS D-ODO	1
	R. Baron, MS D-OP	1
	W. Lokos, MS D-OFS	1
	N. Matheny, MS D-OFV	1
	L. Montoya, MS D-OFA	1
	R. Young, MS D-OFA	1

NASA Langley Research Center
Hampton, VA 23665

Attn:	R. Doggett, MS 340	1
	J. Pride, MS 432	1
	C. Ruhlin, MS 340	1
	L. Williams, MS 286	1

Allison Gas Turbine Operations
P.O. Box 420
Indianapolis, IN 46206-0420

Attn:	K. D. Anderson	1
	B. Jay	1
	T. Lindsey	1
	A. S. Novick	2
	L. Snyder	1

Boeing Commercial Airplane Company
P.O. Box 3707
Seattle, WA 98124

Attn:	G. W. Hanks	2

General Electric Company
1 Neumann Way
Cincinnati, OH 45215

Attn:	R. Harris	1
	P. Niskode	1
	V. Simon	1
	M. Stallone	1

Hamilton Standard Division, UTC
Windsor Locks, CT 06096

Attn:	J. Beggs	1
	R. Cornell	1
	A. Dale	1
	S. Josephson	1
	D. Leishman	1

Rohr Industries
P. O. Box 878
Chula Vista, CA 92012-0878

Attn:	R. A. Bradlaugh - Dredge, MZ 19S	1

Lockheed-California Company
P. O. Box 551
Burbank, California 91520

Attn:		
	Technical Information Center, D/82-40, Bldg. U-51	1
	H. Hassig, D/76-12, Bldg. 63-G	1

Lockheed-Georgia Company
86 South Cobb Dr.
Marietta, Georgia 30063

Attn:		
	Technical Information Dept. 72-34, Zone 235	1
	W. E. Arndt, D/72-17, Zone 418	1
	O. J. Crooks, D/72-73, Zone 406	1
	C. M. J. Jenness, D/72-17, Zone 418	1
	P. L. Kesler, D/72-17, Zone 418	1
	J. M. McAvoy, D/72-73, Zone 406	1
	R. L. McDougal, D/72-03, Zone 80	1
	D. T. Poland, D/72-17, Zone 418	1
	T. M. Rice, D/72-73, Zone 419	1
	J. K. Spitler, D/72-24, Zone 450	1

[redacted]

1. Report No.	2. Government Accession No.	3. Recipient's Catalog No.
CR-179458		

4. Title and Subtitle

Propfan Test Assessment Testbed Aircraft Flutter Model Test Report

5. Report Date

June 1986

6. Performing Organization Code

7. Author(s)

C. M. J. Jenness

8. Performing Organization Report No.

LG85ER0187

10. Work Unit No.

9. Performing Organization Name and Address

Lockheed-Georgia Company
86 South Cobb Drive
Marietta, GA 30063

11. Contract or Grant No.

NAS3-24339

13. Type of Report and Period Covered

Contractor Report

12. Sponsoring Agency Name and Address

NASA Lewis Research Center
21000 Brookpark Road
Cleveland, OH 44135

14. Sponsoring Agency Code

15. Supplementary Notes

Project Manager: E. J. Graber

16. Abstract

A 1/9-th scale high speed flutter model of the Gulfstream II, modified to the PTA testbed aircraft configurations, was tested during August 1985 in the NASA-Langley Transonic Dynamics Tunnel. The dynamically scaled propfan powerplants included windmilling propfans. Tests of the unsymmetric single and symmetric twin propfan configurations revealed no wing or propfan whirl flutter instabilities within the scaled aircraft flight envelope, expanded by a 20% flutter speed margin. Test data were also acquired with destabilizing wing tip booms for the purpose of analysis validation. Excellent correlations with the data were achieved in post-test flutter analyses using actual model properties and modified doublet lattice aerodynamic derivatives. It is concluded that the analysis method provides accurate flutter predictions for verification of the PTA testbed aircraft final design.

17. Key Words (Suggested by Author(s))	18. Distribution Statement
Prop-fan Wind Tunnel Testing Aircraft Flutter Model	Unclassified - [redacted]

19. Security Classif. (of this report)	20. Security Classif. (of this page)	21. No. of pages	22. Price*
unclassified	unclassified		

*For sale by the National Technical Information Service, Springfield, Virginia 22161